

©2018  
NA CAI

ALL RIGHTS RESERVED

THE FUNCTIONAL INTERPLAY BETWEEN TRPM7 CHANNEL-KINASE  
AUTOPHOSPHORYLATION AND ITS CELLULAR REGULATION

by

NA CAI

A dissertation submitted to the  
School of Graduate Studies  
Rutgers, The State University of New Jersey

In partial fulfillment of the requirements

For the degree of

Doctor of Philosophy

Graduate Program in Cellular and Molecular Pharmacology

Written under the direction of

Loren W. Runnels, Ph.D.

And approved by

---

---

---

---

---

New Brunswick, New Jersey

May, 2018

## ABSTRACT OF THE DISSERTATION

### THE FUNCTIONAL INTERPLAY BETWEEN TRPM7 CHANNEL-KINASE AUTOPHOSPHORYLATION AND ITS CELLULAR REGULATION

By NA CAI

Dissertation Director:

Loren W. Runnels, Ph.D.

As a member of the transient receptor potential ion channel subfamily, TRPM7 is a remarkable ion channel in possession of its own functional kinase domain. TRPM7 is ubiquitously expressed and permeable to divalent cations, allowing  $Mg^{2+}$ ,  $Ca^{2+}$ , and trace metals ions such as  $Zn^{2+}$  to constitute the channel's characteristic small inward current. The channel's functional kinase domain is located at the protein's cytosolic COOH terminus, placing TRPM7 also into a family of serine/threonine-phosphorylating alpha-kinases. It is not intuitively clear why a channel is covalently linked to a kinase, especially as it has been found that the kinase activity of TRPM7 is not required for channel gating. Previous studies have shown that TRPM7 is autophosphorylated, and yet the functional outcome of this autophosphorylation remain unknown. Motivated to understand the impact of phosphorylation on the function and regulation of this channel-kinase, I performed a comprehensive phosphoproteomic analysis of TRPM7 by mass spectrometry to identify

the major *in vivo* phosphorylation sites on TRPM7. The results of the mass spectrometry study uncovered potential mechanisms by which the catalytic activity of TRPM7 kinase is regulated through autophosphorylation. My experiments also revealed a significant role of TRPM7's kinase activity in regulating the posttranslational processing of TRPM7. Utilizing the TRPM7-K1646R kinase-inactive mutant, I discovered that TRPM7 kinase inactivation leads to faster protein degradation and intracellular retention of the channel in polarized epithelial cells compared to the wildtype protein. Mutational analysis of TRPM7 autophosphorylation sites further revealed a role for S1360 as a key residue mediating both protein stability and intracellular trafficking of TRPM7. In addition, I discovered that the intrinsic kinase activity of TRPM7 mediates the interaction of the channel with the signaling protein 14-3-3 $\theta$ , whose binding sites on TRPM7 also contribute to the regulation of TRPM7 trafficking. Overall, these findings expand our knowledge of the *in vivo* phosphorylation profile of TRPM7 and, more importantly, increase our understanding of the significance of TRPM7's kinase for functional regulation of the channel.

## ACKNOWLEDGMENTS

It is a great pleasure to express my gratitude to many people who helped in making this thesis possible. First and foremost, I would like to thank my supervisor Dr. Loren W. Runnels for all of his guidance and support. I am deeply honored to become a student of Loren's and carry on the scientific inquiry he started twenty years ago. I admire Loren for his passion for science, his dedication to students, and his kindness and generosity to everyone surrounding. Loren has taught me more than just research but more importantly about how to recognize and trust my potential. His continuous encouragement and support guided me through every step of the journey, especially at some of the more difficult moments. I am deeply grateful for his support and mentorship.

I would also like to express my sincere gratitude to my committee members, Dr. Nancy C. Walworth, Dr. Ann M. Stock, Dr. Victor Jin and Dr. Kiran Madura, whose advice and support are invaluable to my progress. Their passion for research inspires me to continue pursuing my own.

I wish to thank Dr. Vikas Nanda at the Department of Biochemistry for his helpful discussion on the kinase project and expertise in molecular modeling. I am also grateful to Dr. Peter Lobel, director of the Biological Mass Spectrometry Facility, for giving me introduction lectures on mass spectrometry that allowed me to take on my project.

I am thankful to my lab members who accompanied me in the past years. I am lucky to have Liping Lou as my twin sister in the lab. I thank her for always being so cheerful and putting up with my stress temperament from time to time. I would also like to thank Dr. Yuko Komiya for sharing with me many of her research techniques. I enjoyed her company and learned a great deal from her strong work ethics. I appreciate Namariq Al-

Saadi for helping me with experiments in the past a couple of months as I was racing across the finish line. Other current and former members of the lab, Sandra Tetteh, Dr. Zhiyong Bai, Dr. Jeffrey Overton, and Shufei Tao, have also offered me help and support. I would like to express my gratitude to all the faculty, students, and staff members of the Pharmacology Department. The department has become my second home because of all you lovely people, and I will miss our monthly gatherings and Christmas parties.

I want to say thanks to my close friends, Chen Wang and Liping Lou, for standing by my side all the way through and giving me unconditional support. I see them as my sisters and will always cherish our friendships. I am also grateful for the company of many good friends: Yijun Zhou, Jing Lin, Huirong Zhang, Wurihan, Yuanwang Pan, Chengshen Zhu, Zhichao Song, and many more. Their presence made my graduate life joyful and unforgettable. I sincerely wish every one of them a very bright future.

I want to dedicate this thesis especially to my grandfather, who had great faith in me since I was little. He installed me with the idea of growing up and becoming a female scientist. I am sure he would be very proud of me now. Lastly, and most importantly, I want to thank my parents for their endless love, encouragement, and support. I have been away from home for too long, but there was not a single day that I don't feel their unconditional love for me. I want to say “mom and dad, thank you for your sacrifices. I am proud to be your daughter, and I love you two so deeply.”

Na Cai

New Jersey, United States

March 2018

## TABLE OF CONTENTS

ABSTRACT OF THE DISSERTATION .....	ii
ACKNOWLEDGMENTS .....	iv
LIST OF FIGURES .....	viii
LIST OF TABLES .....	ix
INTRODUCTION .....	1
1. TRPM7.....	1
2. The functional interplay between TRPM7 channel and kinase domain .....	3
3. Cellular and physiological functions of TRPM7 kinase.....	4
4. Functional significance of TRPM7 phosphorylation.....	6
5. Regulation of TRPM7 kinase activity .....	7
6. Rationale and hypothesis .....	9
MATERIALS AND METHODS .....	10
SECTION I: MASS SPECTROMETRIC ANALYSIS OF TRPM7 AND TRPM6 <i>IN VIVO</i> PHOSPHORYLATION .....	10
1.1 Constructs .....	10
1.2 Cell lines .....	10
1.3 Expression and purification of TRPM7 kinases for MS analysis.....	11
1.4 Phosphorylation sites identification by LC-MS/MS .....	13
1.5 <i>In vitro</i> kinase assay for TRPM7 proteins expressed in HEK-293 cells .....	14
1.6 Immunoblotting .....	14
SECTION II: TRPM7 KINASE ACTIVITY IS REGULATED BY AUTOPHOSPHORYLATION.....	16
2.1 Constructs .....	16
2.2 Sumo-TRPM7-kinase purification .....	16
2.3 MS analysis of Sumo-TRPM7-kinase .....	17
2.4 <i>In vitro</i> kinase assay of Sumo-TRPM7-kinase .....	18
2.5 GST-exchange peptide pulldown GFP-TRPM7-Cterm .....	18
SECTION III: TRPM7 KINASE ACTIVITY REGULATES THE PROTEIN STABILITY AND CELLULAR LOCALIZATION OF THE CHANNEL .....	20
3.1 Constructs .....	20
3.2 Cell culture and transfection.....	20
3.3 Protein stability assay .....	20
3.4 Detection of TRPM7 protein levels.....	21
3.5 TRPM7 ubiquitylation assay .....	21
3.6 Proteasome inhibition assay with MG132.....	22
3.7 Immunocytochemistry .....	23
SECTION IV: AUTOPHOSPHORYLATION-DEPENDENT INTERACTION WITH 14-3-3 $\theta$ REGULATES TRPM7 CELLULAR LOCALIZATION .....	24
4.1 Constructs .....	24
4.2 GST-14-3-3 $\theta$ pulldown assays .....	25
4.3 TRPM7 and 14-3-3 $\theta$ co-immunoprecipitation .....	26
4.4 Detection of <i>in vivo</i> 14-3-3 $\theta$ binding motifs on TRPM7.....	26
4.5 <i>In vitro</i> kinase assay to assess the effect of 14-3-3 $\theta$ binding to TRPM7 .....	27
EXPERIMENTAL RESULTS.....	28

<b>SECTION I: MASS SPECTROMETRIC ANALYSIS OF TRPM7 AND TRPM6 <i>IN VIVO</i> PHOSPHORYLATION .....</b>	<b>28</b>
1.1 Identification of <i>in vivo</i> autophosphorylation sites on full-length TRPM7 .....	28
1.2 Identification of <i>in vivo</i> autophosphorylation sites on TRPM7 COOH terminus .....	33
1.3 Identification of <i>in vivo</i> TRPM7 transphosphorylation sites introduced by TRPM635 .....	38
1.4 Identification of <i>in vivo</i> TRPM6 phosphorylation sites .....	38
<b>SECTION II: TRPM7 KINASE ACTIVITY IS REGULATED BY AUTOPHOSPHORYLATION.....</b>	<b>42</b>
2.1 TRPM7 COOH terminus is heavily phosphorylated <i>in vitro</i> under ATP stimulation .....	42
2.2 TRPM7 kinase activity is affected by phosphorylation of residues located in the kinase catalytic domain .....	45
2.3 Mutations at S1777 differentially affect TRPM7's kinase activity .....	49
2.4 Phosphorylation of the TRPM7 S1565 in the exchange domain disrupts TRPM7 kinase activity without affecting kinase dimerization .....	51
2.5 A survey of potential regulatory phosphorylation residues on TRPM7 kinase.....	59
<b>SECTION III: TRPM7 KINASE ACTIVITY REGULATES THE PROTEIN STABILITY AND CELLULAR LOCALIZATION OF THE CHANNEL .....</b>	<b>62</b>
3.1 TRPM7 kinase inactivation leads to faster protein turnover .....	62
3.2 TRPM7 kinase inactive mutants are targeted by ubiquitin-proteasome degradation pathway.....	64
3.3 TRPM7 S1360 phosphorylation is involved in proteasome-mediated TRPM7 turnover.....	68
3.4 TRPM7 kinase affects cellular localization of the channel in polarized epithelial cells.....	72
3.5 TRPM7 S1360 phosphorylation regulates TRPM7 peripheral localization in OK cells.....	75
<b>SECTION IV: AUTOPHOSPHORYLATION-DEPENDENT INTERACTION WITH 14-3-3<math>\theta</math> REGULATES TRPM7 CELLULAR LOCALIZATION .....</b>	<b>77</b>
4.1 Identification of the phospho-binding protein 14-3-3 $\theta$ as a binding partner of TRPM7 .....	77
4.2 The interaction between 14-3-3 $\theta$ and TRPM7 requires TRPM7 autophosphorylation .....	80
4.3 Binding of 14-3-3 $\theta$ to TRPM7 requires autophosphorylation of TRPM7 on residue S1403 .....	83
4.4 Mutation in TRPM7's 14-3-3 $\theta$ -binding sites affect the distribution of the channel in polarized epithelial cells .....	87
4.5 The interaction with 14-3-3 $\theta$ does not affect TRPM7 kinase's catalytic activity or the overall protein levels .....	92
<b>DISCUSSION .....</b>	<b>95</b>
<b>REFERENCES.....</b>	<b>109</b>
<b>ABBREVIATIONS .....</b>	<b>119</b>
<b>APPENDICES .....</b>	<b>122</b>

## LIST OF FIGURES

Figure 1. TRPM7 topology and its current-voltage relationship. ....	3
Figure 2. Identification of <i>in vivo</i> phosphorylation sites on full length TRPM7. ....	30
Figure 3. Identification of <i>in vivo</i> phosphorylation on a kinase-containing TRPM7- Cterm protein. ....	33
Figure 4. Identification of <i>in vivo</i> transphosphorylation sites on mTRPM7 introduced by hTRPM6. ....	36
Figure 5. Identification of <i>in vivo</i> phosphorylation sites on full length hTRPM6. ....	39
Figure 6. Identification of <i>in vitro</i> . phosphorylation sites on TRPM7-kinase. ....	43
Figure 7. Mutagenesis screen of TRPM7 kinase domain phosphorylation sites. ....	46
Figure 8. Mutations of residues in the kinase domain leads to TRPM7 kinase inactivation. ....	47
Figure 9. TRPM7 kinase activity is affected by phosphorylation of residue S1777 located in the kinase catalytic domain. ....	50
Figure 10. S1565 in the TRPM7 kinase dimerization exchange segment regulates its catalytic activity. ....	52
Figure 11. Phosphorylation of the TRPM7 S1565 disrupts TRPM7 kinase activity without affecting kinase dimerization. ....	55
Figure 12. Phosphorylation of the TRPM7 S1565 potentially causes structural perturbation at the catalytic core of the TRPM7 kinase. ....	58
Figure 13. Mutagenesis screen of serine and threonine residues on TRPM7 with regulatory potential. ....	61
Figure 14. Inactivation of TRPM7 kinase increases the rate of channel turnover. ....	63
Figure 15. Inactivation of TRPM7 kinase leads to targeting of the protein by the ubiquitin-proteasome pathway. ....	66
Figure 16. A survey of TRPM7 phosphorylation sites that potentially regulate proteasome-dependent TRPM7 degradation. ....	70
Figure 17. Phosphorylation of the TRPM7 S1360 is involved in channel turnover. ....	71
Figure 18. Inactivation of TRPM7 kinase affects the cellular localization of the channel in polarized epithelial cells. ....	73
Figure 19. S1360 phosphorylation alters the localization of TRPM7 in polarized epithelial cells. ....	76
Figure 20. TRPM7 interacts with the phospho-binding protein 14-3-30 <i>in vitro</i> . ....	79
Figure 21. TRPM7 and 14-3-30 interacts in a phosphorylation-dependent manner. ....	81
Figure 22. Identification of S1403 as a major 14-3-30 binding site on TRPM7. ....	85
Figure 23. Alanine substitution at TRPM7 phosphorylation sites alters TRPM7 localization in polarized epithelial cells. ....	89
Figure 24. Phosphomimetic substitutions at S1403 and S1567 differentially affects TRPM7's localization in polarized epithelial cells. ....	90
Figure 25. Interactin with 14-3-30 does not affect TRPM7 kinase activity or protein levels. ....	93
Figure 26. Summary of identified regulatory TRPM7 phosphorylation sites. ....	98
Figure 27. Proposed model of TRPM7 kinase function in mediating TRPM7 protein stability and cellular localization. ....	103

## LIST OF TABLES

<b>Table 1.</b> Phosphopeptides identified from tryptic digestions of HA-mTRPM7-WT and K1646R overexpressed in HEK-203T cells.....	31
<b>Table 2.</b> Phosphopeptides identified from tryptic digestions of FLAG-mTRPM7 constitutively expressed in HEK-293-TRPM7 cells.....	32
<b>Table 3.</b> Phosphopeptides identified from tryptic digestions of GFP-mTRPM7-Cterm-WT and K1646R overexpressed in HEK-293T cells.....	34
<b>Table 4.</b> Phosphopeptides identified from tryptic digestions of SBP-mTRPM7-K1646R.....	37
<b>Table 5.</b> Phosphopeptides identified from tryptic digestions of HA-hTRPM6 transiently expressed in HEK-293T cells. ....	41
<b>Table 6.</b> Phosphopeptides identified from tryptic digestions of Sumo-mTRPM7-Kinase-WT and K1646R purified from <i>E. coli</i> and stimulated with ATP <i>in vitro</i> .....	44

## INTRODUCTION

Ion channels are membrane proteins that act as pores in the cell membrane and permit the selective passage of ions such as sodium, potassium, calcium, and magnesium. Essential for mammalian cell survival and proliferation, ion channels are controlled through multiple mechanisms, including whether the pores are open or closed and the number of ion channels in cellular membranes. Regulation of the channel gating, the transition between open and closed states, and cell surface presentation of an ion channel, a result of channel turnover and subcellular trafficking, are essential for the physiological control of ion channels and often involve phosphorylation of the ion channels. In this dissertation project, we explored the function and regulation of TRPM7, transient receptor potential cation channel melastatin 7, which is not only an active ion channel but is also the first ion channel identified to have its own kinase domain. Why nature endowed TRPM7 with its own kinase has remained an enigma for many years. In this introduction, I will provide essential background on the channel and kinase properties of TRPM7 and point out gaps in our current knowledge of the function and regulation of the TRPM7 kinase.

### 1. TRPM7

TRPM7 was simultaneously discovered by three independent research groups as a bifunctional protein composed of a transmembrane TRP channel domain fused to a cytosolic alpha-kinase domain (1-3) (Figure 1A). This constitutively active TRP channel is permeable to divalent cations including  $\text{Ca}^{2+}$ ,  $\text{Mg}^{2+}$ ,  $\text{Zn}^{2+}$ , and other trace metals (1,4). The kinase domain belongs to a family of serine/threonine protein kinases that share little sequence homology to conventional protein kinases (5). TRPM6, a close homolog of

TRPM7, was also identified as a bifunctional channel-kinase protein (6). Orthologues of TRPM7 were identified in all vertebrates, including rodents, frogs, and zebrafish (7) and paralogues of the channel were found in *Drosophila* and *C. elegans*, though they lack the kinase domain (8,9). TRPM7 is ubiquitously expressed in mammals across major organs such as heart, kidney, intestine, liver, and brain, whereas TRPM6 is more selectively expressed in the kidney and intestine (1,2,10).

Numerous physiological and pathological functions have been attributed to TRPM7. The channel is required for early embryogenesis in mice and *Xenopus laevis* frogs (11-14). Mice homozygous for TRPM7 deletion die at embryonic day 6.5-7.5 (11). In *Xenopus laevis*, knockdown of TRPM7 protein expression with morpholino antisense nucleotides produced severe neural tube closure defects, causing the embryos to die at the early larva stage (12). In Zebrafish, where the channel is not needed for early development, broader roles for the channel have been uncovered in the proliferation of pigment cells and pancreatic epithelial cells, and the differentiation and function of sensory neurons and kidney (14-17).

At the cellular level, TRPM7 is implicated in cellular  $Mg^{2+}$  homeostasis and  $Mg^{2+}$ -dependent cell survival, proliferation, as well as cell adhesion and motility (18-20). TRPM7-mediated intracellular  $Ca^{2+}$  signaling has also been implicated in cell motility, as well as in the control of cell differentiation, basal autophagy, and store-operated calcium entry (21-25). At the physiological level, TRPM7 is linked to the regulation of vertebrate magnesium homeostasis through the channel's association with its homolog TRPM6, which is mutated in human hypomagnesemia with secondary hypocalcemia disease (6,26-29). TRPM7's impact on whole-body magnesium homeostasis was later confirmed in mice

(30). Other studies have linked the TRPM7 channel to pathological processes such as cell death during organ ischemia and tumor proliferation and metastasis (31-39).

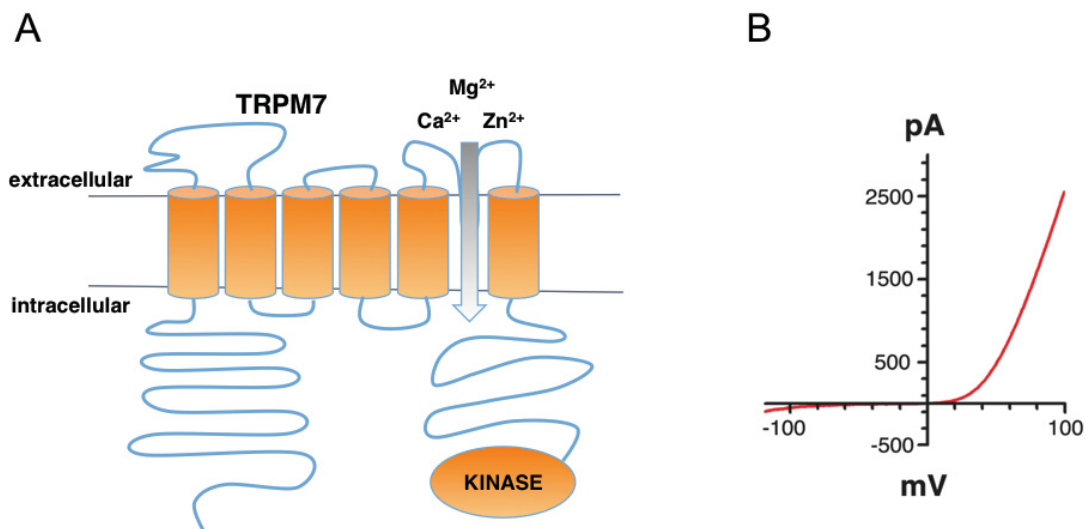


**Figure 1. TRPM7 topology and its current-voltage relationship.**

(A) TRPM7 is a fusion protein of a cation-permeating ion channel and an alpha-kinase. TRPM7's pore domain is located between its fifth and sixth transmembrane domains, and its alpha-kinase domain is located at its COOH terminus. (B) TRPM7 exhibits a strongly outwardly rectifying current at positive potentials and a small inward current at physiologically relevant negative potentials (20).

## 2. The functional interplay between TRPM7 channel and kinase domain

Due to TRPM6 and TRPM7's unique status as the first identified channel-kinase fusion proteins, the functional interrelationship between the channel and kinase has been extensively investigated. The native current constituted by TRPM7 is characterized by a small inward rectifying current at negative potential and a large outward rectifying current

at positive potential (Figure 1B) (1,4). TRPM7 current is inhibited by intracellular  $Mg^{2+}$ ,  $Mg^{2+}$ -ATP, and  $Mg^{2+}$ -GTP, and was originally referred to as magnesium nucleotide-regulated metal ion (MagNuM) or magnesium-inhibited cation (MIC) current (40). Surprisingly, it was found that the catalytic activity of TRPM7's kinase is not required for channel gating (18,41,42). Biophysical assessment of TRPM7 mutants carrying kinase-inactive point mutations (K1646R or G1799D) revealed that the kinase-inactive mutants have normal channel activity but have a reduced sensitivity inhibition by  $Mg^{2+}$  and  $Mg^{2+}$ -ATP (18,41). In contrast, a TRPM7 kinase-truncation mutant (TRPM7- $\Delta$ kinase) was found to have significantly reduced channel conductance and increased sensitivity to inhibition by  $Mg^{2+}$  and  $Mg^{2+}$ -ATP (18,41,42). Based on the aforementioned findings, a model was proposed in which TRPM7 possesses two  $Mg^{2+}$  and  $Mg^{2+}$ -ATP binding sites: one located within the kinase domain and the second one proximal to the transmembrane domain on the COOH terminus (41). The increased sensitivity of TRPM7- $\Delta$ kinase to inhibition by  $Mg^{2+}$  and  $Mg^{2+}$ -ATP is thought to occur because truncation of the kinase domain exposes the second  $Mg^{2+}$  binding site on TRPM7, which leads to the suppression of channel activity by intracellular  $Mg^{2+}$  at physiological levels (41). Therefore, it has been proposed that the kinase domain might play a regulatory role in mediating the sensitivity of the channel to  $Mg^{2+}$  and  $Mg^{2+}$ -nucleotide inhibition.

### **3. Cellular and physiological functions of TRPM7 kinase**

The function of TRPM7 kinase activity was explored by different research groups using TRPM7 transgenic mice models. Mice homozygous for TRPM7 kinase-deletion (*Trpm7* <sup>$\Delta$ kinase/ $\Delta$ kinase</sup>) are embryonic lethal, likely due to impaired channel activity, whereas

TRPM7 knockin mice carrying a kinase-inactive point mutation at K1646R (Trpm7<sup>R/R</sup>) are viable and have normal serum Mg<sup>2+</sup> levels (43,44). Characterization of the Trpm7<sup>R/R</sup> mice revealed that global inactivation of TRPM7 kinase activity made mice resistant to the effect of dietary Mg<sup>2+</sup> deprivation, suggesting a role for TRPM7's kinase as a sensor of cellular Mg<sup>2+</sup> status that coordinates with the channel function in regulating whole-body Mg<sup>2+</sup> homeostasis (44). Subsequent studies using the Trpm7<sup>R/R</sup> mice further identified a broad range of cellular functions that require TRPM7 kinase activity, including murine mast cell degranulation, intra-epithelial T cell gut-homing, splenic T cell proliferation, ameloblast differentiation, and store-operated Ca<sup>2+</sup> entry in platelet cells (45-49).

What is extraordinary about the TRPM7's kinase domain, apart from being a moiety of the fusion protein, is that it can function independently *in vivo* when released from the channel domain (50). It was first discovered by the Clapham group that the carboxyl terminus of TRPM7 containing its kinase domain is proteolytically cleaved off by caspases and that the liberated TRPM7 kinase translocates to the nucleus to interact with chromatin remodeling complex and phosphorylate serine/threonine residues on histones (50,51). The same group later made a similar observation for TRPM6 kinase and proposed a role of TRPM7 and TRPM6 kinases in regulating gene transcription by affecting histone posttranslational modifications (52).

During the course of investigating TRPM7's kinase function, additional *in vitro* substrates of TRPM7 have been identified, including non-muscle myosin heavy chain IIA, annexin I, phospholipase C gamma-2 (PLC-2), eukaryotic elongation factor-2 kinase (eEF2K), tropomodulin, and stromal interaction molecule 2 (STIM2) (19,25,53-58). It is not clear whether the identified *in vitro* substrates are *bona fide* substrates of TRPM7 *in*

*vivo* nor what the functional significance of these substrates' phosphorylation would be. Nonetheless, these observations may suggest a broad role of the TRPM7 kinase in regulating a wide range of cellular and physiological activities. These emerging findings highlight the need to study the mechanisms that regulate TRPM7's kinase activity in order to fully understand the functional significance of the TRPM7 kinase *in vivo*.

#### **4. Functional significance of TRPM7 phosphorylation**

One known substrate of the TRPM7 kinase is the channel-kinase protein itself, with multiple serine and threonine phosphorylation sites having been identified (42,59,60). Using tandem mass spectrometry (MS) techniques, Clark and colleagues identified more than 40 autophosphorylation sites *in vitro* on an ATP-stimulated COOH-terminal fragment of TRPM7, and Kim and colleagues similarly found more than a dozen *in vivo* phosphorylation sites on a full-length TRPM7 protein (59,60). How autophosphorylation of TRPM7 affects the channel remains unclear. An early study by Matsushita and colleagues identified two major *in vitro* TRPM7 autophosphorylation sites, S1511 and S1567, but reported that alanine substitutions at these two sites did not alter the channel's ion conductivity (42). Whether TRPM7 autophosphorylation may impact the stability, cellular localization, and intracellular molecular interactions of the channel with other proteins has not been investigated.

Members of the TRP family channels are known to be subject to phosphorylation as a mechanism to regulate their post-translational activity. For example, the thermosensing channel TRPV1 is regulated by protein kinase A (PKA) and protein kinase C (PKC)-mediated serine phosphorylation for channel conductance and is also tyrosine-

phosphorylated by Src for surface expression (61). The osmosensor channel TRPV4 is phosphorylated by glycogen synthase kinase (GSK) at S824, which alters the channel's interaction with cytoskeleton components for the trafficking of the channel to the cell membrane (62). TRPM7, when in the heteromeric complex with its homolog TRPM6, is cross-phosphorylated by TRPM6's kinase domain (63). Characterization of the TRPM7/TRPM6 interaction revealed that, though the two kinases have virtually identical biochemical activities, only TRPM7 can be cross-phosphorylated by TRPM6, but not vice versa (63). There are indications that TRPM7 subcellular localization and trafficking are also affected by TRPM6's kinase activity in response to changing concentrations in extracellular  $Mg^{2+}$  (64). It is not clear yet what sites on TRPM7 are unique to TRPM6 cross-phosphorylation, and how the cross-phosphorylation sites, as well as autophosphorylation sites of TRPM7, affect the protein subcellular localization.

### **5. Regulation of TRPM7 kinase activity**

TRPM7 and TRPM6 kinases are members of the atypical alpha-kinase family, so named after initial members of the family *Dictyostelium* myosin heavy chain kinase A, B, C (MHCK A, B, C), which primarily phosphorylate their substrates within alpha-helical domains rather than within flexible loops and turns, as generally done by conventional protein kinases (65). Structural analysis of TRPM7 kinase reveals that despite little sequence similarity to conventional protein kinases, the tertiary structure of the kinase resembles the structure of conventional protein kinases like protein kinase A with some exceptions (66,67). The kinase domain of TRPM7 assembles into dimers through an exchange of a short stretch of amino acids NH<sub>2</sub>-terminal to the core catalytic domain (68).

This exchange segment is highly conserved in both TRPM7 and TRPM6 and is required for kinase dimerization and the catalytic activity of both kinases (68,69).

So far, the mechanisms that regulate TRPM7's kinase activity remain poorly understood. For conventional serine and threonine kinases, phosphorylation is one of the most common mechanisms for regulating protein kinase activity, which is mainly achieved by phosphorylation of an activation loop located near the kinase's catalytic core (70). Phosphorylation of the activation loop stabilizes the kinase in an active conformation that is more permissive to substrate binding (70). Structural comparison between alpha-kinases and conventional kinases revealed a conserved asparagine/aspartate-containing loop (N/D loop) in alpha-kinases located at the equivalent sites at the protein's C-terminal lobe (66,67,71). It is not clear if this N/D loop plays a similar regulatory role for the kinase function of TRPM7. Studies of other members of the alpha-kinases family such as eEF2K and *Dictyostelium* MHCKs revealed regulatory mechanisms for their kinase activities, achieved by autophosphorylation of residues inside or outside of the kinase's catalytic cores (72-75). In comparison, it is not clear whether and how autophosphorylation of TRPM7 affects its own kinase activity. TRPM7 contains a heavily phosphorylated serine/threonine-rich region (S/T domain) N-terminal of its kinase domain, yet it appears that this S/T-rich segment does not directly affect TRPM7 kinase's catalytic activity but may facilitate substrate binding (59). Since the kinase activity of TRPM7 is found to be critical in the regulation of a number of cellular activities, it is essential to have a better understanding of the mechanisms that control the activity of the kinase in order to better appreciate its functional significance in the cells.

## 6. Rationale and hypothesis

The motivation for this thesis project is that even though phosphorylation sites have been identified on TRPM7, the effect of TRPM7 autophosphorylation on the function and regulation of the channel-kinase remains unknown. In this study, I performed an MS analysis of TRPM7 phosphorylation as a first step towards understanding the impact of phosphorylation on the function and regulation of the protein. By identifying the key *in vivo* phosphorylation sites, our intention, in part, was to identify potential molecular mechanisms important for regulation of the catalytic activity of TRPM7 kinase. We also expected that a closer examination of TRPM7 phosphorylation would also provide useful information regarding the functional significance of TRPM7 kinase activity in terms of channel regulation. Given that phosphorylation is a common form of post-translational modification regulating protein function and activity, and that the functional significance of TRPM7 kinase activity remains unclear, we hypothesize that the intrinsic kinase activity of TRPM7 plays regulatory roles in affecting TRPM7 protein stability, cellular localization, and cellular interactions with other proteins. In the following sections, we will describe the results of our experiments and discuss its impact on our understanding of the regulation of the TRPM7 channel.

## MATERIALS AND METHODS

### SECTION I: MASS SPECTROMETRIC ANALYSIS OF TRPM7 AND TRPM6 *IN VIVO* PHOSPHORYLATION

#### 1.1 Constructs

The pcDNA5/FRT/TO-HA-mTRPM7 (HA-TRPM7), pcDNA5-SBP-CBP-mTRPM7 (SBP-TRPM7), pcDNA6-mfGFP-mTRPM7-Cterm (a.a. 1120-1863) containing a streptavidin binding protein (SBP) tag (GFP-TRPM7-Cterm), and the pcDNA5/FRT/TO-HA-hTRPM6 (HA-hTRPM6) were generated in earlier studies (20,76). Site-directed mutations were introduced into HA-TRPM7 and GFP-TRPM7-Cterm using the QuickChange mutagenesis kit (Stratagene, CA).

#### 1.2 Cell lines

The 293T cell line (CRL-3216) was purchased from American Type Culture Collection (Manassas, VA). The HEK-293-TRPM7 cells expressing recombinant FLAG-tagged mouse TRPM7 was described in an earlier publication (1). HEK-293T and HEK-293-TRPM7 cells were maintained in a Dulbecco's Modified Eagle Medium (DMEM), high glucose media with 10% fetal bovine serum in a humidified 37°C, 5% CO<sub>2</sub> incubator. For biochemical analysis, transient transfections were performed using the Turbofect transfection reagent (Thermo Fisher, MA) according to the manufacturer's protocol.

### 1.3 Expression and purification of TRPM7 kinases for MS analysis

To identify autophosphorylation sites of TRPM7, HA-TRPM7-WT and K1646R and GFP-TRPM7-Cterm-WT and K1646R were transiently expressed in HEK-293T cells. Approximately  $0.3 \times 10^6$  HEK-293T cells were plated on 10 cm culture dishes overnight and reached 70% confluence the next day. Ten  $\mu\text{g}$  of HA-TRPM7-WT, HA-TRPM7-K1646R, GFP-TRPM7-Cterm-WT, and GFP-TRPM7-Cterm-K1646R were transfected into the HEK-293T cells and expressed for 24 h. Cells were rinsed with phosphate buffered saline (PBS) (137 mM NaCl, 2.7 mM KCl, 10 mM Phosphate, pH 7.4) and lysed in 1 mL lysis buffer (50 mM Tris (pH 7.4), 150 mM NaCl, 1% IGEPAL CA-630 (Sigma-Aldrich, MO)) containing protease inhibitor cocktail (Roche Life Sciences, IN) and phosphatase inhibitor cocktail (EMD Millipore, Germany). HA-TRPM7 proteins were immunoprecipitated by 50  $\mu\text{l}$  HA-agarose (Roche Life Sciences, IN) overnight, washed three times with PBS-1% Triton-X100 (PBST), and then eluted with 50  $\mu\text{l}$  1 mg/ml HA-peptide dissolved in PBS overnight at 4°C by rotation (Roche Life Sciences, IN). The GFP-TRPM7-Cterm proteins containing an SBP tag was immunoprecipitated by 50  $\mu\text{l}$  streptavidin agarose (Stratagene, CA) overnight at 4°C by rotation, washed three times with PBST, and eluted with 10 mM biotin dissolved in PBS overnight at 4°C by rotation.

FLAG-tagged TRPM7 was obtained from the HEK-293-TRPM7 cells expressing recombinant mouse FLAG-TRPM7 at a basal level without tetracycline induction (1). TRPM7-expressing cells grown on 15 mm culture plates were harvested at 70% confluence and a plate of cells were lysed in a total of 5 mL lysis buffer containing protease inhibitor cocktail (Roche Life Sciences, IN) and phosphatase inhibitor cocktail (EMD Millipore, Germany). FLAG-TRPM7 proteins were immunoprecipitated by 100  $\mu\text{l}$  M2 anti-FLAG

agarose (Sigma, MO) overnight at 4°C by rotation, washed three times with PBST, and eluted directly into 50 µl SDS sample buffer.

To identify cross-phosphorylation sites on TRPM7, 7.5 µg kinase-inactive mouse SBP-TRPM7-K1646R was co-expressed with 7.5 µg HA-tagged human TRPM6 into HEK-293T cells grown on 10 cm culture plates. Proteins were expressed for 24 hours and cells were harvested in 1 mL lysis buffer containing protease inhibitor cocktail (Roche Life Sciences, IN) and phosphatase inhibitor cocktail (EMD Millipore, Germany). HA-hTRPM6 was immunoprecipitated by 50 µl HA-agarose (Roche Life Sciences, IN) overnight, washed three times with PBST, and eluted with 50 µl 1 mg/ml HA-peptide dissolved in PBS overnight at 4°C by rotation (Roche Life Sciences, IN). As a negative control, 7.5 µg of SBP-TRPM7-K1646R was expressed alone in HEK-293T cells, immunopurified by 50 µl streptavidin agarose (Stratagene, CA) overnight at 4°C by rotation, and eluted with 10 mM biotin/PBS overnight at 4°C by rotation.

To identify TRPM6 phosphorylation sites, 7.5 µg of HA-hTRPM6 plasmids were transiently transfected into 10 cm HEK-293T cells for 24 h and harvested in 1 mL lysis buffer containing protease inhibitor cocktail (Roche Life Sciences, IN) and phosphatase inhibitor cocktail (EMD Millipore, Germany). HA-hTRPM6 proteins were immunoprecipitated by 50 µl HA-agarose (Roche Life Sciences, IN) overnight, washed three times with PBST, and eluted with 50 µl 1 mg/ml HA-peptide dissolved in PBS overnight at 4°C by rotation (Roche Life Sciences, IN).

#### **1.4 Phosphorylation sites identification by LC-MS/MS**

For phosphorylation site identification, purified TRPM6 and TRPM7 were resolved in a 10% Bis-Tris polyacrylamide gel. Protein bands separated on the gel were visualized by Coomassie blue staining and cut out from the gel for MS analysis performed by the Biological Mass Spectrometry Facility at Rutgers Robert Wood Johnson Medical School. To briefly describe the MS procedure, each gel band was subjected to in-gel reduction, alkylation, tryptic digestion and peptide extraction with a standard protocol. Peptides were solubilized in 0.1% trifluoroacetic acid, and analyzed by Nano LC-MS/MS with Dionex Ultimate 3000 RLSC Nano System interfaced with a Velos-LTQ-Orbitrap (ThermoFisher, CA) or a QExactive HF (ThermoFisher, CA) based on instrument availability. Samples were loaded onto a self-packed 100  $\mu\text{m}$  x 2 cm trap (Magic C18AQ, 5  $\mu\text{m}$  200  $\text{\AA}$ ; Michrom Bioresources, Inc., PA) and washed with Buffer A (0.2% formic acid) for 5 min with a flow rate of 10  $\mu\text{L}/\text{min}$ . The trap was brought in-line with the analytical column (Magic C18AQ, 3  $\mu\text{m}$  200  $\text{\AA}$ , 75  $\mu\text{m}$  x 50 cm; Michrom Bioresources, Inc., PA) and peptides fractionated at 300 nL/min using a segmented linear gradient 4-15% Buffer B (0.2% formic acid in acetonitrile) in 35 min, 15-25% Buffer B in 65 min, 25-50% Buffer B in 55 min. MS data was acquired using a data-dependent acquisition procedure with a cyclic series of a full scan acquired with a resolution of 60,000 (Velos-LTQ-Orbitrap) or 120,000 (QExactive HF) followed by MS/MS of the 20 most intense ions and a dynamic exclusion duration of 30 sec for both instruments. Proteome Discoverer was used for database search and analysis. Data were searched against most updated SwissProt database using MASCOT (v 2.3). Precursor ion mass error tolerance was set to  $\pm 10$  ppm (Velos-LTQ-Orbitrap) or  $\pm 7$  ppm (QExactive HF) and fragment mass error tolerance to  $\pm 0.4$  Da

(Velos-LTQ-Orbitrap) and +/-20 ppm (QExactive HF). Cysteine carbamidomethylation was set as a complete modification, acetylation on NH<sub>2</sub> terminus of protein, oxidation on methionine, phosphorylation on serine, threonine and tyrosine were set as variable modifications. Site localization was analyzed using PTMRS. Only spectra of high confidence (FDR were set at 0.01 for PSM) were reported. Interested sites were further validated manually.

### **1.5 *In vitro* kinase assay for TRPM7 proteins expressed in HEK-293 cells**

Prior to analyzing TRPM7 WT and kinase-inactive mutants by MS, the catalytic activities of the proteins were varified by *in vitro* kinase assays. Purified TRPM7 proteins were dialyzed into kinase buffer (50 mM MOPS (pH 7.2), 100 mM NaCl, 2.5 mM MnCl<sub>2</sub>, 0.5 mM ATP). The kinase reactions were performed at 30°C for 20 min in a 50 µl reaction in the presence of 4 µCi of [ $\gamma$ -<sup>32</sup>P]ATP with 5 µg of myelin basic protein (MBP) as a substrate. Reactions were stopped by the addition of SDS sample buffer, and the reaction mix was resolved by SDS-PAGE. Proteins were detected by Coomassie blue staining and gels were dried completely using a gel dryer (BioRad Laboratories, CA). Incorporation of [ $\gamma$ -<sup>32</sup>P]ATP into substrates was analyzed by autoradiography using Cyclone Plus Phosphor Imager (PerkinElmer, CT).

### **1.6 Immunoblotting**

For detection of proteins, the proteins resolved by SDS-PAGE and Western blotting using standard protocols. A rat monoclonal antibody anti-HA antibody (3F10; Roche Life Sciences, IN) was used to detect HA-tagged TRPM7 and TRPM6. Anti-FLAG M2

antibody (Sigma, MO) was used to detect FLAG-TRPM7. A mouse monoclonal antibody anti-SBP (sc-101595; Santa Cruz Biotechnology, Inc., TX) and a rabbit polyclonal anti-TRPM7-C47 were used to detect SBP-TRPM7 (20). An anti-GFP antibody (sc-9996; Santa Cruz Biotechnology, Inc., TX) was used to detect GFP-TRPM7-Cterm. An anti-pSer antibody (#2981; Cell Signalling Technology, Inc., MA) was used to detect phosphorylated TRPM6 protein.

## SECTION II: TRPM7 KINASE ACTIVITY IS REGULATED BY AUTOPHOSPHORYLATION

### 2.1 Constructs

To generate the Sumo-TRPM7-Kinase, mouse TRPM7 cDNA (a.a. 1384-1863) was amplified by PCR and subcloned into the BamHI/EcoRI sites of a pTrcHis2 A vector (Thermo Fisher Scientific, MA) modified to contain a NH<sub>2</sub>-terminal His6-Sumo-SBP tag between NcoI/BamHI. Site-directed point mutations were introduced into TRPM7 using the QuickChange mutagenesis kit (Stratagene, CA). To generate the GST-fused exchange peptide of TRPM7, residues 1548-1576 of mouse TRPM7 were amplified by PCR and fused in-frame to GST by cloning into the BamHI and EcoRI cloning sites of the pGEX-6P3 vector (Addgene, MA) using primers 5'-CATCATGGATCCGATACAAATTACTATTATTCAGCTGTGGAAAG-3' and 5'-CATCATGAATTCTCGTGGAGGTACAGGAACGAAGGG-3'. GFP-TRPM7-Cterm mutants were generated by site-directed mutagenesis (QuickChange; Stratagene, CA).

### 2.2 Sumo-TRPM7-kinase purification

The Sumo-TRPM7-Kinase WT and mutants were expressed in transformed *E. coli* BL21-DE3 cells (Stratagene, CA). Bacteria were grown in 200 mL culture at 37°C to OD<sub>600</sub> of 0.6-0.8, cooled to 16°C and induced at 16°C for 16-18 h with 1 mM isopropyl-β-D-1-thiogalactopyranoside (IPTG) (Gold Biotechnology, MO). Harvested bacterial cells were re-suspended and lysed by sonication in 10 mL ice-cold PBS containing a final concentration 1 mM protease inhibitor PMSF and 1% Triton-X10. Bacterial cell lysates

were collected by spinning down the lysed bacteria at 6000g at 4°C for 30 min. Sumo-TRPM7-Kinase proteins were pulled down from the cell lysate supernatant by 100 µl streptavidin agarose (Stratagene, CA), washed three times with washing buffer containing 100 mM Tris/Cl (pH 8.0), 150 mM NaCl, and 0.1% Triton X-100. Proteins were eluted with 100 µl of elution buffer containing 10 mM biotin and 0.1 mg/ml BSA dissolved in the washing buffer. Elution was performed by rotating the beads overnight at 4°C. After elution, purified kinase proteins were dialyzed with 500 mL ice-cold dialysis buffer containing 50 mM MOPS (pH 7.2), 100 mM NaCl, 3.5 mM MnCl<sub>2</sub>, and 1 M ZnCl<sub>2</sub> using Slide-A-Lyzer<sup>TM</sup> MINI Dialysis Devices (ThermoFisher, MA) at 4°C for 2 h. Protein concentrations of purified Sumo-TRPM7-Kinase were measured against serial diluted BSA proteins (1 - 10 µg) by visualizing the proteins dissolved on a SDS-PAGE gel and stained with Coomassie blue.

### **2.3 MS analysis of Sumo-TRPM7-kinase**

Two µg of purified Sumo-TRPM7-Kinase-WT and Sumo-TRPM7-Kinase-K1646R proteins were stimulated with ATP *in vitro* in a kinase reaction containing 50 µl kinase buffer (50 mM MOPS (pH 7.2), 100 mM NaCl, 2.5 mM MnCl<sub>2</sub>, 0.5 mM ATP) at 30°C for 2 min. Reactions were stopped by the addition of SDS sample buffer. ATP stimulated Sumo-TRPM7-kinases were resolved on a 10% Bis-Tris polyacrylamide gel and cut out for MS analysis.

#### **2.4 *In vitro* kinase assay of Sumo-TRPM7-kinase**

*In vitro* kinase assays were performed containing 1 µg of purified Sumo-TRPM7-kinase WT and 5 µg pf substrate MBP dissolved in in 50 µl kinase buffer (50 mM MOPS (pH 7.2), 100 mM NaCl, 2.5 mM MnCl<sub>2</sub>, 0.5 mM ATP). The reactions were performed at 30°C for 2 min in the presence of 4 µCi of [ $\gamma$ -<sup>32</sup>P]ATP. Reactions were stopped by the addition of SDS sample buffer, and the reaction mix was resolved by SDS-PAGE. Proteins were detected by Coomassie blue staining and gels were dried completely using a gel dryer (BioRad Laboratories, CA). Incorporation of [ $\gamma$ -<sup>32</sup>P]ATP into substrates was analyzed by autoradiography using Cyclone Plus Phosphor Imager (PerkinElmer, CT).

#### **2.5 GST-exchange peptide pulldown GFP-TRPM7-Cterm**

Recombinant GST-exchange peptide and GST were expressed in *E. coli* BL21-DE3 cells (Agilent Technologies, CA). Bacteria in 200 mL cultures were grown at 37°C to OD600 of 0.6-0.8 and induced overnight with 1 mM IPTG (Gold Biotechnology, MO). Bacterial cells were lysed by sonication in 20 mL of ice-cold PBS containing 1% Triton-X100 and protease inhibitor phenylmethylsulfonyl fluoride (Sigma-Aldrich, MO). The bacterial cell lysates were then incubated with 1 mL glutathione agarose (Sigma-Aldrich, MO) overnight at 4°C with rotation. The agarose beads were washed with 50 mL PBST three times by rotation. The protein concentrations of GST pulldown samples were measured by resolving the proteins on a SDS-PAGE gel and compare the protein levels with serial diluted BSA proteins (5 - 50 µg) by Coomassie staining.

For GST pulldown assays, 10 µg of GFP-TRPM7-Cterm-WT, L1564P, S1565A, and S1565D plasmids were transfected in 10 cm HEK-293T cells and expressed for 24 h.

Cell lysates were harvested in 1 mL lysis buffer containing protease inhibitor cocktail (Roche Life Sciences, IN) and phosphatase inhibitor cocktail (EMD Millipore, Germany) and incubated with 5  $\mu$ g GST-exchange peptide or GST proteins bound on glutathione agarose for overnight at 4°C. Cell lysate input (20  $\mu$ l) and GST pulldown samples were separated by SDS-PAGE and analyzed by immunoblotting. An anti-GFP antibody (sc-9996; Santa Cruz Biotechnology, Inc., TX) was used to detect GFP-TRPM7-Cterm.

## **SECTION III: TRPM7 KINASE ACTIVITY REGULATES THE PROTEIN STABILITY AND CELLULAR LOCALIZATION OF THE CHANNEL**

### **3.1 Constructs**

A pcDNA3/HA-Ubiquitin construct (HA-ubiquitin, item #18712) was also purchased from Addgene (77). The ubiquitin sequence was subcloned into the pcDNA6-FLAG vector between the BamHI and EcoRI sites (pcDNA6-FLAG-Ub). FLAG-NHERF1 was from Addgene (pCMV-NHERF1-FL, item #28291) (78).

### **3.2 Cell culture and transfection**

293-TRPM7-WT and 293-TRPM7-K1646A cells have been described previously (20). The cells were cultured under standard conditions in DMEM supplemented with 10% FBS. For biochemical analysis, transient transfections were performed using the Turbofect transfection reagent (ThermoFisher, MA) according to the manufacturer's protocol. Opossum Kidney (OK) cell line was a generous gift of Dr. Judith A Cole (Department of Biological Sciences, The University of Memphis). OK cells were cultured in DMEM/F12 medium supplemented with 5% FBS. Transfections of OK cells were performed with Lipofectamine 3000 (ThermoFisher, MA) according to the manufacturer's protocol.

### **3.3 Protein stability assay**

Approximately  $0.6 \times 10^6$  293-TRPM7-WT and 293-TRPM7-K1646A cells were seeded onto Poly-L-lysine (Sigma-Aldrich, MO) coated 6-well plates. Two hours after seeding, cells were added with 5  $\mu\text{g/ml}$  tetracycline to induce protein expression for 24 hours. To

arrest protein synthesis, cell medium was replaced with fresh medium containing 10 µg/ml cycloheximide (CHX). At various time points following CHX treatment, cells were lysed in 200 µl lysis buffer containing protease inhibitor cocktail (Roche Life Sciences, IN). Protein concentrations of the cell lysates were measured using Bradford assays (ThermoFisher, MA).

### **3.4 Detection of TRPM7 protein levels**

Equal amounts of cell lysates (40 – 80 µg/well) were resolved by SDS-PAGE and Western blotting following standard protocols. The rabbit polyclonal TRPM7 antibody (anti-TRPM7) was used to probe for HA-TRPM7; its characterization has been previously described as anti-C47 (20). Vinculin, which was used as loading control, was detected by Western blotting using a monoclonal anti-vinculin antibody (clone hVIN-1; Sigma-Aldrich, MO). Immunochemiluminescence signals were detected by X-ray film exposure. Quantification of protein levels was performed by analyzing scanned film images using LI-COR Image Studio software (LI-COR Biotechnology, NE). The protein half-life of TRPM7-K1646A was calculated by fitting the turnover curve to a one-phase exponential decay using GraphPad Prism 7 (GraphPad Software, Inc., CA).

### **3.5 TRPM7 ubiquitylation assay**

Approximately  $3 \times 10^6$  293-TRPM7-WT and 293-TRPM7-K1646A cells were seeded onto 10 cm culture plates. After attachment overnight, cells were treated with 5 µg/ml tetracycline to induce TRPM7 expression and transfected with 5 µg FLAG-tagged ubiquitin (pcDNA6-FLAG-Ub). After 24 h of protein expression, cells were then treated

with 10  $\mu$ M of the proteasome inhibitor MG132 (Sigma-Aldrich, MO) for 8 hours and lysed in lysis buffer containing protease inhibitor cocktail (Roche Life Sciences, IN) and 20 mM of deubiquitinase inhibitor *N*-ethylmaleimide (NEM) (Sigma-Aldrich, MO). To detect ubiquitinated TRPM7, ubiquitinated proteins from cell lysates were immunoprecipitated using ANTI-FLAG® M2 Agarose Affinity Gel (Sigma-Aldrich, MO), washed three times with lysis buffer, and eluted to 50  $\mu$ l SDS sample buffer. Cell lysates and immunoprecipitated samples were resolved by SDS-PAGE and Western blotting following standard protocols. Ubiquitinated TRPM7 in the FLAG-IP samples was detected using a rat monoclonal anti-HA antibody (3F10; Roche Life Science, IN). The total amounts of TRPM7 and ubiquitinated proteins in the lysates were analyzed with the anti-HA antibody (3F10; Roche Life Science, IN) and an anti-FLAG antibody (Sigma-Aldrich, MO).

### **3.6 Proteasome inhibition assay with MG132**

Approximately  $0.7 \times 10^6$  293-TRPM7-WT and 293-TRPM7-K1646A cells were seeded on Poly-L-lysine coated 6-well plates. Two hours after seeding, 5  $\mu$ g/ml tetracycline was added to induce protein expression. After 24 h of expression, cell culture medium of 293-TRPM7-WT and 293-TRPM7-K1646A cells were replaced with fresh medium containing DMSO or 1  $\mu$ M MG132. Cells were harvested at 8 h and 24 h after MG132 treatments in 200  $\mu$ l lysis buffer containing protease inhibitor cocktail (Roche Life Sciences, IN).

Alternatively, HEK-293T cells were seeded onto Poly-L-lysine coated 12-well plates at  $0.3 \times 10^6$  cells/well. Cells were transfected with 0.5  $\mu$ g HA-TRPM7-WT and mutants at 70% confluence the next day. After 24 h of expression, cell culture medium was replaced with

fresh medium containing DMSO or 1  $\mu$ M MG132 to inhibit proteasome activity. Cells were harvested 24 hours after MG132 treatment and lysed in 100  $\mu$ l lysis buffer containing protease inhibitor cocktail (Roche Life Sciences, IN). Protein concentrations of the cell lysates were measured using Bradford assays (ThermoFisher, MA). Quantification of TRPM7 protein levels were performed as described above.

### **3.7 Immunocytochemistry**

OK cells were seeded on glass coverslips in 24-well plates at  $0.1 \times 10^6$  density. To observe TRPM7 cellular localization, OK cells were co-transfected with 1  $\mu$ g HA-TRPM7-WT and 0.5  $\mu$ g FLAG-NHERF1 plasmids for 24 h. To compare the cellular localization between WT TRPM7 and mutants, 0.5  $\mu$ g of HA-TRPM7-WT and mutant plasmids were transiently expressed in the OK cells for 48 h. For immunochemical staining, cells were fixed with 4% formaldehyde at room temperature for 30 min, permeabilized in PBS with 0.1% Triton at 30°C for 20 min, and blocked with 5% FBS/ PBS at 30°C for 1 hour. A rabbit monoclonal anti-HA antibody (C29F4; Cell Signaling Technology, MA) was used to detect the HA-tagged TRPM7, and a mouse anti-FLAG antibody (Sigma-Aldrich, MO) was used to detect FLAG-NHERF1. Alexa Fluor™ 488 and Alexa Fluor™ 568 goat antibodies raised against rat and mouse were used as secondary antibodies (Thermo Fisher, MA). F-actin was detected with Alexa Fluor™ 568 phalloidin (Thermo Fisher, MA). Images were obtained at the Rutgers RWJMS CORE Confocal Facility using a Yokogawa CSUX1-5000 microscope under 63X magnification using 488 nm and 561 nm excitation wavelengths. Quantification of TRPM7 cellular localization was performed under 40X magnification with an inverted fluorescent microscope.

## SECTION IV: AUTOPHOSPHORYLATION-DEPENDENT INTERACTION WITH 14-3-3 $\theta$ REGULATES TRPM7 CELLULAR LOCALIZATION

### 4.1 Constructs

14-3-3 $\theta$  cDNA was amplified by PCR using mouse brain RNA after reverse transcription with the following primer pair: 5'- ATGGAGAAGACCGAGCTGATCCAG-3' and 5'- TTAGTTTTTCGGCCCCCTCTGCTG-3'. The open reading frame of 14-3-3 $\theta$  was then cloned into the pGEX-6P3 vector into the BamHI and EcoRI sites using primers 5'- CATCATGGATTCATGGAGAAGACCGAGCTGATCCAG-3' and 5'- CATCATGAATTCTTAGTTTTTCGGCCCCCTCTGCTG-3' to make a pGEX-14-3-3 $\theta$  construct. The open reading frame of 14-3-3 $\theta$  was also cloned into the HindIII and BamHI sites of pcDNA6-V5-HisB vector containing the FLAG epitope (pcDNA6-FLAG) using primers 5'- CATCATAAGCTTATGGAGAAGACCGAGCTGATCCAG-3' and 5'- CATCATGGATCCTTAGTTTTTCGGCCCCCTCTGCTG-3' to make a pcDNA6-FLAG-14-3-3 $\theta$  construct. The 14-3-3 $\theta$ -K49E binding-deficient mutant was created using the site-directed mutagenesis system (QuickChange, Stratagene, CA). cDNAs encoding various 14-3-3 isoforms were acquired from Addgene: GST-14-3-3wt(pGEX) (14-3-3 $\zeta$ , item #1944) (79), pGEX-2TK 14-3-3 sigma GST (14-3-3 $\sigma$ , item #11944), pGEX-2TK-14-3-3beta GST (14-3-3 $\beta$ , item #13276), pGEX-2TK-14-3-3 eta-GST (14-3-3 $\eta$ , item #13277), pGEX-4T1-14-3-3gamma GST (14-3-3 $\gamma$ , item #13280), and pGEX-4T1-epsilon-GST (14-3-3 $\epsilon$ , item #13279) (80).

#### 4.2 GST-14-3-30 pulldown assays

To purify GST-tagged proteins, GST-14-3-3 fusion proteins were expressed in transformed BL21-DE3 cells (Stratagene, CA). Bacteria in 200 mL cultures were grown at 37°C to OD600 of 0.6-0.8 and induced overnight with 1 mM IPTG (Gold Biotechnology, MO). Bacterial cells were lysed by sonication in 20 mL of ice-cold PBS containing 1% Triton-X100 and protease inhibitor PMSF (Sigma-Aldrich, MO). The bacterial cell lysates were then incubated with 1 mL glutathione agarose (Sigma-Aldrich, MO) overnight at 4°C with rotation. The glutathione agarose beads bound with GST-tagged proteins were washed with 50 mL PBST three times by rotation. Protein concentrations of GST pulldown samples were measured on Coomassie stained SDS-PAGE gel using serial diluted BSA proteins (0.5 - 5 µg) as controls.

For GST pulldown assays, 10 µg of HA-TRPM7 or GFP-TRPM7-Cterm plasmids were transiently transfected in 293T cells in 10 cm dish for 24 h. Cells were lysed in 1 mL mild lysis buffer containing protease inhibitor cocktail (Roche Life Sciences, IN) and phosphatase inhibitor cocktail (EMD Millipore, Germany). Cell lysate supernatants were collected after spinning down lysed cell at 14,000g for 10 min at 4°C, and pulled down by 20 µg of GST-14-3-30 proteins or GST proteins bound on glutathione agarose overnight at 4°C with rotation. The bound proteins were washed with 1 mL PBST three times by rotation, and eluted into 50 µl SDS sample buffer. Lysates input (20 µl) and pulldown samples were separated on SDS-PAGE gels and analyzed by immunoblotting. The rat monoclonal anti-HA (3F10, Roche) and a mouse monoclonal anti-GFP antibody (sc-9996; Santa Cruz Biotechnology, CA) were used to probe HA-TRPM7 and GFP-TRPM7-Cterm proteins respectively. GST-14-3-30 and GST proteins were visualized by SDS-PAGE and

Coomassie staining. For experiments where protein dephosphorylation was conducted, a Lambda Phosphatase (New England Biolabs, MA) was added to the lysis buffer in the absence of the phosphatase inhibitor.

#### **4.3 TRPM7 and 14-3-30 co-immunoprecipitation**

Approximately  $1.0 \times 10^6$  HEK-293T cells were seeded onto 60 mm dish. Two-and-half  $\mu\text{g}$  of HA-TRPM7-WT/K1636R plasmids were co-transfected with 1  $\mu\text{g}$  of FLAG-14-3-3 in the cells the next day. After 48 h of expression, cell lysates were collected in 1 mL mild lysis buffer containing protease inhibitor cocktail (Roche Life Sciences, IN) and phosphatase inhibitor cocktail (EMD Millipore, Germany), immunoprecipitated by 20  $\mu\text{l}$  HA-agarose (Sigma-Aldrich, MO) overnight at 4°C. Lysates input (20  $\mu\text{l}$ ) and IP samples were separated on SDS-PAGE gels and analyzed by immunoblotting. The rabbit polyclonal anti-TRPM7 antibody was used to detect HA-TRPM7, and a mouse anti-FLAG antibody was used to detect FLAG-14-3-30.

#### **4.4 Detection of *in vivo* 14-3-30 binding motifs on TRPM7**

HEK-293T cells in 60 mm dish were transfected with 3  $\mu\text{g}$  of HA-TRPM7-WT and mutants plasmids. After 24 h of expression, cells were lysed in 1 mL lysis buffer containing protease inhibitor cocktail (Roche Life Sciences, IN) and phosphatase inhibitor cocktail (EMD Millipore, Germany), and immunoprecipitated by 20  $\mu\text{l}$  HA-agarose (Sigma-Aldrich, MO) overnight at 4°C. TRPM7 proteins from the IP were separated on SDS-PAGE gels and analyzed by immunoblotting. The *in vivo* 14-3-3 binding motifs were detected with a mouse monoclonal Phospho-(Ser)-14-3-3 Binding Motif (4E2) antibody (item #9606; Cell

Signaling Technology, MA). The total amounts of TRPM7 proteins in the IP samples were detected by a rat anti-HA antibody (3F10; Roche Life Science, IN).

#### **4.5 *In vitro* kinase assay to assess the effect of 14-3-30 binding to TRPM7**

HA-TRPM7 and GFP-TRPM7-Cterm proteins were transiently expressed in HEK-293T cells and immunoprecipitated by HA-agarose (Sigma-Aldrich, MO) and streptavidin agarose (Stratagene, CA). To test the effect of 14-3-30 binding on the catalytic activity of HA-TRPM7 and GFP-TRPM7-Cterm, 5  $\mu$ g of glutathione-eluted GST or GST-14-3-30 proteins were added into the reaction in kinase buffer containing 50 mM MOPS (pH 7.2), 100 mM NaCl, 2.5 mM MnCl<sub>2</sub>, and 0.5 mM ATP. The kinase reactions were performed at 30°C for 2 min in the presence of 4  $\mu$ Ci of [ $\gamma$ -<sup>32</sup>P]ATP with 5  $\mu$ g of MBP as a substrate. To test the catalytic activity of HA-TRPM7-WT and 14-3-30 binding-deficient mutant, the kinase assays were performed at 30°C for 20 min. Reactions were stopped by the addition of SDS sample buffer and proteins in the reaction mix were resolved by SDS-PAGE. Proteins were detected by Coomassie blue staining and gels were dried completely using a gel dryer (Bio-Rad, CA). Incorporation of [ $\gamma$ -<sup>32</sup>P]ATP into substrates was analyzed by autoradiography using Cyclone Plus Phosphor Imager (PerkinElmer, CT).

## EXPERIMENTAL RESULTS

### SECTION I: MASS SPECTROMETRIC ANALYSIS OF TRPM7 AND TRPM6 *IN VIVO* PHOSPHORYLATION

#### 1.1 Identification of *in vivo* autophosphorylation sites on full-length TRPM7

A number of TRPM7 phosphorylation sites have been identified by other research groups using MS analysis. As technological advances have improved the sensitivity for identifying phosphorylation sites on proteins, we were motivated to discover *in vivo* TRPM7 sites that may have been missed in previous analysis of TRPM7, as well as to identify phosphorylation sites on TRPM6, whose phosphorylation has not yet been systematically investigated.

We employed liquid chromatography tandem mass spectrometry (LC-MS/MS) to identify residues phosphorylated on TRPM7 *in vivo* when the protein was expressed in mammalian cells (Figure 2A). We first purified wild-type (WT) HA-tagged mouse TRPM7 (HA-TRPM7) or a kinase-inactive mutant (HA-TRPM7-K1646R) transiently expressed in HEK-293T cells. The kinase activities of purified proteins were tested *in vitro* via kinase assays using MBP as a substrate (Figure 2B). Our MS analysis identified a total of twenty-three phosphorylated serine/threonine residues on the full-length TRPM7, among which fifteen were exclusive to the WT kinase and nine were also found on the kinase-inactive mutant (Figure 2C). By comparing the relative abundance of each of the phosphopeptides on the MS/MS spectra, we identified S1567 as the major phosphorylation site on the overexpressed TRPM7 (Table 1).

We previously showed that overexpressing HA-TRPM7 in HEK-293T cells could lead to successful localization of the channel to the cell surface, but also leave behind many overexpressed proteins in the endoplasmic reticulum (ER) (20,76). We were, therefore, concerned that phosphorylation events that occur at the plasma membrane could potentially be underrepresented in our sample. To obtain a more physiologically representative analysis of the phosphorylation state of TRPM7 *in vivo*, we employed a tetracycline-inducible HEK-293-TRPM7 cell line created by Nadler and colleagues (1). In this cell line, constitutively expressed FLAG-tagged mouse TRPM7 (FLAG-TRPM7) can be detected in the absence of tetracycline (Figure 2D), with the added benefit that the cells are not stressed and are in equilibrium with a modestly high expression of TRPM7. LC-MS/MS analysis identified a more selective twenty phosphorylation sites on the constitutively expressed TRPM7 (Figure 2C). Under this condition, residue S1360 was recognized as the most frequently phosphorylated site (Table 2).

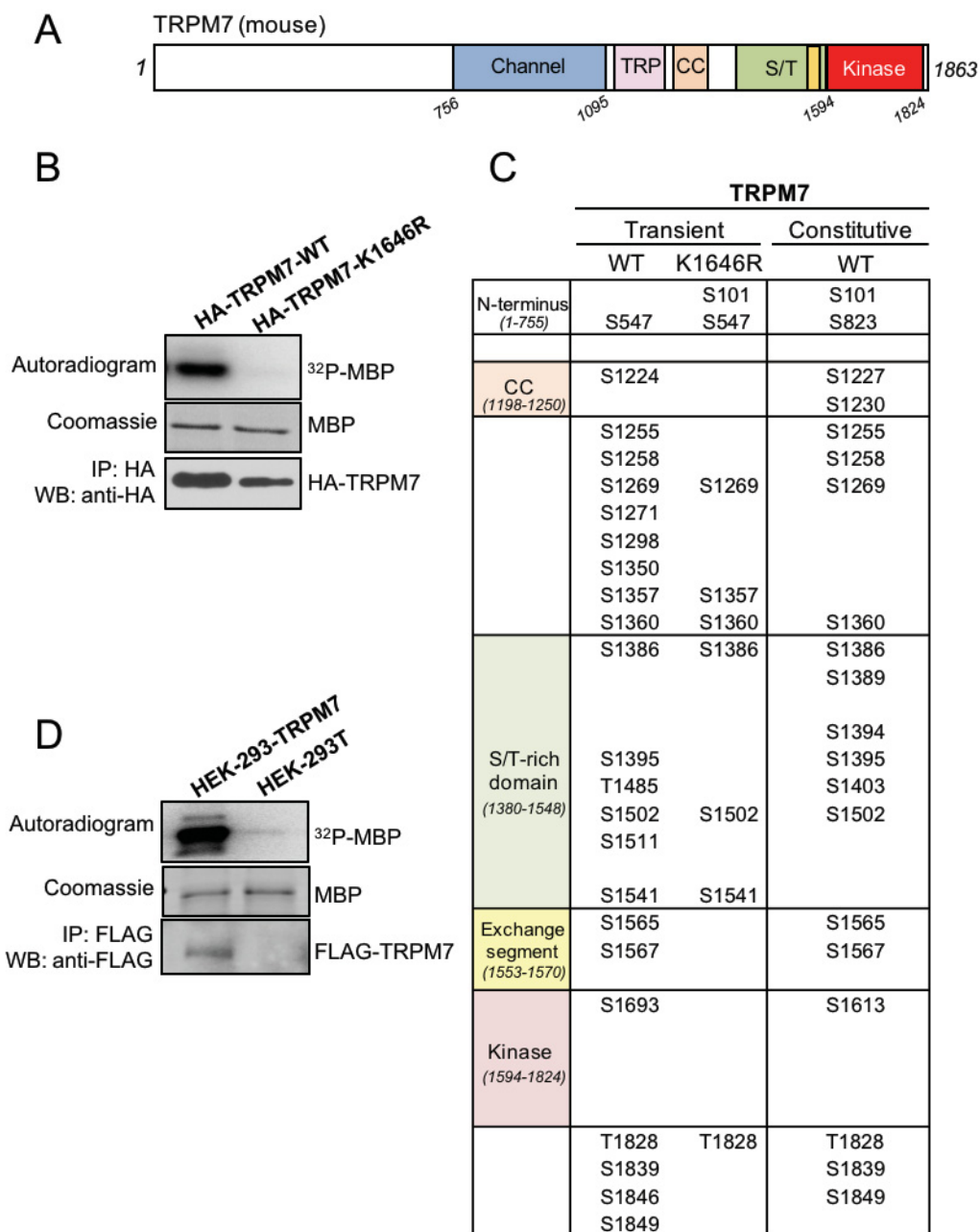


**Figure 2. Identification of *in vivo* phosphorylation sites on full length TRPM7.**

(A) A schematic diagram showing the domain organization of mouse TRPM7. Between the ion channel and the functional alpha-kinase domain there resides a conserved TRP box (TRP), a coiled-coil domain (CC), a serine/threonine-rich domain (S/T), and an exchange-segment of the kinase lighted in yellow. (B) The kinase activities of overexpressed HA-

TRPM7-WT and HA-TRPM7-K1646R were assessed with *in vitro* kinase assays using MBP as a substrate. **(C)** Summary of phosphorylation residues identified on the full-length TRPM7. **(D)** FLAG-mTRPM7 was immuno-purified from constitutively expressing HEK-293-TRPM7 cells. *In vitro* kinase assay confirmed the kinase activity of the protein.

**Table 1.** Phosphopeptides identified from tryptic digestions of HA-mTRPM7-WT and K1646R overexpressed in HEK-203T cells.

HA-mTRPM7 Phosphorylation				#PSMs	
Positions in Master Proteins	Sequence	Modifications	Phosphorylation in Master Proteins	WT	K1646R
Q923J1 [83-105]	HTEQSPTDAYGVINFGGSHSYR	S101+Phospho;	S101		1
Q923J1 [547-560]	SGRNTSSSTPQLRK	N550+Deamidated; S547+Phospho;	S547	1	1
Q923J1 [1224-1247]	SLQSLDSQIGHLQDLSALTVDTLK	S1224+Phospho;	S1224	1	
Q923J1 [1248-1259]	TLTAQKASEASK	S1255+Phospho;	S1255	1	
Q923J1 [1248-1266]	TLTAQKASEASKVHNEITR	S1255+Phospho;	S1255	2	
Q923J1 [1254-1266]	ASEASKVHNEITR	S1258+Phospho;	S1258	1	
Q923J1 [1267-1289]	ELSISKHLAQNLIIDVVPVRPLWK	S1269+Phospho;	S1269	3	1
Q923J1 [1267-1289]	ELSISKHLAQNLIIDVVPVRPLWK	S1271+Phospho;	S1271	1	
Q923J1 [1290-1306]	KPSAVNTLSSSLPQGDR	S1298+Phospho;	S1298	3	
Q923J1 [1340-1365]	KEFNIPEAGSSCGALFPSAVSPPELR	C1351+Carbamidomethyl; S1360+Phospho;	S1360	1	
Q923J1 [1341-1365]	EFNIPEAGSSCGALFPSAVSPPELR	C1351+Carbamidomethyl; S1360+Phospho;	S1360	3	2
Q923J1 [1350-1365]	SCGALFPSAVSPPELR	C1351+Carbamidomethyl; S1350+Phospho;	S1350	1	
Q923J1 [1351-1365]	CGALFPSAVSPPELR	C1351+Carbamidomethyl; S1357+Phospho;	S1357	4	1
Q923J1 [1383-1399]	LGSSPNSSPHMSSPPTK	M1393+Oxidation; S1395+Phospho;	S1395	1	
Q923J1 [1383-1399]	LGSSPNSSPHMSSPPTK	S1386+Phospho;	S1386	1	1
Q923J1 [1485-1498]	TSTSLHSVQESCSR	C1496+Carbamidomethyl; T1485+Phospho;	T1485	1	
Q923J1 [1500-1512]	RASTEDSPEVDSK	S1502+Phospho;	S1502	1	1
Q923J1 [1500-1521]	RASTEDSPEVDSKAALLPDWLR	S1511+Phospho;	S1511	1	
Q923J1 [1528-1558]	EMPSEGGTLNGLASPFKPVLDNTYYSAVER	M1529+Oxidation; S1541+Phospho;	S1541	1	1
Q923J1 [1564-1576]	LSQSIPFVPPVPPR	S1565+Phospho;	S1565	3	
Q923J1 [1564-1576]	LSQSIPFVPPVPPR	S1567+Phospho;	S1567	27	
Q923J1 [1564-1584]	LSQSIPFVPPVPPRGEVTVYR	S1567+Phospho;	S1567	6	
Q923J1 [1693-1699]	SIPYSR	S1693+Phospho;	S1693	1	
Q923J1 [1825-1851]	NDYTPDKIIFPQDESSDLNLQSGNSTK	S1839+Phospho;	S1839	1	
Q923J1 [1825-1851]	NDYTPDKIIFPQDESSDLNLQSGNSTK	T1828+Phospho;	T1828	1	1
Q923J1 [1825-1860]	NDYTPDKIIFPQDESSDLNLQSGNSTKESEAT	S1846+Phospho;	S1846	1	
Q923J1 [1825-1860]	IIFPQDESSDLNLQSGNSTKESEATNSVR	S1849+Phospho;	S1849	1	

**Table 2.** Phosphopeptides identified from tryptic digestions of FLAG-mTRPM7 constitutively expressed in HEK-293-TRPM7 cells.

FLAG-mTRPM7 Phosphorylation				
Positions in Master Proteins	Sequence	Modifications	Phosphorylation in Master Proteins	# PSMs
Q923J1 [83-105]	HTEQSPDAYGVINFQGGSHSYR	S101+Phospho	S101	4
Q923J1 [820-835]	ILDSSDGKNEMEIHK	S823+Phospho;	S823	1
Q923J1 [1224-1247]	SLQSLDSQIGHLQDLSALTVDLTK	Q1236+Deamidated; S1227+Phospho;	S1227	1
Q923J1 [1224-1247]	SLQSLDSQIGHLQDLSALTVDLTK	S1230+Phospho;	S1230	1
Q96QT4 [1248-1259]	TLTAQKASEASK	S1255+Phospho	S1255	1
Q923J1 [1248-1266]	TLTAQKASEASKVHNEITR	S1255+Phospho;	S1255	1
Q923J1 [1254-1266]	ASEASKVHNEITR	S1255+Phospho; S1258+Phospho;	S1255/S1258	1
Q923J1 [1267-1289]	ELSIKHLAQNLIIDVPPRPLWK	S1269+Phospho;	S1269	1
Q923J1 [1341-1365]	EFNIPEAGSSCGALFPSAVSPPELR	C1351+Carbamidomethyl; S1360+Phospho;	S1360	11
Q923J1 [1383-1399]	LGSSPNSSPHMSSPPTK	S1386+Phospho;	S1386	1
Q923J1 [1383-1399]	LGSSPNSSPHMSSPPTK	S1389+Phospho;	S1389	2
Q923J1 [1383-1399]	LGSSPNSSPHMSSPPTK	S1394+Phospho;	S1394	1
Q923J1 [1383-1399]	LGSSPNSSPHMSSPPTK	S1395+Phospho;	S1395	2
Q923J1 [1383-1399]	LGSSPNSSPHMSSPPTK	M1393+Oxidation; S1386+Phospho;	S1386	2
Q923J1 [1383-1399]	LGSSPNSSPHMSSPPTK	M1393+Oxidation; S1389+Phospho;	S1389	1
Q923J1 [1383-1399]	LGSSPNSSPHMSSPPTK	M1393+Oxidation; S1394+Phospho;	S1394	1
Q923J1 [1383-1399]	LGSSPNSSPHMSSPPTK	M1393+Oxidation; S1395+Phospho;	S1395	1
Q923J1 [1400-1411]	FSVSTPSQPSCCK	C1410+Carbamidomethyl; S1403+Phospho;	S1403	1
Q923J1 [1500-1512]	RASTEDSPEVDSK	S1502+Phospho;	S1502	2
Q923J1 [1564-1576]	LSQSIPIFVPVPPR	S1565+Phospho;	S1565	1
Q923J1 [1564-1576]	LSQSIPIFVPVPPR	S1567+Phospho;	S1567	5
Q923J1 [1564-1584]	LSQSIPIFVPVPPRGEVTVYR	S1567+Phospho;	S1567	1
Q923J1 [1609-1622]	IEFLSKEEMGGGLR	S1613+Phospho;	S1613	1
Q923J1 [1824-1851]	RNDYTPDKIIFPQDESSDLNLQSGNSTK	T1828+Phospho;	T1828	1
Q923J1 [1825-1860]	IIFPQDESSDLNLQSGNSTKESEATNSVR	S1839+Phospho;	S1839	2
Q923J1 [1825-1860]	NDYTPDKIIFPQDESSDLNLQSGNSTKESEATNSVR	Q1836+Deamidated; S1839+Phospho;	S1839	1
Q923J1 [1825-1860]	IIFPQDESSDLNLQSGNSTKESEATNSVR	S1839+Phospho; S1840+Phospho;	S1839/S1840	1
Q923J1 [1825-1860]	IIFPQDESSDLNLQSGNSTKESEATNSVR	S1849+Phospho;	S1849	1

## 1.2 Identification of *in vivo* autophosphorylation sites on TRPM7 COOH terminus

Recently, TRPM7 has been reported to be subject to proteolytic cleavage at its COOH terminus, releasing fragments containing the catalytically active kinase (50). We thus undertook an analysis of the phosphorylation pattern of the COOH-terminal fragment of TRPM7 (Figure 3A). We employed a construct where the COOH-terminal fragment of mouse TRPM7 (a.a. 1120–1863) was fused to a multifunctional GFP-tag containing a streptavidin binding protein motif (GFP-TRPM7-Cterm) (Figure 3B). When GFP-TRPM7-Cterm is transiently expressed in HEK-293T cells, it is localized to the cytoplasm (76). LC-MS/MS analysis of purified GFP-TRPM7-Cterm WT and GFP-TRPM7-Cterm-K1646R revealed a total of twelve phosphorylation sites, with eight of them exclusive to the WT kinase (Figure 3C and Table 3).

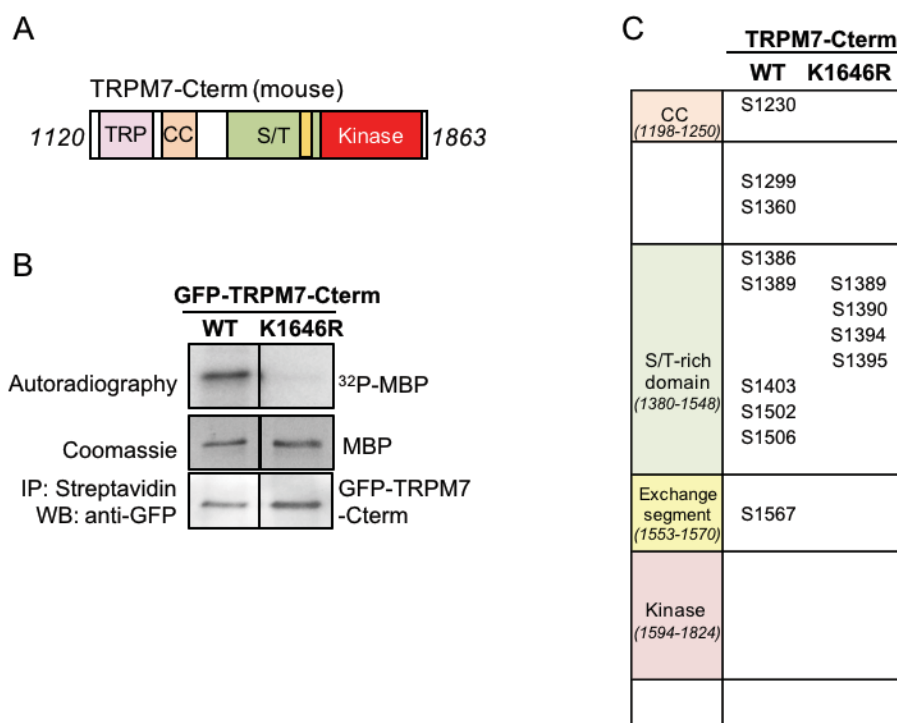


**Figure 3. Identification of *in vivo* phosphorylation on a kinase-containing TRPM7-Cterm protein.**

(A) A schematic diagram showing the domain organization of mouse TRPM7-Cterm protein. (B) The kinase activities of overexpressed GFP-TRPM7-Cterm-WT and GFP-TRPM7-Cterm-K1646R were assessed with *in vitro* kinase assays using MBP as a substrate. (C) Summary of identified phosphorylation residues on TRPM7-Cterm proteins.

**Table 3.** Phosphopeptides identified from tryptic digestions of GFP-mTRPM7-Cterm-WT and K1646R overexpressed in HEK-293T cells.

GFP-mTRPM7-Cterm Phosphorylation				#PSMs	
Positions in Master Proteins	Sequence	Modifications	Phosphorylation in Master Proteins	WT	K1646R
Q923J1 [1224-1147]	SLQSLDSQIGHLQDLSALTVDLTK	S1230+Phospho;	S1230	1	
Q923J1 [1290-1306]	KPSAVNTLSSSLPQGDR	S1299+Phospho;	S1299	1	
Q923J1 [1341-1365]	EFNIPEAGSSCGALFPSAVSPPELR	C1351+Carbamidomethyl; S1360+Phospho;	S1360	1	
Q923J1 [1383-1399]	LGSSPNSSPHMSSPPTK	M1393+Oxidation; S1386+Phospho;	S1386	2	
Q923J1 [1383-1399]	LGSSPNSSPHMSSPPTK	M1393+Oxidation; S1389+Phospho;	S1389	1	
Q923J1 [1383-1399]	LGSSPNSSPHMSSPPTK	M1393+Oxidation; S1390+Phospho;	S1390		1
Q923J1 [1383-1399]	LGSSPNSSPHMSSPPTK	M1393+Oxidation; S1395+Phospho;	S1395		1
Q923J1 [1383-1399]	LGSSPNSSPHMSSPPTK	S1389+Phospho;	S1389	4	1
Q923J1 [1383-1399]	LGSSPNSSPHMSSPPTK	S1394+Phospho;	S1394		2
Q923J1 [1400-1411]	FSVSTPSQPSCK	C1410+Carbamidomethyl; S1403+Phospho;	S1403	2	
Q923J1 [1500-1512]	RASTEDSPEVDSK	S1502+Phospho;	S1502	5	
Q923J1 [1500-1521]	ASTEDSPEVDSKAALLPDWLR	S1506+Phospho;	S1506	1	
Q923J1 [1564-1576]	LSQSIPFVPPR	S1567+Phospho;	S1567	10	

### 1.3 Identification of *in vivo* TRPM7 transphosphorylation sites introduced by TRPM6

It has been reported that TRPM7 can be phosphorylated by TRPM6 and that the phosphorylation events may be important for intracellular trafficking of TRPM7 (63,64). To identify potential transphosphorylation sites on TRPM7 introduced by TRPM6, we employed a kinase-inactive mouse TRPM7 mutant tagged with streptavidin binding protein (SBP-TRPM7-K1646R) to be expressed alone or co-expressed with wild-type HA-tagged human TRPM6 (HA-hTRPM6) in HEK-293T cells. *In vitro* kinase assays verified that SBP-TRPM7-K1646R is indeed catalytically inactive (Figure 4B). A co-immunoprecipitation assay confirmed that TRPM6 and TRPM7-K1646R assemble into a complex when co-expressed in HEK-293T cells (Figure 4C). The MS analysis uncovered a large number of transphosphorylation sites on the kinase-inactive TRPM7 that were introduced by co-expressed TRPM6. Seven transphosphorylation residues found on the kinase-inactive TRPM7 were previously identified as TRPM7 autophosphorylation sites (TRPM7 S1224, S1255, S1299, S1403, S1565, S1567, and S1693) (Figure 4D). In this analysis, S1255 and S1567 were the two most prominently transphosphorylated sites (Table 4).

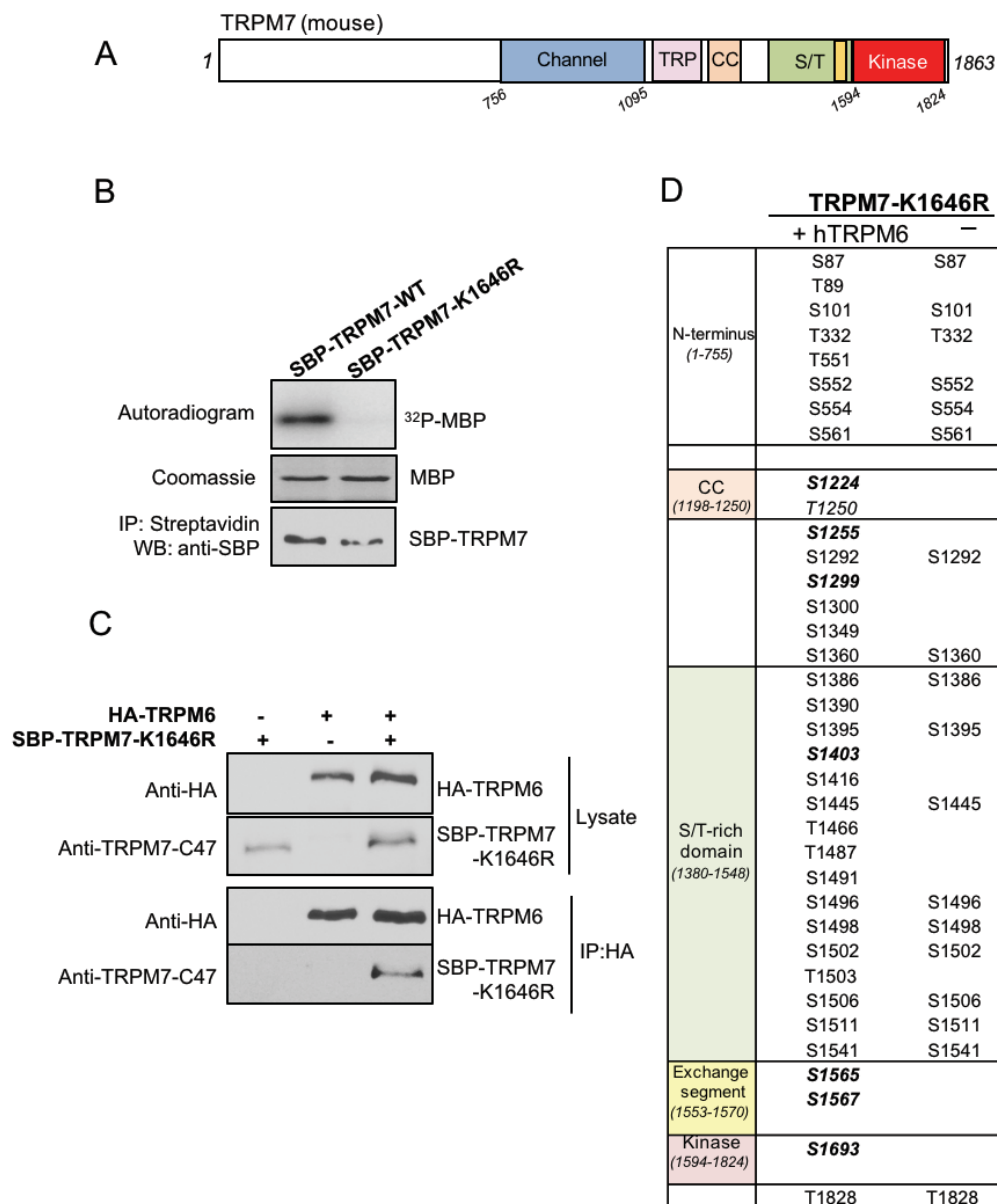


**Figure 4. Identification of *in vivo* transphosphorylation sites on mTRPM7 introduced by hTRPM6.**

(A) A schematic diagram showing the domain organization of mouse TRPM7. (B) *In vitro* kinase assays confirmed that the SBP-TRPM7-WT-K1646R protein was devoid of kinase activity. (C) A kinase-inactive SBP-TRPM7-K1646R was co-expressed with HA-hTRPM6 in HEK-293T cells and pulled down by HA-agarose. Co-immunoprecipitation assay confirmed the heteromeric TRPM6/7 complex formation. Proteins in the lysate and the

immunoprecipitated samples were resolved by SDS-PAGE and analyzed by Western blotting. (D) Summary of phosphorylation residues identified on SBP-TRPM7-K1646R when the protein was expressed alone or with HA-hTRPM6. Residues that are both autophosphorylated by TRPM7 and transphosphorylated by TRPM6 are highlighted in bold.

**Table 4.** Phosphopeptides identified from tryptic digestions of SBP-mTRPM7-K1646R.

Cross-phosphorylation of mTRPM7 by hTRPM6			#PSMs	
Positions in Master Proteins	Sequence	Phosphorylation in Master Proteins	Co-expression with HA-hTRPM6	Expressed alone
Q923J1 [83-105]	HTEQSPDAYGVINFGGSHSYR	S87+Phospho;	4	4
Q923J1 [83-105]	HTEQSPDAYGVINFGGSHSYR	T89+Phospho;	1	
Q923J1 [83-105]	HTEQSPDAYGVINFGGSHSYR	S101+Phospho;	7	5
Q923J1 [331-351]	QTEEGGNLPDAAEPDIISTIK	T332+Phospho;	1	1
Q923J1 [550-559]	NTSSSTPQLR	T551+Phospho;	1	
Q923J1 [550-559]	NTSSSTPQLR	S552+Phospho;	2	3
Q923J1 [550-559]	NTSSSTPQLR	S553+Phospho;		1
Q923J1 [550-559]	NTSSSTPQLR	S554+Phospho;	2	
Q923J1 [550-560]	NTSSSTPQLRK	S552+Phospho;	2	4
Q923J1 [550-560]	NTSSSTPQLRK	S554+Phospho;	1	1
Q923J1 [550-568]	NTSSSTPQLRKSHETFGNR	S561+Phospho;	2	2
Q923J1 [780-816]	AEMSHIPQSQDAHQMTEDESENNFHNITEEIPMEVFK	S788+Phospho;		1
Q923J1 [1248-1259]	TLTAQKASEASK	S1255+Phospho;	3	
Q923J1 [1248-1266]	TLTAQKASEASKVHNEITR	T1250+Phospho;	2	
Q923J1 [1248-1266]	TLTAQKASEASKVHNEITR	S1255+Phospho;	10	
Q923J1 [1290-1306]	KPSAVNTLSSSLPQGDR	S1292+Phospho;	1	2
Q923J1 [1290-1306]	KPSAVNTLSSSLPQGDR	S1299+Phospho;	2	
Q923J1 [1290-1306]	KPSAVNTLSSSLPQGDR	S1300+Phospho;	2	
Q923J1 [1341-1365]	EFNIPEAGSSCGALFPSAVSPPELR	S1349+Phospho;	1	
Q923J1 [1340-1365]	KEFNIPEAGSSCGALFPSAVSPPELR	S1360+Phospho;	2	1
Q923J1 [1341-1365]	EFNIPEAGSSCGALFPSAVSPPELR	S1360+Phospho;	7	6
Q923J1 [1383-1399]	LGSSPNSSPHMSSPPTK	S1386+Phospho;		4
Q923J1 [1383-1399]	LGSSPNSSPHMSSPPTK	S1390+Phospho;	1	
Q923J1 [1383-1399]	LGSSPNSSPHMSSPPTK	S1395+Phospho;	9	4
Q923J1 [1383-1411]	LGSSPNSSPHMSSPPTKFSVSTPSQPSCK	S1386+Phospho;	4	4
Q923J1 [1383-1411]	LGSSPNSSPHMSSPPTKFSVSTPSQPSCK	S1390+Phospho;	1	
Q923J1 [1383-1411]	LGSSPNSSPHMSSPPTKFSVSTPSQPSCK	S1395+Phospho;	5	5
Q923J1 [1400-1411]	FSVSTPSQPSCK	S1403+Phospho;	3	
Q923J1 [1412-1427]	SHLESTTKDQEPIFYK	S1416+Phospho;	2	
Q923J1 [1428-1450]	AAEGDNIEFGAFVGHRSMDLQR	S1445+Phospho;	5	1
Q923J1 [1460-1472]	ELLSNDTPENTLK	T1466+Phospho;	2	
Q923J1 [1485-1498]	TSTSLHSVQESCSR	T1487+Phospho;	4	
Q923J1 [1485-1498]	TSTSLHSVQESCSR	S1495+Phospho;		1
Q923J1 [1485-1512]	TSTSLHSVQESCSRRASTEDSPEVDSK	S1491+Phospho; S1495+Phospho;	1	
Q923J1 [1485-1512]	TSTSLHSVQESCSRRASTEDSPEVDSK	S1495+Phospho; S1497+Phospho;	1	2
Q923J1 [1500-1512]	RASTEDSPEVDSK	S1502+Phospho;	7	9
Q923J1 [1500-1512]	RASTEDSPEVDSK	S1506+Phospho;	4	2
Q923J1 [1501-1512]	ASTEDSPEVDSK	S1506+Phospho;	1	2
Q923J1 [1501-1521]	ASTEDSPEVDSKAALLPDWLR	S1502+Phospho; S1506+Phospho;	1	
Q923J1 [1500-1521]	RASTEDSPEVDSKAALLPDWLR	S1502+Phospho; S1506+Phospho; T1503+Phospho;	2	
Q923J1 [1500-1521]	RASTEDSPEVDSKAALLPDWLR	S1502+Phospho; S1511+Phospho;	2	
Q923J1 [1501-1521]	ASTEDSPEVDSKAALLPDWLR	S1506+Phospho;	2	1
Q923J1 [1500-1521]	RASTEDSPEVDSKAALLPDWLR	S1506+Phospho; S1511+Phospho;	1	
Q923J1 [1501-1521]	ASTEDSPEVDSKAALLPDWLR	S1511+Phospho;		1
Q923J1 [1528-1558]	EMPSGEGTGLASPFKVLDTNYYSAVER	S1541+Phospho;	3	3
Q923J1 [1564-1576]	LSQSIPFVPPVPR	S1567+Phospho;	15	
Q923J1 [1564-1584]	LSQSIPFVPPVPRGEPVTVYR	S1565+Phospho;	3	
Q923J1 [1564-1584]	LSQSIPFVPPVPRGEPVTVYR	S1567+Phospho;	4	1
Q923J1 [1693-1699]	SIPYSPR	S1693+Phospho;	1	
Q923J1 [1825-1851]	NDYTPDKIIFPQDESSDLNLQSGNSTK	S1839+Phospho;		1
Q923J1 [1824-1851]	RNDYTPDKIIFPQDESSDLNLQSGNSTK	T1828+Phospho;	6	6
Q923J1 [1825-1851]	NDYTPDKIIFPQDESSDLNLQSGNSTK	T1828+Phospho;	3	5

#### 1.4 Identification of *in vivo* TRPM6 phosphorylation sites

To understand how TRPM6 is regulated by autophosphorylation, we analyzed TRPM6 autophosphorylation by expressing HA-hTRPM6 alone in HEK-293T cells (Figure 5A and 5B). Our MS analysis indeed identified a large number of *in vivo* phosphorylation sites on TRPM6, and some of which have analogues on TRPM7 that are also phosphorylated (e.g. TRPM6-S1226, T1724, S1986 versus TRPM7-T1250, S1567, T1828) (Figure 5C). Interestingly, the most prominently phosphorylated residue on TRPM6 S552 was on its NH<sub>2</sub> terminus (Table 5). TRPM7 had been reported to not phosphorylate TRPM6 (63,64). However, by co-expressing a kinase-inactive TRPM6 (TRPM6-K1804R) with a TRPM7-WT (SBP-TRPM7), we identified a weak transphosphorylation of TRPM6 by TRPM7, though not as robust as TRPM6 autophosphorylation (Figure 5D).

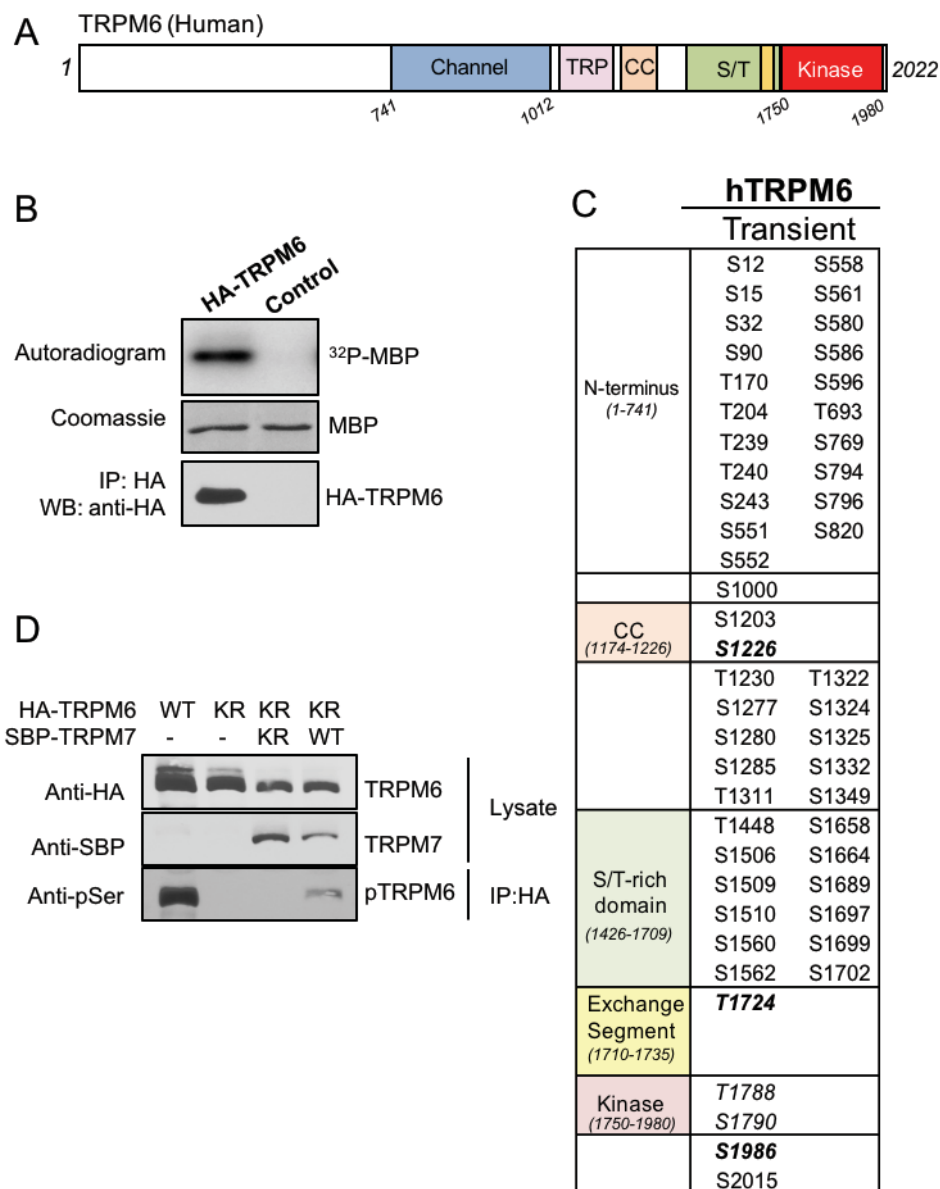


**Figure 5. Identification of *in vivo* phosphorylation sites on full length hTRPM6.**

(A) A schematic diagram showing the domain organization of human TRPM6. (B) The kinase activities of overexpressed HA-hTRPM6 was assessed with *in vitro* kinase assays. (C) Summary of identified phosphorylation residues on transiently expressed TRPM6 from HEK-293T cells. (D) HA-TRPM6-WT and HA-TRPM6-K1804R (KR) were transiently expressed individually or co-expressed with SBP-TRPM7-WT and SBP-TRPM7-K1646R (KR) in HEK-293T cells. TRPM6 is weakly transphosphorylated by TRPM7's kinase *in*

*vivo*. The proteins were immunopurified by HA-agarose. Proteins in the lysates and in the immunoprecipitated samples were resolved by SDS-PAGE. TRPM6 phosphorylation was probed by an anti-Ser antibody.

**Table 5.** Phosphopeptides identified from tryptic digestions of HA-hTRPM6 transiently expressed in HEK-293T cells.

HA-hTRPM6 Phosphorylation			
Positions in Master Protein Sequence	Master Protein Sequence	Phosphorylation in Master Proteins	# PSMs
Q9BX84[10-18]	LQSQKSWIK	S12+Phospho;	3
Q9BX84[10-18]	LQSQKSWIK	S15+Phospho;	1
Q9BX84[25-38]	ECSTIIPSSKNPHR	S32+Phospho;	2
Q9BX84[86-110]	HHTKSPTDTFGTINFQDGEHTTHAK	S90+Phospho;	1
Q9BX84[86-110]	HHTKSPTDTFGTINFQDGEHTTHAK	S90+Phospho;	4
Q9BX84[116-185]	AAETTGAWIITEGINTGVSK	T170+Phospho;	3
Q9BX84[201-217]	KIWTVGIPPWGVIENQR	T204+Phospho;	2
Q9BX84[202-217]	IWTVGIPPWGVIENQR	T204+Phospho;	1
Q9BX84[238-258]	LTTLNSMHSFILSDDGTGK	T239+Phospho;	4
Q9BX84[238-258]	LTTLNSMHSFILSDDGTGK	T240+Phospho;	2
Q9BX84[238-258]	LTTLNSMHSFILSDDGTGK	S243+Phospho;	2
Q9BX84[547-569]	HQRHSSGNRNESAESTLHSQFIR	S551+Phospho;	1
Q9BX84[547-569]	HQRHSSGNRNESAESTLHSQFIR	S551+Phospho; S552+Phospho;	1
Q9BX84[550-569]	HSSGNRNESAESTLHSQFIR	S551+Phospho; S552+Phospho;	2
Q9BX84[547-569]	HQRHSSGNRNESAESTLHSQFIR	S551+Phospho; S558+Phospho;	1
Q9BX84[550-569]	HSSGNRNESAESTLHSQFIR	S552+Phospho;	48
Q9BX84[550-569]	HSSGNRNESAESTLHSQFIR	S558+Phospho;	4
Q9BX84[556-569]	NESAESTLHSQFIR	S558+Phospho;	3
Q9BX84[550-569]	HSSGNRNESAESTLHSQFIR	S561+Phospho;	2
Q9BX84[576-585]	FKEKSIVLHK	S580+Phospho;	1
Q9BX84[580-587]	SIVLHKSR	S586+Phospho;	1
Q9BX84[588-619]	KKSKEQNVSDPESTGFLYPYNDLLVWAVLMK	S596+Phospho;	1
Q9BX84[686-700]	QNERMAMTLTYELR	T693+Phospho;	2
Q9BX84[766-792]	AEMSHVPQSQDFQFMWYSDQNASSSK	S769+Phospho;	3
Q9BX84[793-804]	ESASVKEYDLER	S794+Phospho;	4
Q9BX84[793-804]	ESASVKEYDLER	S796+Phospho;	6
Q9BX84[805-829]	GHDEKLDENQHFGLESQHPWTR	S820+Phospho;	1
Q9BX84[997-1011]	AILSPKEPPWSLAR	S1000+Phospho;	5
Q9BX84[1199-1223]	DSLLSLSQVGHQLDLSALTVDTLK	S1203+Phospho;	1
Q9BX84[1224-1240]	VLSAVDTLQDEALLAK	S1226+Phospho;	3
Q9BX84[1224-1240]	VLSAVDTLQDEALLAK	T1230+Phospho;	1
Q9BX84[1272-1284]	KYQYYSMPSSLLR	S1277+Phospho;	6
Q9BX84[1273-1284]	YQYYSMPSSLLR	S1277+Phospho;	6
Q9BX84[1273-1284]	YQYYSMPSSLLR	S1277+Phospho; S1280+Phospho;	1
Q9BX84[1272-1284]	KYQYYSMPSSLLR	S1280+Phospho;	1
Q9BX84[1273-1284]	YQYYSMPSSLLR	S1280+Phospho;	3
Q9BX84[1285-1294]	SLAGGRHPPR	S1285+Phospho;	3
Q9BX84[1315-1335]	NDQERQETQSSIVVSGVSPNR	S1324+Phospho;	1
Q9BX84[1308-1335]	REATNVRNDQERQETQSSIVVSGVSPNR	S1324+Phospho; T1311+Phospho; T1322+Phospho;	1
Q9BX84[1315-1335]	NDQERQETQSSIVVSGVSPNR	S1325+Phospho;	1
Q9BX84[1315-1335]	NDQERQETQSSIVVSGVSPNR	S1332+Phospho;	6
Q9BX84[1315-1340]	NDQERQETQSSIVVSGVSPNRQAHSK	S1332+Phospho;	2
Q9BX84[1320-1335]	QETQSSIVVSGVSPNR	S1332+Phospho;	10
Q9BX84[1320-1340]	QETQSSIVVSGVSPNRQAHSK	S1332+Phospho;	1
Q9BX84[1341-1352]	YGQFLLVPSNLK	S1349+Phospho;	2
Q9BX84[1341-1353]	YGQFLLVPSNLKR	S1349+Phospho;	1
Q9BX84[1445-1470]	IMQTTGGGVNNAFSEGEDTGVFSIKK	T1448+Phospho;	2
Q9BX84[1506-1531]	SAQSSECSEVGPWLQPNNTSFWINPLR	S1506+Phospho;	1
Q9BX84[1506-1532]	SAQSSECSEVGPWLQPNNTSFWINPLRR	S1506+Phospho;	1
Q9BX84[1506-1531]	SAQSSECSEVGPWLQPNNTSFWINPLR	S1509+Phospho;	1
Q9BX84[1506-1532]	SAQSSECSEVGPWLQPNNTSFWINPLRR	S1509+Phospho;	1
Q9BX84[1506-1532]	SAQSSECSEVGPWLQPNNTSFWINPLRR	S1510+Phospho;	1
Q9BX84[1556-1572]	IKNLGSSSEIGQGAWVK	S1560+Phospho;	3
Q9BX84[1558-1572]	NLSGSSSEIGQGAWVK	S1560+Phospho;	1
Q9BX84[1556-1572]	IKNLGSSSEIGQGAWVK	S1562+Phospho;	1
Q9BX84[1558-1572]	NLSGSSSEIGQGAWVK	S1562+Phospho;	1
Q9BX84[1647-1662]	TKEIGQCAIQISDYLK	S1658+Phospho;	1
Q9BX84[1647-1670]	TKEIGQCAIQISDYLKQSQEDLSK	S1658+Phospho;	2
Q9BX84[1647-1670]	TKEIGQCAIQISDYLKQSQEDLSK	S1664+Phospho;	2
Q9BX84[1649-1670]	EIGQCAIQISDYLKQSQEDLSK	S1664+Phospho;	3
Q9BX84[1684-1695]	NLLKSSIGVDK	S1689+Phospho;	1
Q9BX84[1689-1701]	SSIGVDKISASLK	S1697+Phospho;	1
Q9BX84[1689-1715]	SSIGVDKISASLKSPQEPHHHYSIAIER	S1697+Phospho;	1
Q9BX84[1696-1715]	ISASLKSPQEPHHHYSIAIER	S1699+Phospho;	3
Q9BX84[1696-1715]	ISASLKSPQEPHHHYSIAIER	S1702+Phospho;	3
Q9BX84[1721-1742]	LSQTIPTFPVQLFAGEEITVYR	T1724+Phospho;	3
Q9BX84[1721-1753]	LSQTIPTFPVQLFAGEEITVYRLEESSPLNLDK	T1724+Phospho;	1
Q9BX84[1785-1804]	VVSTWSEDDILKPGQVFVK	T1788+Phospho;	1
Q9BX84[1785-1804]	VVSTWSEDDILKPGQVFVK	S1790+Phospho;	1
Q9BX84[1983-1999]	NDYSPERINSTFGLEIK	S1986+Phospho;	5
Q9BX84[2010-2022]	ETGRNSPEDDMQL	S2015+Phospho;	7

## SECTION II: TRPM7 KINASE ACTIVITY IS REGULATED BY AUTOPHOSPHORYLATION

In section I, we showed that TRPM7 is very robustly phosphorylated *in vivo*. Most of the identified phosphorylation sites are located on the cytosolic COOH terminus, agreeing with the previous report by Kim and colleagues, and new sites are also found on the cytosolic NH<sub>2</sub>-terminal domain. Our analysis also identified phosphorylation sites on the kinase catalytic core domain, though less than the number identified by Clark and colleagues where they used a TRPM7-COOH fragment under ATP stimulation *in vitro* (59). As we hypothesized that TRPM7's kinase activity could be directly regulated by phosphorylation, we therefore adopted an *in vitro* phosphorylation strategy to capture the maximal number of TRPM7 autophosphorylation sites and to investigate more closely the impact of phosphorylation on TRPM7 kinase's catalytic activity.

### 2.1 TRPM7 COOH terminus is heavily phosphorylated *in vitro* under ATP stimulation

To study potential regulatory phosphorylation sites governing the catalytic activity of TRPM7 kinase, we generated a Sumo-tagged TRPM7 kinase construct (Sumo-TRPM7-Kinase) containing the S/T domain and the kinase domain (a.a. 1384-1863) of TRPM7 (Figure 6A). The sumo-TRPM7-kinase was purified from *E. coli* and stimulated with ATP *in vitro* before MS analysis. A catalytically inactive mutant of TRPM7 kinase was also analyzed as a negative control (Figure 6B). *In vitro*, ATP stimulation enriched the number

of autophosphorylation sites identified and in particular, revealed five additional phosphorylation sites within the kinase's catalytic core domain (Figure 6C and Table 6).

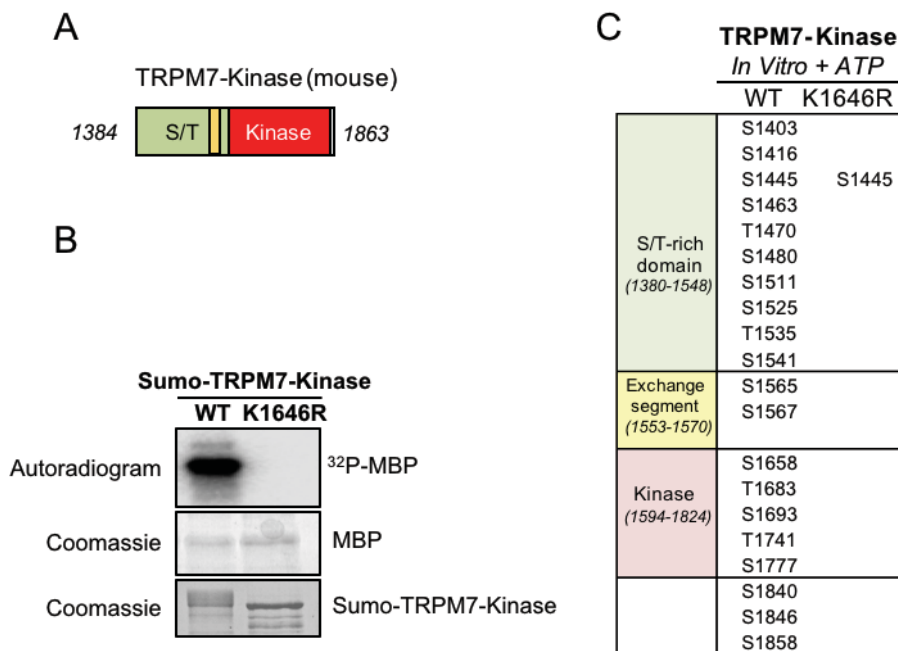


**Figure 6. Identification of *in vitro* phosphorylation sites on TRPM7-kinase**

(A) A schematic diagram showing the structure of a cytosolic fragment of TRPM7 containing the S/T domain and the kinase domain (TRPM7-Kinase). (B) *In vitro* kinase assays assess the kinase activities of Sumo-TRPM7-Kinase-WT and Sumo-TRPM7-Kinase-K1646R using MBP as a substrate. (C) Summary of identified phosphorylation residues on sumo-TRPM7-Kinases.

**Table 6.** Phosphopeptides identified from tryptic digestions of Sumo-mTRPM7-Kinase-WT and K1646R purified from *E. coli* and stimulated with ATP *in vitro*

Sumo-mTRPM7-Kinase Phosphorylation				#PSMs	
Positions in Master Prote Sequence	Modifications	Phosphorylation in Master Proteins	WT	K1646R	
Q923J1 [1400-1411]	FSVSTPSQPSCK	1xCarbamidomethyl; 1xPhospho	S1403	1	
Q923J1 [1400-1411]	FSVSTPSQPSCK	1xCarbamidomethyl; 1xPhospho	S1403	1	
Q923J1 [1412-1427]	SHLESTTKDQEPIFYK	1xPhospho	S1416/S1417/T1418	8	
Q923J1 [1428-1450]	AAEGDNIEFGAFVGHRSMDLQR	1xPhospho	S1445	8	
Q923J1 [1428-1450]	AAEGDNIEFGAFVGHRSMDLQR	1xOxidation; 1xPhospho	S1445	6	
Q923J1 [1428-1450]	AAEGDNIEFGAFVGHRSMDLQR	1xPhospho	S1445	2	2
Q923J1 [1428-1450]	AAEGDNIEFGAFVGHRSMDLQR	1xOxidation; 1xPhospho	S1445	2	2
Q923J1 [1458-1472]	IRELLSNDTPENTLK	1xPhospho	T1470	4	
Q923J1 [1458-1472]	IRELLSNDTPENTLK	1xPhospho	T1470	1	
Q923J1 [1460-1472]	ELLSNDTPENTLK	2xPhospho	S1463; T1470	2	
Q923J1 [1460-1472]	ELLSNDTPENTLK	1xPhospho	T1470	8	
Q923J1 [1460-1472]	ELLSNDTPENTLK	1xPhospho	T1470	3	
Q923J1 [1473-1484]	HVGAAGYSECK	2xCarbamidomethyl; 1xPhospho	S1480	1	
Q923J1 [1500-1512]	RASTEDSPEVDSK	1xPhospho	S1511	3	
Q923J1 [1500-1521]	RASTEDSPEVDSKAALLPDWLR	1xPhospho	S1511	2	
Q923J1 [1500-1521]	RASTEDSPEVDSKAALLPDWLR	1xPhospho	S1511	1	
Q923J1 [1501-1512]	ASTEDSPEVDSK	1xPhospho	S1511	2	
Q923J1 [1501-1512]	ASTEDSPEVDSK	1xPhospho	S1511	1	
Q923J1 [1501-1521]	ASTEDSPEVDSKAALLPDWLR	1xPhospho	S1511	4	
Q923J1 [1501-1521]	ASTEDSPEVDSKAALLPDWLR	1xPhospho	S1511	5	
Q923J1 [1522-1558]	DRPSNREMPSEGGTLNGLASPFKPVLDNTNYYSAVER	1xOxidation; 1xPhospho	S1525	1	
Q923J1 [1528-1558]	EMPSEGGTLNGLASPFKPVLDNTNYYSAVER	1xOxidation; 1xPhospho	S1541	8	
Q923J1 [1528-1558]	EMPSEGGTLNGLASPFKPVLDNTNYYSAVER	1xOxidation; 1xPhospho	T1535	1	
Q923J1 [1564-1576]	LSQSIPIFVPVPPR	1xPhospho	S1565	19	
Q923J1 [1564-1576]	LSQSIPIFVPVPPR	1xPhospho	S1567	8	
Q923J1 [1564-1584]	LSQSIPIFVPVPPRGPVTVYR	1xPhospho	S1567	5	
Q923J1 [1564-1584]	LSQSIPIFVPVPPRGPVTVYR	1xPhospho	S1567	14	
Q923J1 [1647-1671]	SFLPEVINTWSSYKEDTVLHLCRL	1xCarbamidomethyl; 1xPhospho	S1658	3	
Q923J1 [1647-1671]	SFLPEVINTWSSYKEDTVLHLCRL	1xCarbamidomethyl; 1xPhospho	S1658	1	
Q923J1 [1678-1690]	AAQKLTFAFNQMK	1xOxidation; 1xPhospho	T1683	1	
Q923J1 [1678-1692]	AAQKLTFAFNQMKPK	1xOxidation; 1xPhospho	T1683	2	
Q923J1 [1678-1692]	AAQKLTFAFNQMKPK	1xPhospho	T1683	1	
Q923J1 [1678-1692]	AAQKLTFAFNQMKPK	1xOxidation; 1xPhospho	T1683	3	
Q923J1 [1682-1692]	LTFAFNQMKPK	1xPhospho	T1683	1	
Q923J1 [1682-1692]	LTFAFNQMKPK	1xOxidation; 1xPhospho	T1683	2	
Q923J1 [1682-1699]	LTFAFNQMKPKSIPYSPR	1xOxidation; 1xPhospho	S1693	2	
Q923J1 [1728-1758]	YNNNNGDEIIPNTNLEEIMLAFSHWYTYR	1xPhospho	T1741	3	
Q923J1 [1759-1780]	GELLVLDLQGVGENLTDPSVIK	1xPhospho	S1777	5	
Q923J1 [1759-1784]	GELLVLDLQGVGENLTDPSVIKAEK	1xPhospho	S1777	2	
Q923J1 [1759-1784]	GELLVLDLQGVGENLTDPSVIKAEK	1xPhospho	S1777	1	
Q923J1 [1825-1851]	NDYTPDKIIFPQDESSDLNLQSGNSTK	1xPhospho	S1840	8	
Q923J1 [1825-1851]	NDYTPDKIIFPQDESSDLNLQSGNSTK	1xPhospho	S1840	1	
Q923J1 [1832-1851]	IIFPQDESSDLNLQSGNSTK	1xPhospho	S1846	2	
Q923J1 [1852-1860]	ESEATNSVR	1xPhospho	S1858	1	
Q923J1 [1852-1863]	ESEATNSVRLML	1xOxidation; 1xPhospho	S1858	1	
Q923J1 [1852-1863]	ESEATNSVRLML	1xOxidation; 1xPhospho	S1858	3	

## **2.2 TRPM7 kinase activity is affected by phosphorylation of residues located in the kinase catalytic domain**

To assess the importance of the phosphorylated residues on TRPM7 kinase domain to its catalytic activity we conducted a mutagenesis screen. The five autophosphorylated sites identified on the Sumo-TRPM7-Kinase (S1658, T1683, S1693, T1741, and S1777), S1613, which was discovered on the constitutively expressed FLAG-TRPM7, and S1596, a phosphorylated residue identified in a previous study (59) were mutated to either non-phosphorylatable alanine or the phosphomimetic residue aspartate (Figure 7).

The catalytic activity of WT and mutants were then tested using *in vitro* kinase assays. Our screen identified two autophosphorylation sites, S1596 and S1777, on the kinase catalytic core domain that influenced catalytic activity. We found that substitution at S1596 either to alanine or aspartate compromised catalytic activity (Figure 8A and 8B). Close examination of the kinase structure reveals that S1596 is located on an omega-loop between the  $\beta 2$  and  $\beta 3$  strand, with its side-chain hydroxyl group forming hydrogen bonds with S1588 and E1587 (66) (Figure 8B). Omega-loops are hydrogen bond-rich secondary structures that are often found on the surface of globular proteins and involved in protein folding and stability (81). Substitution of residues at this site likely affected the structural stability of kinase, compromising catalytic activity as a result. Substitution of alanine or aspartate at the five other serine and threonine residues (S1613, S1658, T1683, S1693, and T1741) did not cause a significant change in the catalytic activity. An examination of the kinase structure showed that these five serine and threonine residues are exposed at the protein's surface (Figure 8D), suggesting that substitutions at this site did not cause

structural disruption and that these residues likely do not function as regulatory sites for the kinase.

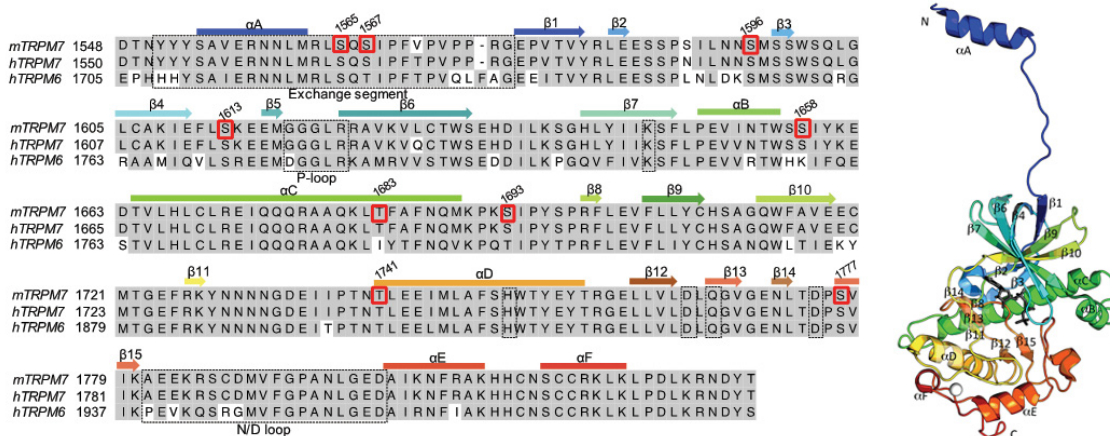


**Figure 7. Mutagenesis screen of TRPM7 kinase domain phosphorylation sites.**

Sequence alignment of mouse TRPM7, human TRPM7, and human TRPM6 (UniProtKB: Q923J1, Q96QT4, and Q9BX84). The position of  $\alpha$  helices (boxes) and  $\beta$  strands (arrows) are shown above the alignment. Functionally important motifs and residues on the mouse TRPM7 sequence are shown in dashed boxes. Seven identified autophosphorylation residues on the mouse TRPM7 sequence are shown in red boxes. On the right, a ribbon diagram depicts the structure of mouse TRPM7 kinase domain (PDB code 1IA9 (66)). The AMPPNP is rendered as gray sticks and the zinc atom as a white sphere. The N and C termini are indicated as "N" and "C".

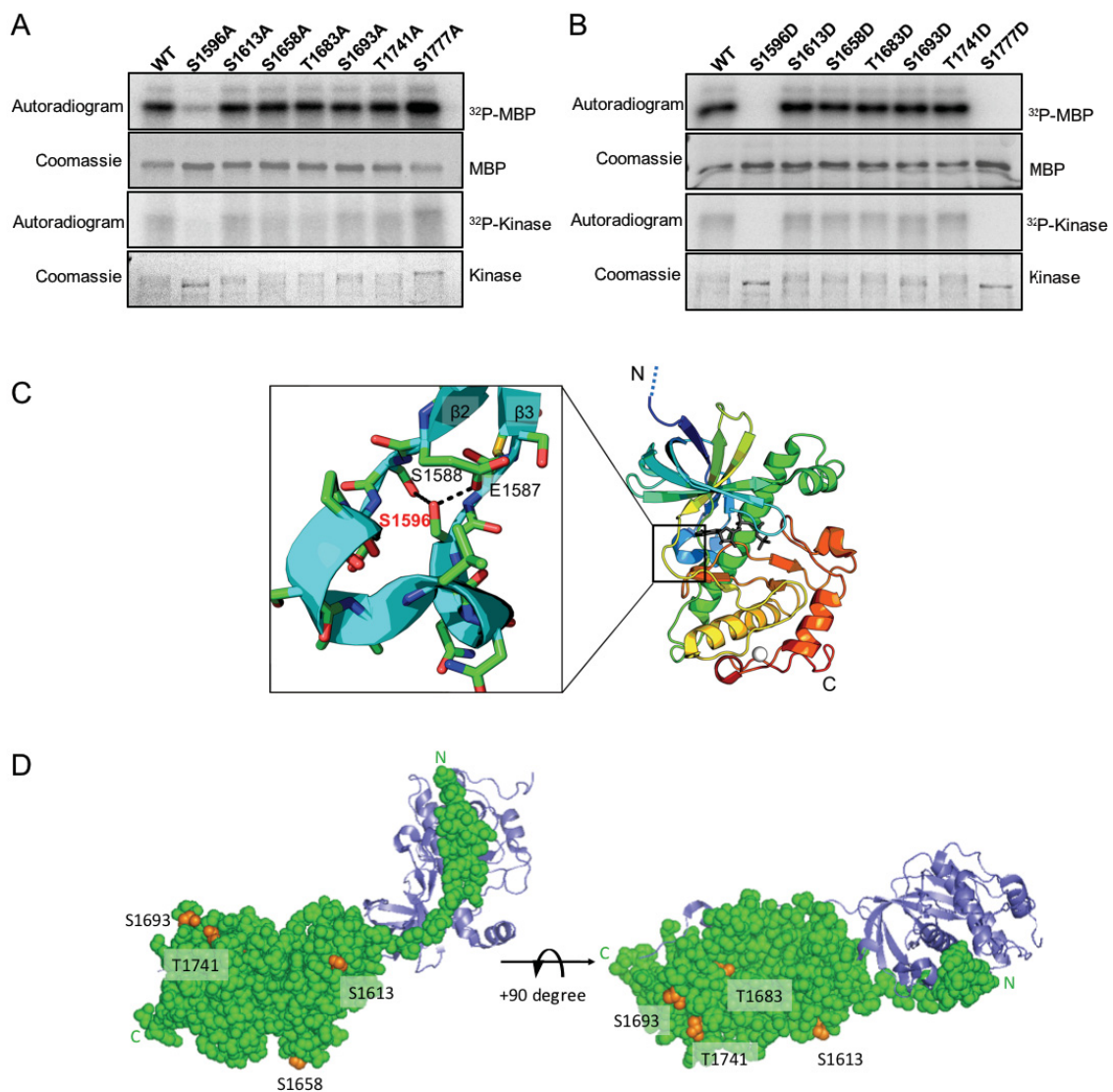


**Figure 8. Mutations of residues in the kinase domain leads to TRPM7 kinase inactivation.**

**(A)** and **(B)** Catalytic activities of the Sumo-TRPM7-Kinase WT and mutants WT and mutant kinases were assessed in *in vitro* kinase assays using MBP as a substrate. **(C)** The expanded view on the left highlights the location of residue S1596 on an omega-loop between the  $\beta 2$  and  $\beta 3$  strands of the kinase domain. Side chains of residues are shown as sticks. Interactions between residues S1596, S1588 and E1587 are indicated with dashed lines.

Ribbon diagram on the right shows the structure the core catalytic domain (a.a. 1575–1828) of mouse TRPM7 kinase (PDB code 1IA9). The AMPPNP is rendered as gray sticks and the zinc atom as a white sphere. The N and C termini are indicated as “N” and “C”. **(D)** Diagram depicts dimerized TRPM7 kinase. Space-filling model shows the location of residue S1613, S1658, T1683, S1693, and T1741 (orange) on the surface of kinase monomer A (green). Purple ribbon depicts the other TRPM7 kinase monomer that dimerizes with A. The N and C termini of the monomer are indicated as “N” and “C”.

### 2.3 Mutations at S1777 differentially affect TRPM7's kinase activity

TRPM7 S1777 is another residue where mutation changes the catalytic activity of the kinase (Figure 8A and 8B). Interesting, we found that the non-phosphorylatable alanine substitution at S1777 significantly increased TRPM7's kinase activity while phosphomimetic mutations to either glutamate or aspartate abolished kinase activity (Figure 8A, 8B, and 9A). S1777 is located near the catalytic center of kinase and forms a hydrogen bond with D1765 (Figure 9B), the invariant key catalytic aspartate residue responsible for properly orientating the hydroxyl group of the substrate towards the  $\gamma$ -phosphate of ATP for catalysis (66,67).

Taking into account the proximity of S1777 to the active site of the TRPM7 kinase, we hypothesized that the negative charge introduced by S1777 phosphorylation could cause a perturbation of the overall electrostatic interactions at the catalytic center and disrupt catalysis. Another possibility we considered is that addition of the large phosphate group on S1777 could be impeding the binding of ATP to the catalytic core, whereas the S1777A substitution would prevent such a modification and also better accommodate ATP for hydrolysis and phosphate transfer. We mutated S1777 to either asparagine (S1777N) or glutamine (S1777Q), two uncharged polar residues that structurally resemble their charged aspartate and glutamate counterparts, and found that these substitutions significantly compromised kinase activity (Figure 9A). By contrast, mutating S1777 to glycine (S1777G), which possesses the smallest side chain and is also non-phosphorylatable, produced a kinase that retained its catalytic activity (Figure 9A). This result indicates that functional catalysis by TRPM7 kinase requires an amino acid at

position 1777 with a relatively small side chain. Thus, the addition of a phosphate group at S1777 by phosphorylation likely disrupts catalysis.

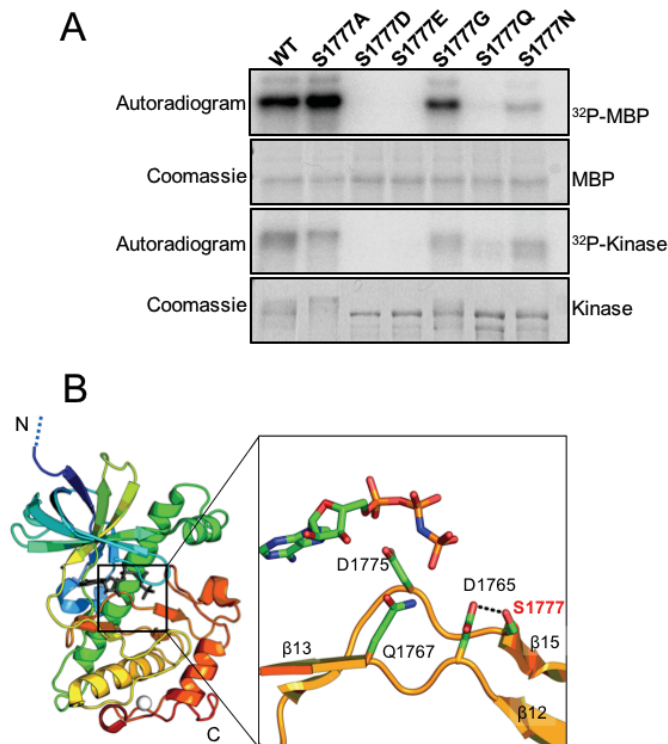


**Figure 9. TRPM7 kinase activity is affected by phosphorylation of residue S1777 located in the kinase catalytic domain.**

(A) The catalytic activities of Sumo-TRPM7-Kinase WT and various S1777 mutants were assessed by an *in vitro* kinase assay using MBP as a substrate. (B) Ribbon diagram shows the structure of the core catalytic domain (a.a. 1575–1828) of mouse TRPM7 kinase (PDB code 1IA9). The AMPPNP is rendered as gray sticks and the zinc atom as a white sphere. The N and C termini are indicated as “N” and “C”. The expanded view on the right shows the position of residue S1777 at the active site along with catalytic residues D1765, Q1767, and D1775. The nucleotide and side-chains of key residues are shown as sticks. The interaction between S1777 and D1765 is shown with a dashed line.

## **2.4 Phosphorylation of the TRPM7 S1565 in the exchange domain disrupts TRPM7 kinase activity without affecting kinase dimerization**

A distinguishing feature of TRPM7 is that the kinase domain forms a dimer in the crystal structure as a consequence of the exchange between monomers of an N-terminal segment that is mainly helical (a.a. 1551-1577) (Figure 8D and 10) (66). Within this exchange segment of TRPM7, two serine residues (S1565 and S1567) have been identified as autophosphorylation sites by our screen and other studies. To determine whether phosphorylation of S1565 and S1567 could potentially affect kinase activity, we mutated these serine residues to alanine or a phosphomimetic amino acid aspartate. We observed that mutation of S1565 to aspartate (S1565D) abolished catalytic activity, whereas the alanine mutation of S1565 (S1565A) did not affect kinase activity (Figure 10B). Mutation of residue S1567 to either alanine or aspartate (S1567A and S1567D) had no effect on the kinase's catalytic activity (Figure 10B).

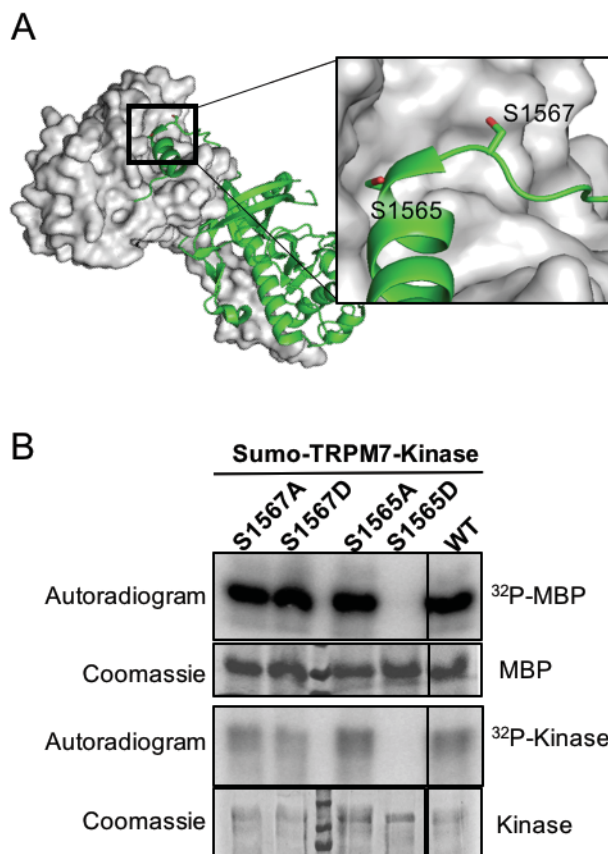


**Figure 10. S1565 in the TRPM7 kinase dimerization exchange segment regulates its catalytic activity.**

**(A)** The structure of a dimerized TRPM7 kinase depicts the N-terminal exchange segment of one kinase monomer (ribbon diagram in green) interacting with another kinase monomer (space-filled surface in gray). The expanded view on the right highlights the location of S1565 and S1567 on the exchange domain of one of the promoters (side-chains shown as sticks) (66). **(B)** An *in vitro* kinase assay assesses the catalytic activities of Sumo-TRPM7-Kinase WT and mutants carrying S1565A, S1565D, S1567A, and S1567D substitutions.

The exchange segment outside of the kinase domain is divided into two functional motifs: an "activation motif" (a.a. 1553-1562) that is essential for kinase activity and a "dimerization motif" (a.a. 1563-1570) that is critical for the functional dimer assembly (Figure 11A) (68). Previous studies have shown that mutation of the L1564 adjacent to the S1565 on the "dimerization motif" abolished kinase catalytic activity by disrupting the dimer formation for TRPM7 kinases (68). Therefore, we speculated that the phosphomimetic substitution S1565D might similarly disrupt the catalytic activity of TRPM7 kinase by interfering with kinase dimerization.

We purified GFP-tagged COOH-terminal fragment of wild-type mTRPM7 kinase (GFP-TRPM7-Cterm-WT) and kinases harboring L1564P, S1565A and S1565D mutations (GFP-TRPM7-Cterm-L1564P, S1565A, and S1566D). *In vitro* kinase assay using MBP as a substrate indeed confirmed the catalytic defects for both L1564P and S1565D mutants (Figure 11B). To test for disruption of dimer formation, we performed an *in vitro* GST pulldown assay using GST-tagged TRPM7 exchange domain containing residue 1548-1576 (GST-exchange) and investigated its ability of the GST-exchange proteins to affinity purify GFP-TRPM7-Cterm WT and mutants from cell lysate (Figure 11C). The rationale is that if dimer formation of the TRPM7 kinases was disrupted, the free GFP-TRPM7-kinase monomers in the cell lysates would then be available to be pulled down by the GST-exchange proteins. As we expected, the WT TRPM7-Cterm protein was not able to be affinity purified by the GST-exchange protein, suggesting that a normal dimer interaction between WT TRPM7 kinase monomers could not be overcome (Figure 11C). By contrast, the GST-exchange proteins successfully affinity purified the GFP-TRPM7-Cterm-L1564P mutant, indicating that the L1565P mutation disrupted the stability of the TRPM7 kinase

dimer (Figure 11C). Surprisingly, the introduction of S1565A or S1565D mutations into TRPM7-Cterm did not disrupt dimerization, as assessed by the inability of GST-exchange to affinity purify GFP-TRPM7-Cterm-S1565A and S1565D proteins (Figure 11C). These data indicate the S1565D mutation in TRPM7's exchange segment disables kinase catalytic activity without significantly interfering with dimerization, suggesting that phosphorylated S1565 may behave similarly.

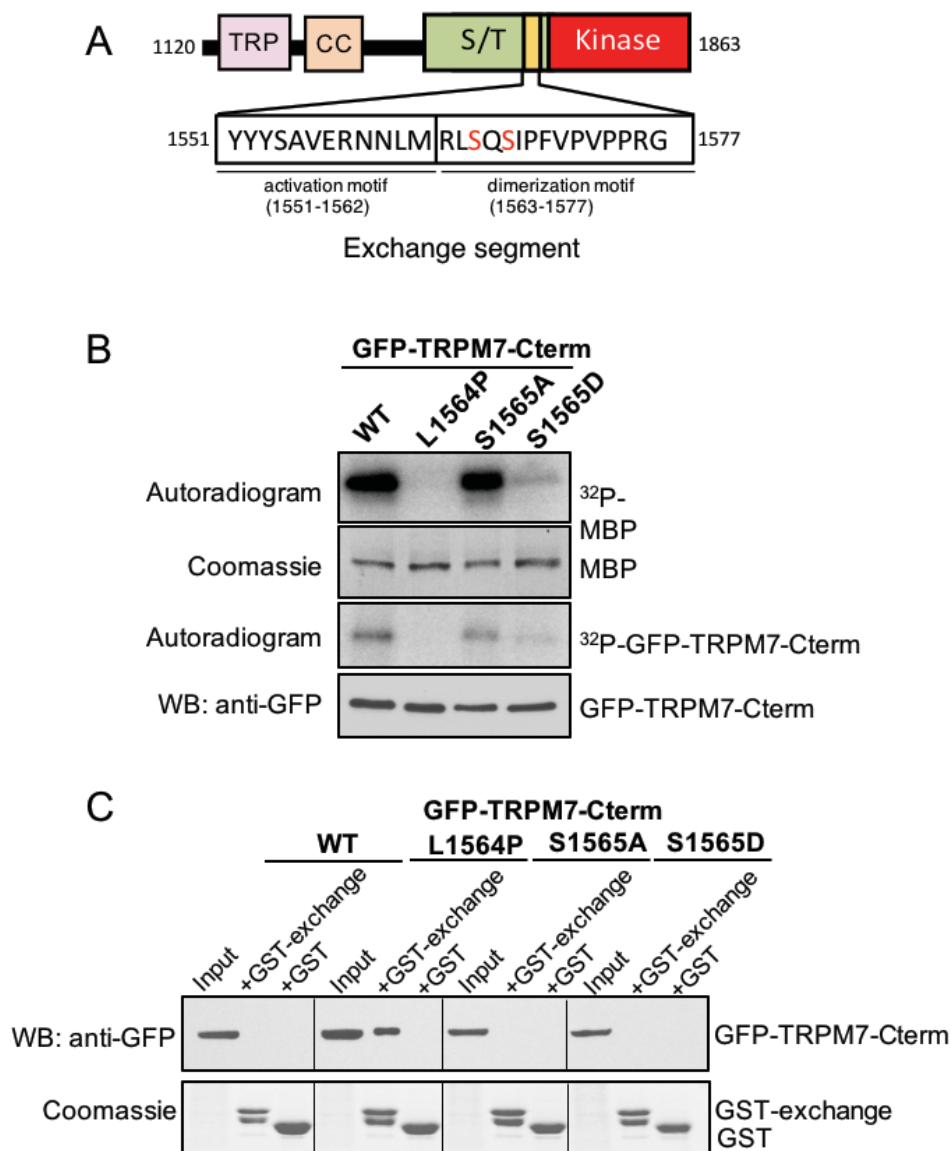


**Figure 11. Phosphorylation of the TRPM7 S1565 disrupts TRPM7 kinase activity without affecting kinase dimerization.**

(A) Schematic representation of TRPM7-Cterm highlighting the sequence of the exchange segment located NH<sub>2</sub>-terminal to the kinase domain. (B) An *in vitro* kinase assay was carried out to validate the catalytic activity of GFP-TRPM7-Cterm containing WT kinase or mutants harboring the L1564P, S1565A, and S1565D. (C) GFP-TRPM7-Cterm-WT, L1564P, S1565A, and S1565D were expressed in HEK-293T cells and pulled down by a

GST-tagged TRPM7 exchange segment (a.a. 1548-1576) (GST-exchange) bound to glutathione agarose. The pulldown samples were resolved by SDS-PAGE and Coomassie blue staining. GFP-TRPM7-Cterm proteins were analyzed by immunoblotting with an anti-GFP antibody.

One explanation for the catalytic defect observed in S1565D mutant comes from the observation that the side chain of S1565 is orientated towards a glycine-rich loop (a.a. 1783-1798) between the  $\beta$ 15 sheet and the  $\alpha$ E strand of the other monomer (Figure 12). This loop of alpha-kinases is referred to as the “N/D loop” due to the presence of an invariant asparagine or aspartate residue (71). The N/D loop of TRPM7 is highly flexible as it is absent in the crystal structure of the kinase without ATP (Figure 12) (66). S1565 in the exchange domain of one TRPM7 kinase monomer faces a wall of negative charges from the side chain carboxylates of E1783 and D1788, and the backbone carbonyls of residues C1787, M1789, and V1790 in the flexible N/D loop of the other TRPM7 kinase monomer (Figure 12).

Molecular modeling indicates that the ATP-binding site at the kinase catalytic core does not have direct contacts with S1565 that would be perturbed upon S1565 mutation to aspartate. Rather, substitution of aspartate at S1565 would introduce a negative charge, which would cause electrostatic repulsion of the N/D loop away from its original location. Studies of this N/D loop in other alpha-kinases have suggested its involvement in the substrate binding (73). Moreover, by comparing the crystal structure of the MHCK A to the TRPM7 kinase structure, Ye and colleagues speculated that “the N/D loop not only dictates the size and shape of the active-site pocket but may also act as a regulatory switch to control access to it” (71). We, therefore, speculate that phosphorylation of S1565 changes the structure of the N/D loop, disrupting the ability of the kinase to bind to its substrate.

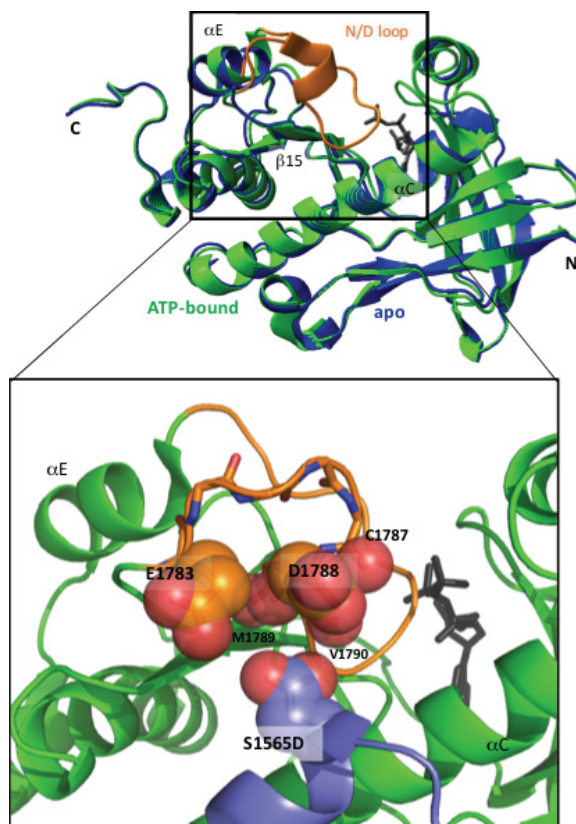


**Figure 12. Phosphorylation of the TRPM7 S1565 potentially causes structural perturbation at the catalytic core of the TRPM7 kinase.**

Overlaying image of the TRPM7 kinase in the ATP-bound state (PDB: 1IA9, green) and the apo-state (PDB: 1IAJ, blue) (66). Orange color highlights the flexible N/D loop (a.a. 1783-1798) that is missing in the apo-state. The AMPPNP is shown as gray sticks. The zoomed panel at the bottom shows the flexible N/D loop (orange) of one kinase monomer, superimposed with the exchange segment of another monomer containing the S1565D mutation (purple). Side chain carboxylates of D1565, E1783, and D1788, and backbone carbonyls of C1787, M1789, and V1790 are shown as red spheres.

## 2.5 A survey of potential regulatory phosphorylation residues on TRPM7 kinase

To complete our investigation of factors that may modulate TRPM7's catalytic activity within the core domain, we explored whether serine or threonine residues not subject to autophosphorylation, but rather located close to functionally important residues of the kinase, could regulate the kinase activity if they become phosphorylated. Residue S1750 is located adjacent to the invariant zinc-binding coordinating residue H1751 on the  $\alpha$ -helix D of the TRPM7 kinase, along with two other highly conserved residues T1753 and T1757 (Figure 7). Substitution of S1750, T1753 and T1757 to the phosphomimetic aspartate and/or glutamate abolished catalytic activity (Figure 13). Analysis of the TRPM7 kinase structure indicated that phosphomimetic substitution of residues on this  $\alpha$  helix might disrupt the overall protein stability. Meanwhile, substitutions at T1774, which is adjacent to the invariant catalytic residue D1775, to alanine, aspartate, and glutamate also produced severe disruption to the catalytic activity (Figure 13). Previous studies found that a threonine to serine substitution at this site also inactivated the kinase, suggesting the importance of the threonine side chain in mediating the catalysis (42,67). We also found that aspartate substitution of S1647, which is adjacent to the invariant catalytic K1646, caused kinase inactivation (Figure 7 and Figure 13). Those above-mentioned serine and threonine residues have not yet been found phosphorylated in any of the current analysis, therefore it is not clear whether they would potentially serve as regulatory sites for TRPM7's kinase activity.

As many conventional kinases and alpha-kinases are subject to regulation by phosphorylation by other kinases, we explored whether serine or threonine residues contained within phosphorylation motifs of other kinases have the potential to influence

TRPM7 kinase activity. For example, we found that S1588 resides within the phosphorylation motif of NIMA-related kinase-6, S1554 and T1630 are within a casein kinase 2 phosphorylation motif, and T1664 is within a motif for proline-directed kinases (82). We generated phosphomimetic substitutions at those sites (S1554A/D, S1558D, T1630D, and T1664D), and also at a few other serine/threonine residues not located within known kinase domain (T1655D, S1697D, T1722D and S1786A/D), but found no change in the kinase's catalytic activity. As members of the alpha-kinases family have regulatory phosphorylation sites outside the catalytic core (72,73), we looked at phosphorylated residues S1502, T1503, S1506, and T1828 that are outside of TRPM7 kinase domain. However, substitution of alanine or aspartate at these sites also had no effect on the kinase's catalytic activity (Figure 13).

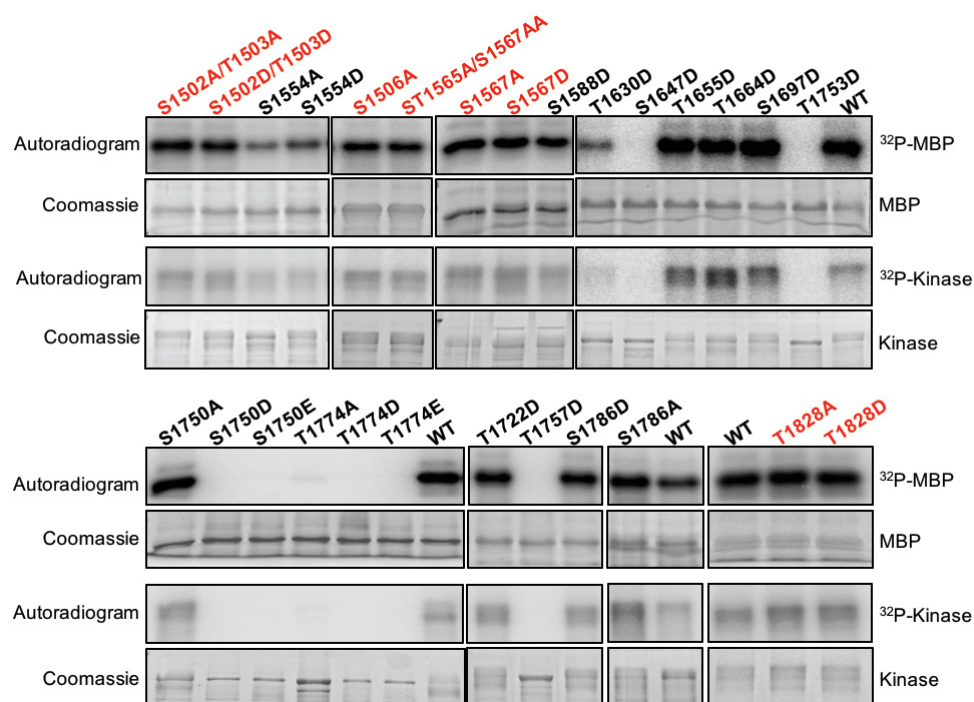


**Figure 13. Mutagenesis screen of serine and threonine residues on TRPM7 with regulatory potential.**

The indicated Sumo-TRPM7-Kinase mutants were purified from *E. coli* and their kinase activities were assayed in *in vitro* kinase assays. Phosphorylated residues identified by our MS analysis are highlighted in red.

### **SECTION III: TRPM7 KINASE ACTIVITY REGULATES THE PROTEIN STABILITY AND CELLULAR LOCALIZATION OF THE CHANNEL**

In the previous sections, we employed a comprehensive analysis of TRPM7 phosphorylation and identified a mechanism by which the kinase activity of TRPM7 is regulated by autophosphorylation. However, we still lack the insights as to what functional roles the kinase activity may play in regulating the channel. In our previous investigations into TRPM7, we observed that protein level of TRPM7 is affected by mutations that inactivate the catalytic activity of TRPM7 kinase. We decided to investigate how the kinase-inactivation of TRPM7 affects the stability and consequently the cellular localization of the channel.

#### **3.1 TRPM7 kinase inactivation leads to faster protein turnover**

To understand the role of TRPM7 kinase activity in regulating protein level, we employed tetracycline-inducible HEK-293 cells expressing HA-TRPM7-WT (293-TRPM7-WT cells) or kinase-inactive mutant HA-TRPM7-K1646A (293-TRPM7-K1646A cells) to follow the kinetics of TRPM7 protein turnover. Following 24 hours of tetracycline induction, the TRPM7-expressing cells were replaced with tetracycline-free medium containing CHX to inhibit protein synthesis. TRPM7 protein levels were then analyzed at various time points over 24 hours. TRPM7-WT proteins were relatively stable compared to TRPM7-K1646A, and the protein levels of TRPM7-WT did not appreciably decrease over 24 hours of CHX treatment (Figure 14A). By contrast, the protein levels of TRPM7-K1646A decreased rapidly over time, with an apparent half-life of 7.1 hours (Figure 14B), suggesting that the kinase-inactive mutant is subjected to increased protein turnover.

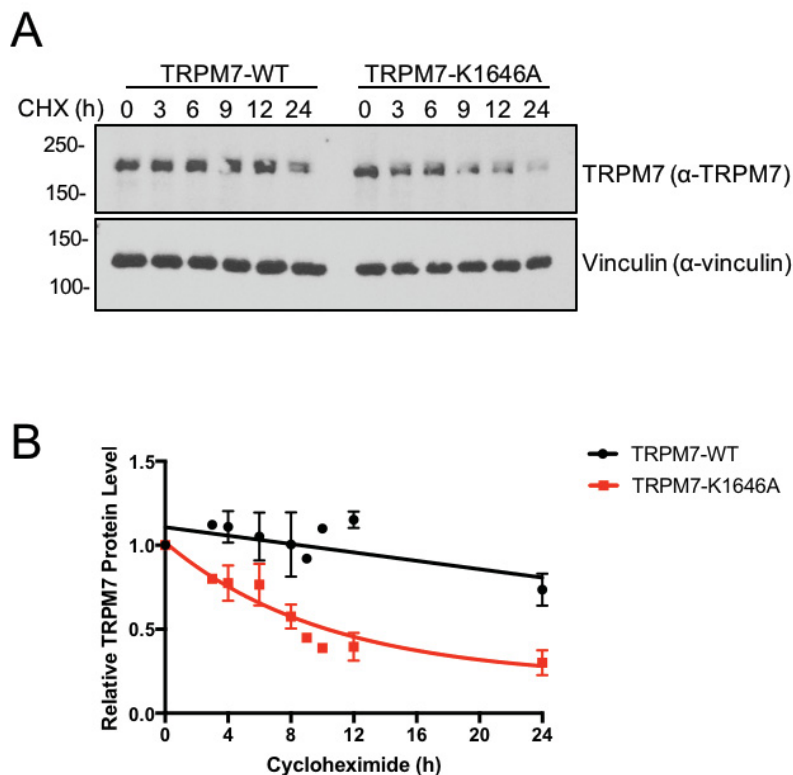


**Figure 14. Inactivation of TRPM7 kinase increases the rate of channel turnover.**

(A) 293-TRPM7-WT and 293-TRPM7-K1646A cells were induced with tetracycline for 24 h and then treated with CHX (10  $\mu$ g/ml) to block protein synthesis. Cell lysates were harvested at various time points. Protein concentrations of the cell lysates were measured with Bradford assays and equal amount of total proteins were loaded on the SDS-PAGE gel. (B) The time courses for turnover of TRPM7-WT and TRPM7-K1646A. The relative TRPM7 protein levels were calculated by normalizing TRPM7 protein levels relative to the vinculin control. Fitting the turnover curve of TRPM7-K1646A to a one-phase exponential decay curve yields a half-life of 7.1 hours. TRPM7-WT turnover could not be fitted to the decay curve. Data from three independent experiments were analyzed.

### **3.2 TRPM7 kinase inactive mutants are targeted by ubiquitin-proteasome degradation pathway**

Ubiquitylation is a frequent post-translational modification targeting proteins for degradation. To probe for TRPM7 ubiquitylation, 293-TRPM7-WT and 293-TRPM7-K1646A cells were first treated with tetracycline and transfected with FLAG-tagged ubiquitin (FLAG-Ub). Next, ubiquitinated TRPM7 in cell lysates was immunoprecipitated with M2 anti-FLAG agarose. TRPM7 protein levels and the degree of ubiquitylation were then resolved by SDS-PAGE and Western blotting. The kinase-inactive TRPM7-K1646A had a higher amount of ubiquitylation compared to the WT protein (Figure 15A).

As ubiquitylation often serves as a signal for protein degradation through the proteasome, we next tested whether application of the proteasome inhibitor MG132 would raise the protein levels of TRPM7-K1646A. 293-TRPM7-WT and 293-TRPM7-K1646A cells were treated with tetracycline for 24 hours, and the media was then replaced with tetracycline-free medium containing MG132. The cells were harvested at 8 hours and 24 hours following MG132 treatment. Proteasome inhibition by MG132 had little effect on TRPM7-WT levels at either 8 hours or 24 hours, but significantly elevated protein levels of TRPM7-K1646A at 24 hours compared to non-treated control cells (Figure 15B). These results support the previous finding that TRPM7-WT is a very long-lived protein for which little ubiquitylation occurs, whereas the kinase-inactive mutant is more unstable and subject to protein turnover by the ubiquitin-proteasome pathway.

We also confirmed that increased proteasome-mediated TRPM7 turnover is independent of the mechanism by which TRPM7 kinase was rendered inactive. TRPM7-WT and two independent kinase-inactive mutants, TRPM7-K1646R and TRPM7-G1618D,

were transiently expressed in HEK-293T cells that were subsequently treated with MG132 for 24 hours (Figure 15C). Following proteasome inhibition, the fold-increase in protein levels was  $3.15 \pm 0.29$  for TRPM7-K14646R and  $2.49 \pm 0.60$  for TRPM7-G1618D, compared to  $1.01 \pm 0.11$  for TRPM-WT (Figure 15D). The fold-increase observed for TRPM7-K14646R and TRPM7-G1618D was similar to what we found for TRPM7-K1646A expressed in the stable 293-TRPM7-K1646A cells. These results point to a role for TRPM7-kinase and autophosphorylation in controlling channel turnover.

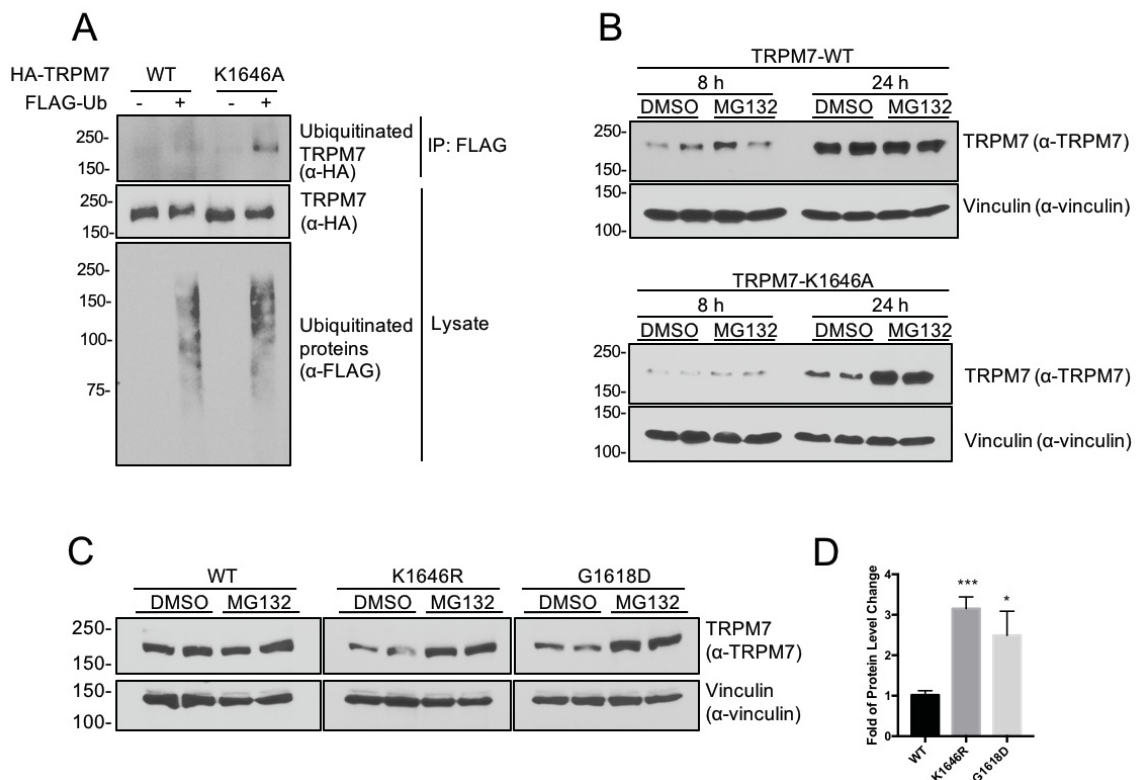


**Figure 15. Inactivation of TRPM7 kinase leads to targeting of the protein by the ubiquitin-proteasome pathway.**

**(A)** A TRPM7 kinase-inactive mutant has higher level of ubiquitylation than the TRPM7-WT. 293-TRPM7-WT and 293-TRPM7-K1646A cells were induced with tetracycline and co-transfected with FLAG-Ubiquitin (FLAG-Ub) for 24 h. FLAG-ubiquitinated proteins were immunoprecipitated with M2 anti-FLAG agarose. The amount of ubiquitinated TRPM7 in the immunoprecipitation (IP) samples and the levels of HA-TRPM7 and FLAG-ubiquitinated proteins in cell lysates were assessed by SDS-PAGE and Western blotting.

**(B)** Proteasome inhibition using MG132 was effective in increasing protein levels of TRPM7-K1646A mutant compared to TRPM7-WT. 293-TRPM7-WT and 293-TRPM7-K1646A cells were induced with tetracycline for 24 h and then replaced with fresh media containing DMSO or MG132 (1  $\mu$ M). Cell lysates were harvested at 8 h and 24 h and

normalized to total protein levels. **(C)** Proteasome inhibition is effective in accumulating two different kinase-inactive TRPM7 mutants. HEK-293T cells transfected with TRPM7-WT or kinase-inactive TRPM7-K1646R and TRPM7-G1618D were treated with DMSO or MG132 (1  $\mu$ M) for 24 h. The proteins were resolved by SDS-PAGE and Western blotting, with equal amounts of lysates loading. **(D)** The fold increase in protein expression was assessed by normalizing TRPM7 protein levels relative to vinculin controls and by calculating the mean between MG132 and DMSO treatment groups (n=2-6, Mean  $\pm$  S.E.M, Student t-test, \*\*\* P<0.0005, \* P=0.0170).

### **3.3 TRPM7 S1360 phosphorylation is involved in proteasome-mediated TRPM7 turnover**

Since kinase-inactivation resulted in faster TRPM7 turnover, we next investigated whether certain key phosphorylation sites are mediating proteasome-dependent degradation of the channel. Our analysis of TRPM7 autophosphorylation uncovered many phosphorylation sites that are commonly phosphorylated on TRPM7. We mutated frequently phosphorylated residues (S1255, S1360, S1403, S1502, T1503, and S1567) to alanine and tested whether these amino acid substitutions affected the channel's sensitivity to proteasome-mediated degradation (Figure 16A). We found that in response to MG132 treatment, the fold increase in TRPM7-S1360A protein levels ( $2.01 \pm 0.34$ ) mimicked the change observed for the kinase-inactive TRPM7 mutants ( $3.15 \pm 0.29$  for TRPM7-K14646R and  $2.49 \pm 0.60$  for TRPM7-G1618D as shown in Figure 15), whereas protein levels of TRPM7 mutants with alanine substitutions at the other TRPM7 autophosphorylation sites were unaffected (Figure 16B).

In our previous study of TRPM7 autophosphorylation, S1360 was found most frequently phosphorylated in HEK-293 cells constitutively expressing the channel. To test whether S1360 phosphorylation affects proteasome-mediated turnover of TRPM7, we introduced phosphomimetic substitutions at S1360 (TRPM7-S1360D and TRPM7-S1360E) and found that both phosphomimetic substitutions were effective in reversing the MG132-sensitivity of the S1360A mutant (Figure 17A). This observation suggests that the phosphorylation of S1360 is important in preventing TRPM7 from being targeted for proteasome-mediated degradation. Our MS analysis also found phosphorylation of S1360 on the TRPM7-K1646R mutant, suggesting this residue can be phosphorylated by

endogenous TRPM7 and TRPM6 or other cellular kinases. We attempted to prevent proteasome-mediated degradation of the kinase-inactive mutant by introducing S1360 phosphomimetic substitutions on TRPM7-K1646R (TRPM7-K1646R/S1360D and TRPM7-K1646R/S1360E). However, either glutamate or aspartate substitutions at S1360 did not prevent proteasome-mediated degradation of the kinase-inactive TRPM7, suggesting that other regulatory phosphorylation sites are involved in mediating TRPM7 protein stability (Figure 17B). Taken together, our results suggest that S1360 phosphorylation is an important posttranslational signal for preventing proteasome-mediated turnover of the channel.

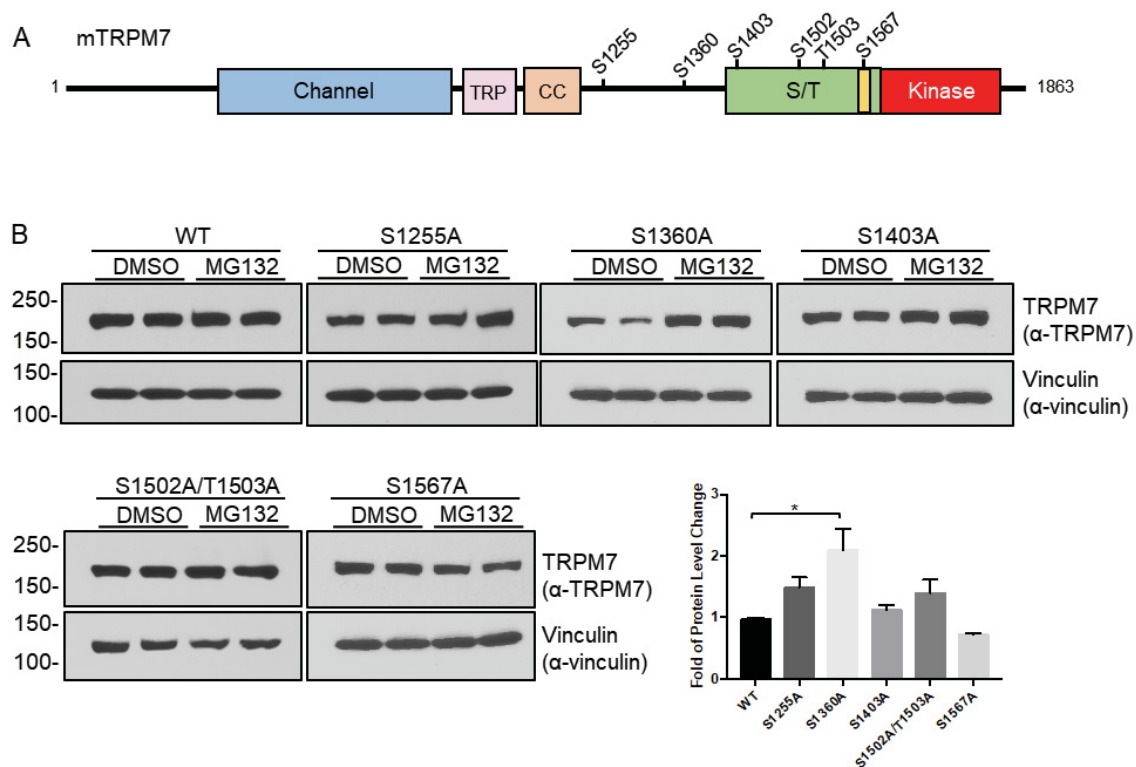


**Figure 16. A survey of TRPM7 phosphorylation sites that potentially regulate proteasome-dependent TRPM7 degradation.**

(A) A schematic representation of a full-length mouse TRPM7 showing the locations of frequently phosphorylated residues. (B) Alanine mutation at S1360 leads to sensitization of TRPM7 to MG132-mediated protein accumulation. HEK-293T cells expressing TRPM7-WT or phosphorylation site mutants (S1255A, S1360A, S1403A, S1502A/T1503A, and S1567A) were treated with DMSO or MG132 (1  $\mu$ M) for 24 h. Cell lysates were normalized and analyzed by Western blotting. Quantification of TRPM7 protein level change was performed from three independent experiments as described above (Mean  $\pm$  S.E.M, Student t-test, \* P=0.0404).

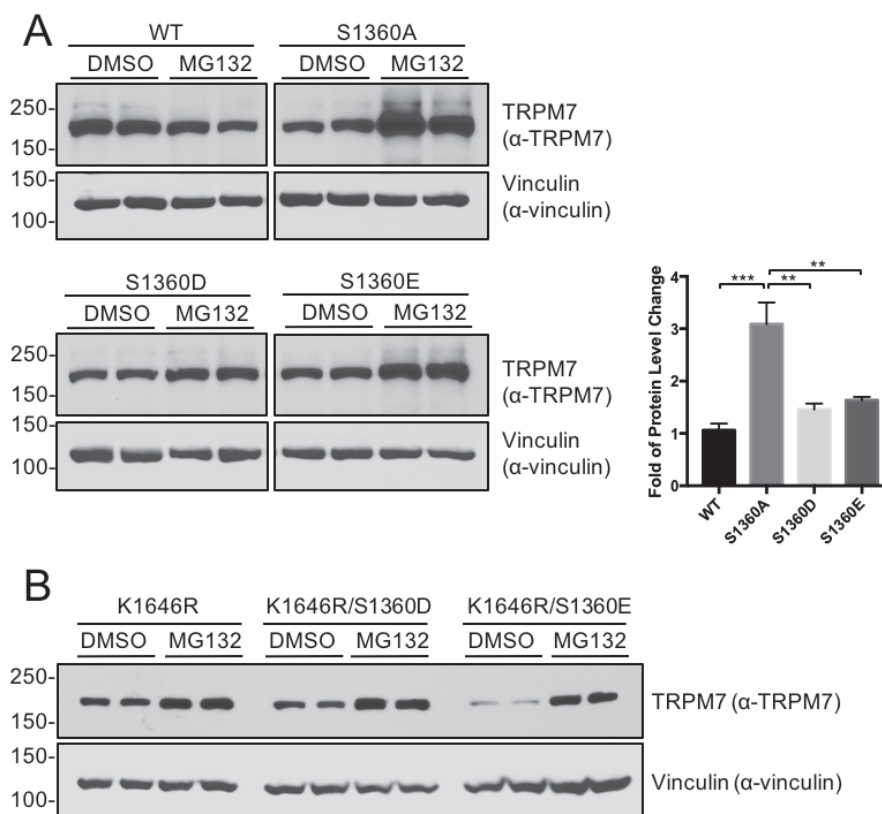


**Figure 17. Phosphorylation of the TRPM7 S1360 is involved in channel turnover.**

(A) Phosphomimetic substitutions at S1360 (TRPM7-S1360D and TRPM7-S1360E) effectively reversed the proteasome-mediated degradation of TRPM7-S1360A. HEK-293T cells transfected with TRPM7-WT, S1360A, S1360D, and S1360E were treated with DMSO or 1  $\mu$ M MG132 for 24 h. Equal amounts of cell lysates were loaded. Quantification of TRPM7 protein level change was performed from three independent experiments as described above (Mean  $\pm$  S.E.M, Student t-test, \*\*P<0.005, \*\*\*P<0.0005) (B) S1360 phosphomimetic substitutions of the TRPM7-K1646R (TRPM7-K1646R/S1360D and TRPM7-K1646R/S1360E) could not rescue the kinase-inactive TRPM7 mutant from proteasome-mediated turnover. HEK-293T cells expressing TRPM7-K1646R, K1646R/S1360D, and K1646R/S1360E were treated with MG132 as described in (B).

### **3.4 TRPM7 kinase affects cellular localization of the channel in polarized epithelial cells**

Our results thus far suggest a role for TRPM7's kinase in controlling protein levels. We next asked whether the kinase influences the cellular localization of the channel. TRPM7 is widely expressed in adult mice with the highest expression in the kidney where the channel contributes to  $Mg^{2+}$  reabsorption (1,2,26). Expression of the native channel, however, was too low for us to detect its cellular localization by immunocytochemistry. Instead, we analyzed the cellular distribution of murine TRPM7 heterologously expressed in OK cells, a model proximal tubule epithelial cell line (83). Using confocal microscopy, we found that TRPM7-WT readily localized to the basal-lateral side of the OK cells (Figure 18A) and could also be found on the apical membrane where it co-localized with the apical and microvilli marker NHERF1, albeit at much lower levels (Figure 18A and 18B). In contrast, TRPM7-K1646R poorly localized to basal-lateral or apical membranes in OK cells, and was instead retained intracellularly (Figure 18C). The percentage of cells displaying peripheral membrane TRPM7 localization for the kinase-inactive mutant ( $18.12 \pm 2.9$  %) was significantly lower than that for TRPM7-WT ( $71.4 \pm 2.5$  %) (Figure 18D), pointing again to a role for autophosphorylation in controlling the cellular localization of the channel.

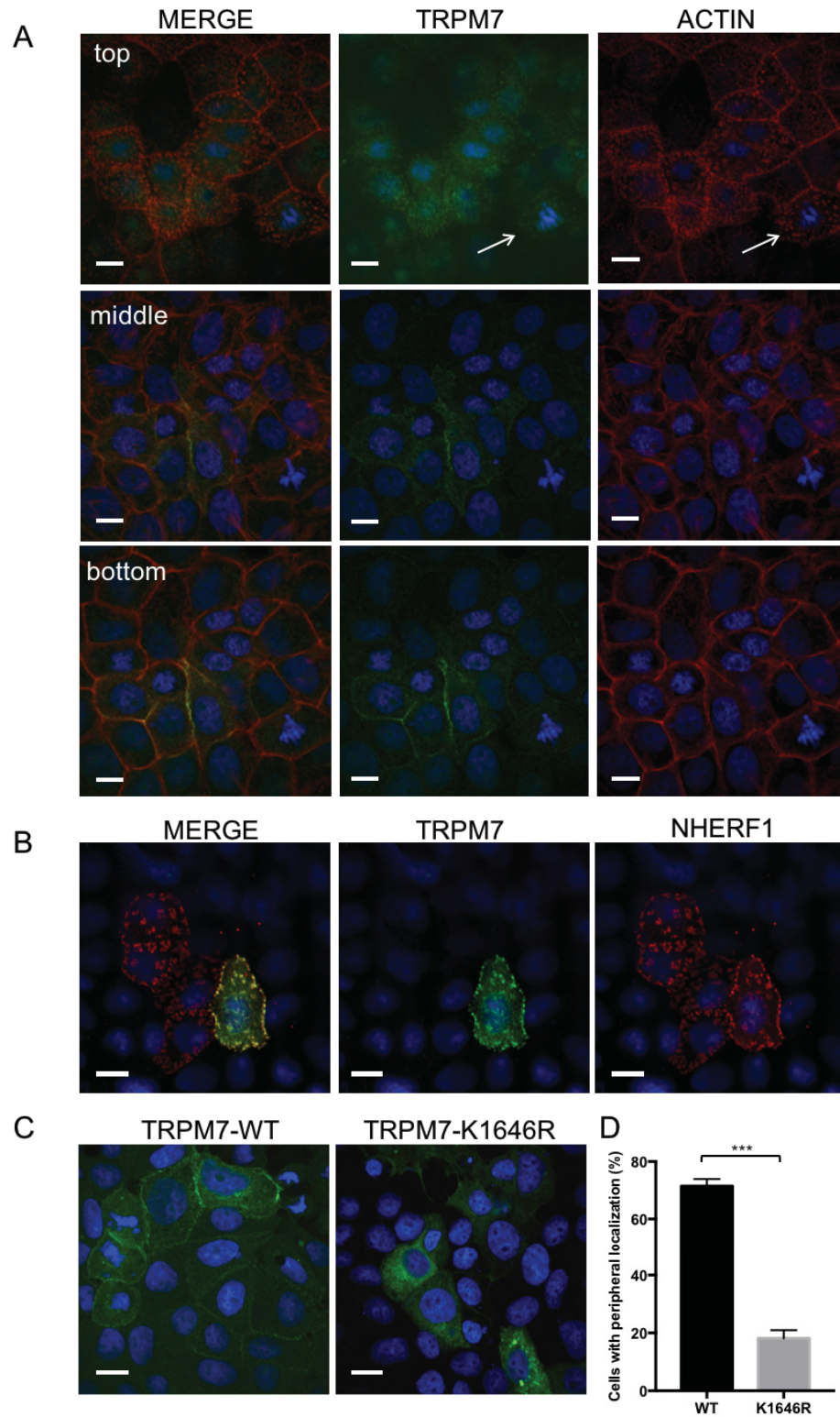


**Figure 18. Inactivation of TRPM7 kinase affects the cellular localization of the channel in polarized epithelial cells.**

(A) Representative confocal Z-stack images of transiently expressed HA-TRPM7 (green) and actin (red) in opossum kidney (OK) proximal tubule epithelial cells (*Scale bar*, 10 microns). HA-TRPM7 was expressed for 24 h. TRPM7 weakly localized to the apical membrane of OK cells in actin patches (*white arrow*) (top) and prominently localized to the basal-lateral sides of OK cells (middle and bottom). (B) On the apical membrane, HA-TRPM7 (green) co-localizes with the microvilli marker FLAG-NHERF1 (red) after co-expression for 24 h. (C) Comparison of HA-TRPM7-WT and K1646R cellular localization in OK cells after 48 h of expression (*Scale bar* 10 microns). TRPM7-WT readily localizes to the lateral membranes whereas the kinase-inactive mutant TRPM7-K1646R is retained intracellularly. (D) Quantification of the percentage of cells expressing TRPM7 localized to apical and basal-lateral sides of OK cells. Cell counting was performed under 40X magnification using an inverted fluorescent microscope. A total of 400-600 positive staining cells from three non-overlapping areas of each slide were analyzed. Three independent experiments were performed. (Mean  $\pm$  S.E.M, Student t-test, \*\*\*  $P < 0.0005$ ).

### **3.5 TRPM7 S1360 phosphorylation regulates TRPM7 peripheral localization in OK cells**

Following the observation that S1360 phosphorylation status affects the protein stability of TRPM7, we next examined whether S1360 phosphorylation also affects the cellular localization of TRPM7. Following the methods described above, HA-TRPM7-WT, S1360A, S1360D, and S1360E were transiently expressed in OK cells for 48 h and stained with an anti-HA antibody (Figure 19A). We found that alanine mutation of S1360 severely affected the peripheral localization of the channel ( $20.25 \pm 2.4$  %) compared to the WT ( $61.43 \pm 1.6$  %) (Figure 19B). Phosphomimetic substitutions at S1360D ( $51.80 \pm 3.6$  %) and S1360E ( $50.97 \pm 2.6$  %) showed peripheral localization slightly below that of WT but significantly higher than that of the S1360A mutant (Figure 19B). These findings suggest that the phosphorylation status of S1360 also affects the post-translational trafficking of the channel.

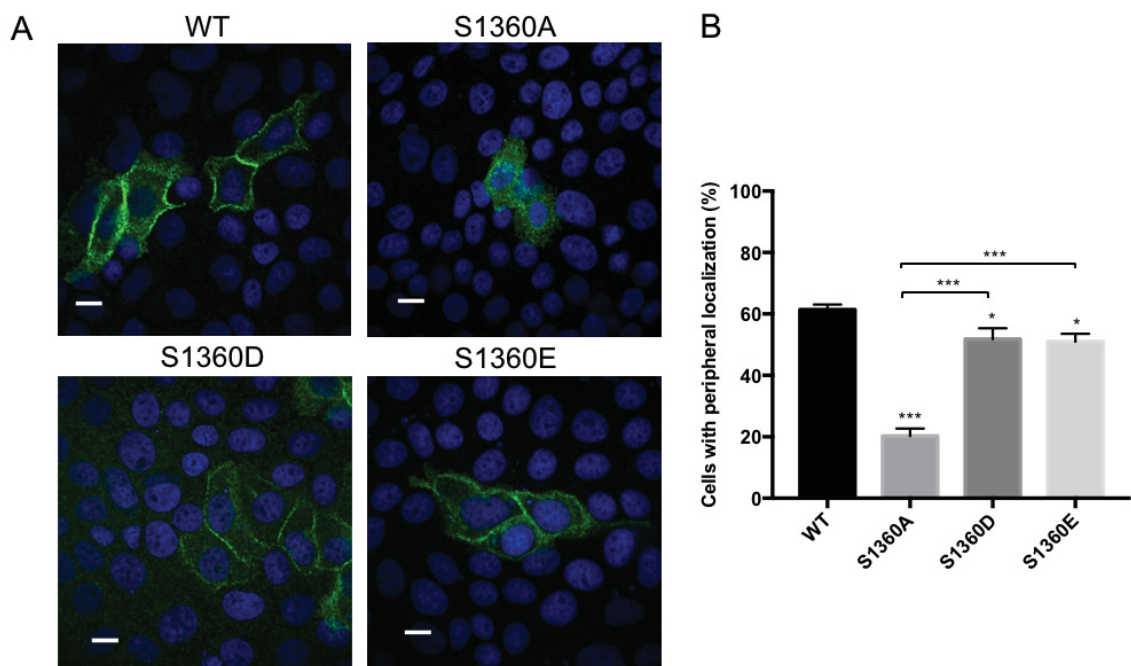


**Figure 19. S1360 phosphorylation alters the localization of TRPM7 in polarized epithelial cells.**

(A) Representative confocal images show cellular localization of HA-TRPM7-WT, S1360A, S1360D, and S1360E (green) in OK cells after 48 h of expression (Scale bar 10 micron). (B) Quantification of the percentage of TRPM7-expressing OK cells with TRPM7 localized to basal-lateral or apical membranes. Cell counting was performed using an inverted fluorescent microscope under 40X magnification as described previously. Results from three independent experiments were analyzed (Mean  $\pm$  S.E.M, Student t-test, \*  $P < 0.05$ , \*\*\*  $P < 0.0005$ ).

## **SECTION IV: AUTOPHOSPHORYLATION-DEPENDENT INTERACTION WITH 14-3-3 $\theta$ REGULATES TRPM7 CELLULAR LOCALIZATION**

To gain insight into the mechanisms by which TRPM7's kinase affects the stability and localization of the channel, we conducted a yeast two-hybrid screen of a rat brain cDNA library by using the COOH terminus of the mouse TRPM7 (a.a. 1120-1863) as the bait (76). One of the positive clones identified by the screen was 14-3-3 $\theta$ . 14-3-3 $\theta$  belongs to a family of highly conserved and ubiquitously expressed proteins involved in cell signaling pathways (84,85). Seven 14-3-3 isoforms are encoded in mammalian genomes, and they exist as homo- and heterodimers with each monomer capable of binding specifically to distinctive phospho-serine/threonine residues on target proteins (84-87). Binding of 14-3-3 proteins to their cognate protein ligands has been shown to regulate protein enzymatic activity, elicit protein conformational changes, influence cellular localization, and mediate cross-bridging with other proteins (88).

### **4.1 Identification of the phospho-binding protein 14-3-3 $\theta$ as a binding partner of TRPM7**

To confirm the interaction between TRPM7 and 14-3-3 $\theta$  in mammalian cells, we first conducted GST pull-down purification assays using GST fused to 14-3-3 $\theta$  (GST-14-3-3 $\theta$ ) and lysates from cells expressing full-length TRPM7 (HA-TRPM7) or a GFP-fusion protein of the kinase-containing TRPM7-COOH-terminal tail (GFP-TRPM7-Cterm) (Figure 20A). A substrate binding-deficient 14-3-3 $\theta$ -K49E mutant was used as a negative control. The charge reversal of K49E in the 14-3-3 substrate-binding groove disrupts 14-3-3's interaction with phosphorylated ligands (50). Strong interactions between both full-

length TRPM7 and GFP-TRPM7-Cterm with GST-14-3-3 $\theta$ -WT were detected (Figure 20A), indicating that TRPM7 is a *bona fide* binding partner of 14-3-3 $\theta$  and that the strong binding between the two proteins occurs on TRPM7's COOH terminus. We also tested whether TRPM7 interacts with other 14-3-3 isoforms. GFP-TRPM7-Cterm was expressed in HEK-293T cells and lysates were applied in a GST-pulldown purification assay using 20  $\mu$ g of GST-14-3-3 $\theta$ , 14-3-3 $\sigma$ , 14-3-3 $\beta$ , 14-3-3 $\eta$ , 14-3-3 $\gamma$ , 14-3-3 $\epsilon$ , 14-3-3 $\theta$ -K49E, and GST. The GST pull-down purification assays demonstrated that all seven isoforms interacted with the GFP-TRPM7-Cterm protein with similar strength (Figure 20B).

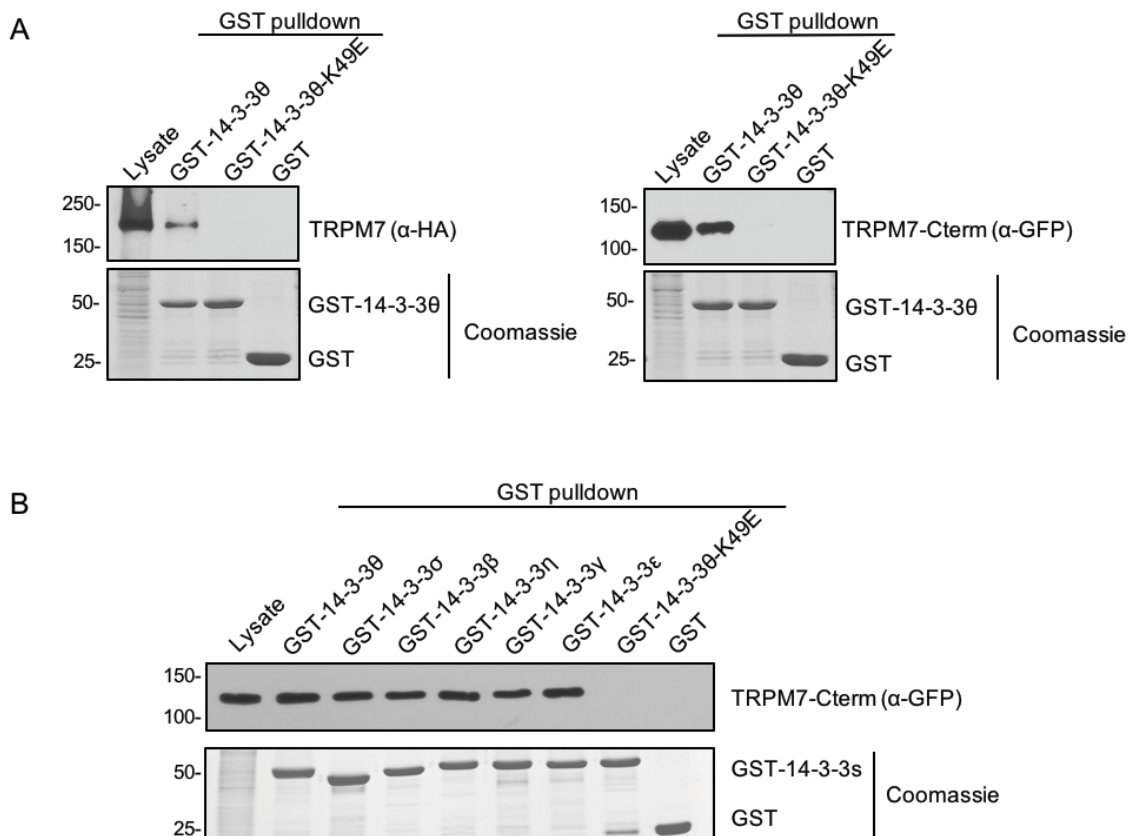


**Figure 20. TRPM7 interacts with the phospho-binding protein 14-3-30 *in vitro*.**

**(A)** GST-pulldown purification assays using glutathione agarose bound with 20  $\mu$ g of GST-14-3-30, GST-14-3-30-K49E or GST proteins were performed to pulldown full-length HA-TRPM7 (left) and GFP-TRPM7-Cterm (right) expressed in HEK-293T cells. HA-TRPM7 and GFP-TRPM7-Cterm were examined by Western blotting using anti-HA and anti-GFP antibodies respectively. GST proteins were visualized by SDS-PAGE and Coomassie staining. **(B)** TRPM7 interacts with all seven 14-3-3 isoforms. Cell lysates containing GFP-TRPM7-Cterm were subjected to pulldown assays using GST-tagged 14-3-3 isoforms. GFP-TRPM7-Cterm in cell lysates and pulldown samples were resolved by SDS-PAGE and Western blotting using an anti-GFP antibody. GST proteins were visualized by Coomassie staining.

## 4.2 The interaction between 14-3-3 $\theta$ and TRPM7 requires TRPM7 autophosphorylation

Since 14-3-3 $\theta$  is a phospho-binding protein, we tested whether the interaction between GFP-TRPM7-Cterm and 14-3-3 $\theta$  is phosphorylation-dependent. A GST-pulldown assay was performed where cell lysates containing GFP-TRPM7-Cterm-WT or GFP-TRPM7-Cterm-K1646R were treated with Lambda phosphatase and then subjected to a pulldown with GST-14-3-3 $\theta$  (Figure 21A). Both Lambda phosphatase treatment of TRPM7 and TRPM7 kinase inactivation abolished the interaction between TRPM7 and 14-3-3 $\theta$ , indicating that the interaction between the two proteins is autophosphorylation-dependent.

To further validate an *in vivo* interaction between TRPM7 and 14-3-3 $\theta$ , HA-TRPM7-WT or the kinase-inactive HA-TRPM7-K1646R were transiently co-expressed with FLAG-tagged 14-3-3 $\theta$  (FLAG-14-3-3 $\theta$ ) or FLAG-14-3-3 $\theta$ -K49E in HEK-293T cells and subjected to immunoprecipitation (Figure 21B and 21C). FLAG-14-3-3 $\theta$ -WT but not the 14-3-3 $\theta$ -K49E mutant readily co-immunoprecipitated with HA-TRPM7, validating an *in vivo* interaction between these two proteins (Figure 19B). Similar to the observation from *in vitro* studies that the interaction between TRPM7 and 14-3-3 $\theta$  requires TRPM7's functional kinase activity, we also found from *in vivo* experiments that FLAG-14-3-3 $\theta$  co-immunoprecipitated with HA-TRPM7-WT but failed to do so with HA-TRPM7-K1646R, confirming that the *in vivo* interaction between 14-3-3 $\theta$  and TRPM7 is autophosphorylation-dependent (Figure 21C).

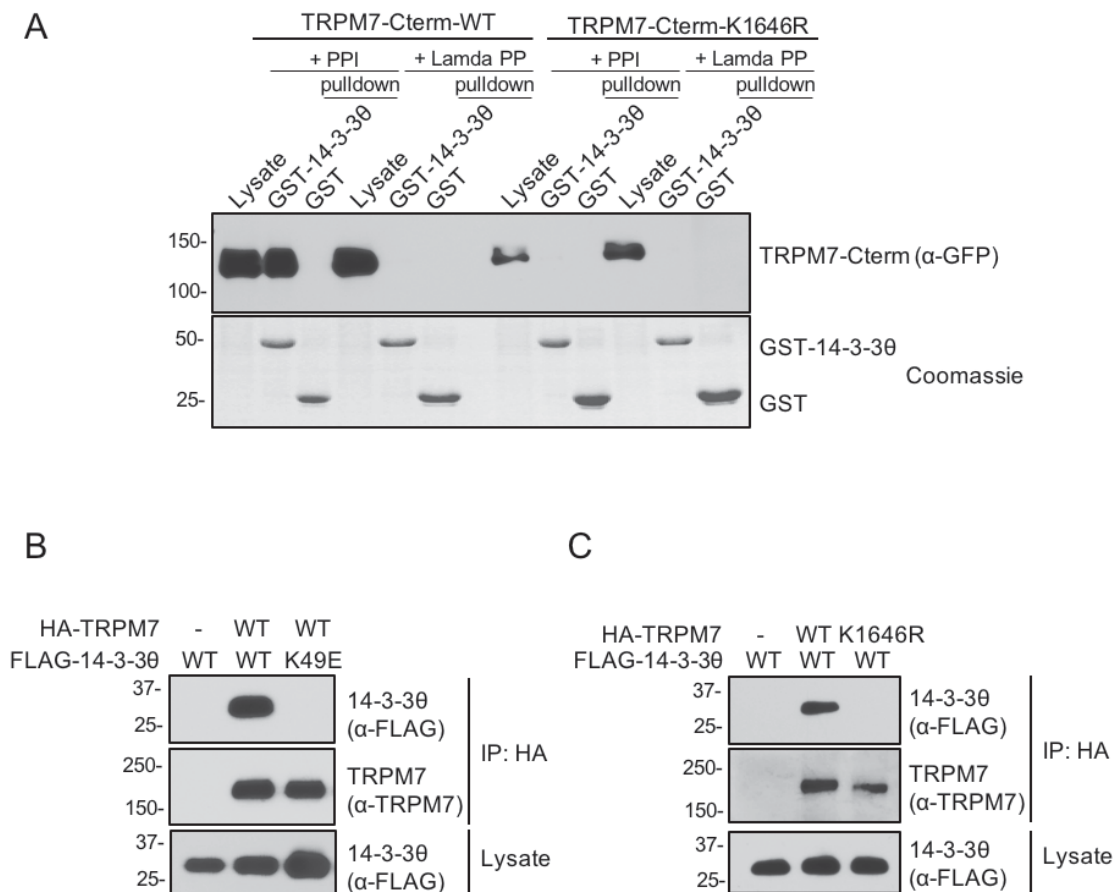


**Figure 21. TRPM7 and 14-3-3θ interacts in a phosphorylation-dependent manner.**

(A) *In vitro* interaction between TRPM7 and 14-3-3 requires TRPM's kinase activity. TRPM7-Cterm-WT and TRPM7-Cterm-K1646R were transiently expressed in HEK-293T cells. At the time of cell harvesting, cell lysates were treated with either phosphatase inhibitor (PPI) or a Lambda phosphatase (Lambda PP) and subjected to a GST-pulldown purification assay. GFP-TRPM7-Cterm proteins were examined by Western blotting using anti-GFP antibodies, and GST proteins were visualized by SDS-PAGE and Coomassie staining. (B) Co-immunoprecipitation of HA-TRPM7 and FLAG-14-3-3θ confirms their interaction *in vivo*. HA-TRPM7-WT was co-expressed with FLAG-14-3-3θ-WT or binding-deficient mutant FLAG-14-3-3θ-K49E in HEK-293T cells for 48h. TRPM7 was immunoprecipitated with HA-agarose and blotted with an anti-FLAG antibody to detect

14-3-3 $\theta$  binding. The total amount of FLAG-14-3-3 $\theta$  protein in cell lysates and the amount of HA-TRPM7 bound on the HA-agarose were blotted by an anti-FLAG and an anti-TRPM7 antibody respectively. (C) *In vivo* interaction between TRPM7 and FLAG-14-3-3 also requires TRPM7 autophosphorylation. HA-TRPM7-WT and K1646R were co-expressed with FLAG-14-3-3 $\theta$ -WT and analyzed similarly as described in (B). FLAG-14-3-3 $\theta$  only co-immunoprecipitated TRPM7-WT but not the kinase-inactive mutant.

### **4.3 Binding of 14-3-30 to TRPM7 requires autophosphorylation of TRPM7 on residue S1403**

Most of the 14-3-3 binding partners bear variations of consensus recognition motifs R-S-X-pS/T-X-P (motif I) or K/R-X-X-X-pS/T-x-P (motif II) containing a phosphoserine/threonine residue (87,89,90). We screened for potential 14-3-30 binding sites on TRPM7 and found three highly conserved serine residues (S1403, S1567, and S1588) within sequences that match 14-3-3 binding motif II and two residues (S1502 and T1503) in sequences partially matching 14-3-3 binding motif I (Figure 22A). Our MS analysis of TRPM7 autophosphorylation provided supporting information that S1403, S1502, T1503, and S1567 are bona fide *in vivo* autophosphorylation sites but S1588 is not.

We created GFP-TRPM7-Cterm mutants bearing alanine substitutions at S1403, S1567, and S1588 and performed GST-pulldown purification assays with the mutants (Figure 22B). The interaction between GFP-TRPM7-Cterm and GST-14-3-30 was completely abolished in the S1403A mutant and partially reduced in S1567A and S1588A mutants. To further explore the requirement of S1403 phosphorylation for 14-3-30 binding, we created phosphomimetic substitutions of aspartate and glutamate at S1403 (S1403D and S1403E) on GFP-TRPM7-Cterm and tested their ability to interact with 14-3-30 (Figure 22C). It has been reported that 14-3-3 binding requires target site phosphorylation and cannot be replaced with phosphomimetic substitutions (91). Both GFP-TRPM7-Cterm-S1403D and S1403E mutants failed to interact with 14-3-30, indicating a specific requirement of S1403 phosphorylation for 14-3-30 binding.

To complete our analysis, we also tested for binding of 14-3-30 to S1502 and T1503 on TRPM7. GST pulldown purification assay using TRPM7-Cterm carrying

S1502A/T1503A double mutation showed a robust yet partially reduced interaction with 14-3-3 $\theta$ , eliminating S1502 and T1503 as strong 14-3-3 $\theta$  binding sites (Figure 22D). We also eliminate S1588 as a potential 14-3-3 $\theta$  binding site as literature review and a database search could not find evidence of this residue being a phosphorylation site.

We examined the status of *in vivo* phosphorylation of the potential 14-3-3 $\theta$  binding sites on TRPM7 using a mouse monoclonal antibody that recognizes phosphorylated 14-3-3 motifs containing phospho-serine residues (R/K-x-x-pS-x-P) (Figure 22E). HA-TRPM7-WT, HA-TRPM7-S1403A, TRPM7-S1502A/T1503A, and TRPM7-S1567A were transiently expressed in HEK-293T cells, immunoprecipitated, and probed with the phospho-14-3-3-motif antibody. The phospho-14-3-3-motif antibody recognized TRPM7-WT, demonstrating that this antibody is suitable for probing potential phosphorylated 14-3-3-binding motifs on TRPM7. Binding of the phospho-14-3-3-motif antibody to TRPM7 was significantly reduced in the TRPM7-S1403A mutant and also to a lesser degree for TRPM7-S1567A (Figure 22E). However, alanine mutations at S1502A/T1503A did not significantly reduce the recognition of TRPM7 by the phospho-14-3-3-motif antibody (Figure 22E), which could be explained by the fact that S1502 and T1503 fall within a partial motif not efficiently recognized by the antibody. There are many examples where dimerized 14-3-3 proteins bind to their targets using a stronger and a weaker binding site (90). Our results, collectively, suggest that S1403 is the major 14-3-3 binding site but that other weaker secondary sites may be involved in mediating the interaction between 14-3-3 $\theta$  and TRPM7 *in vivo*.

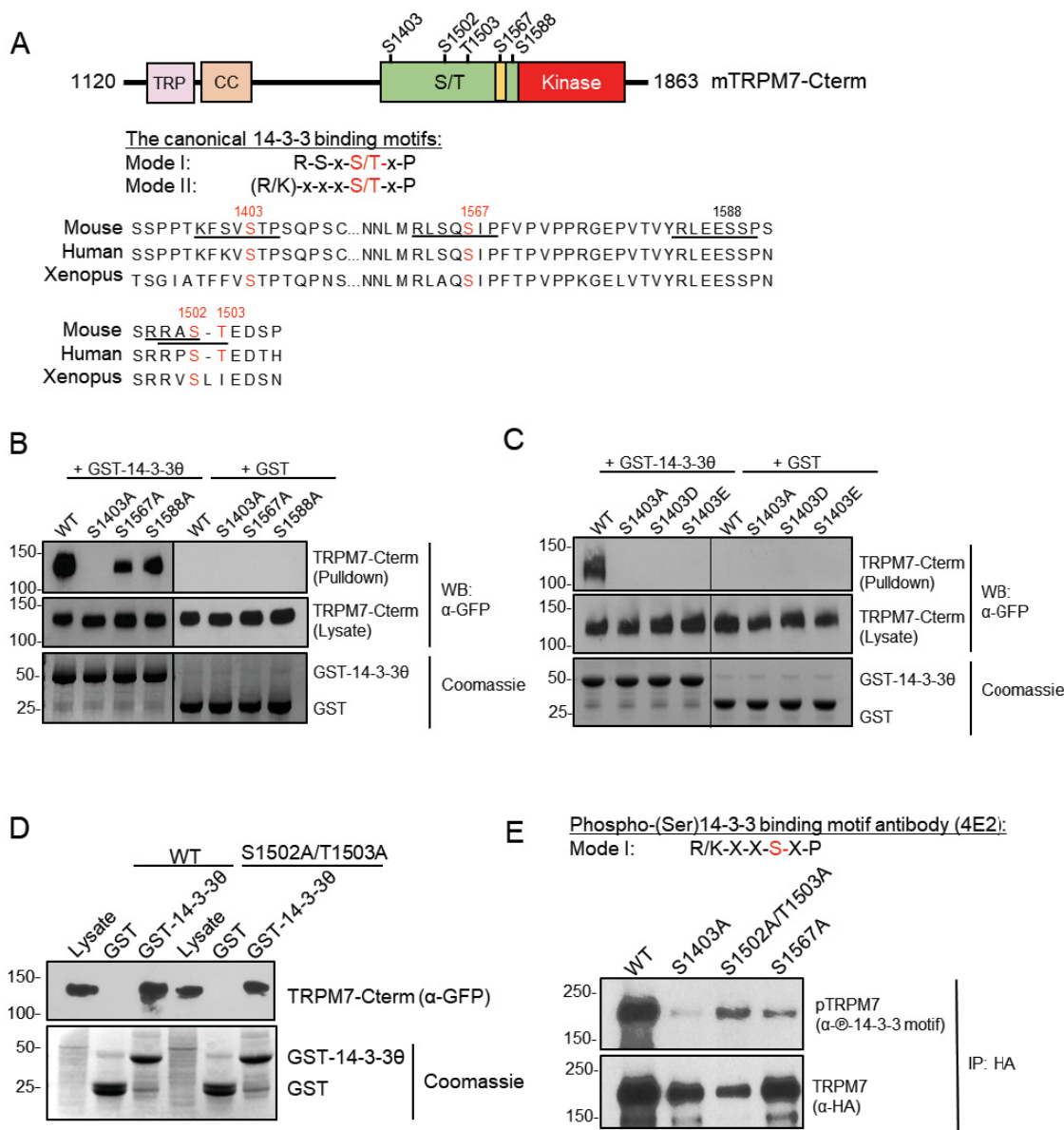


**Figure 22. Identification of S1403 as a major 14-3-30 binding site on TRPM7.**

(A) A schematic representation of TRPM7 shows the location of potential 14-3-3 binding sites on the protein's COOH terminus. Five conserved potential 14-3-3 binding motifs on TRPM7 are highlighted on the sequence alignment of mouse, human, and *Xenopus laevis* TRPM7. Residues identified as TRPM7 phosphorylation sites are highlighted in red. (B)-(D) GFP-TRPM7-Cterm-WT and mutant proteins were expressed in HEK-293T cells and subjected to GST-pull-down assays. (B) GST-14-3-30 failed to pull down GFP-TRPM7-

Cterm-S1403A and weakly pulled down S1567A and S1588A mutants. (C) Phosphomimetic substitutions at S1403 also disrupted binding between TRPM7-Cterm and 14-3-3 $\theta$ , demonstrating a requirement of S1403 phosphorylation for TRPM7 and 14-3-3 $\theta$  interaction. (D) GFP-TRPM7-Cterm-S1502/T1503 mutant showed weaker but robust interaction with GST-14-3-3 $\theta$ . Data combined suggest that S1403 is the major *in vitro* 14-3-3 $\theta$  binding site on GFP-TRPM7-Cterm. (E) TRPM7-S1403 phosphorylation accounts for the majority of the 14-3-3 binding signal on TRPM7 *in vivo*. HA-TRPM7-WT, S1403A, S1502A/T1503A, and S1567A were expressed in HEK-293T cells and immunoprecipitated using HA-agarose. An anti-phospho-(Ser)-14-3-3 motif antibody (4E2) was used to probe phosphorylated 14-3-3 binding sites on TRPM7. The total amount of TRPM7 on the beads were detected by SDS-PAGE and Western blotting using an anti-HA antibody.

#### **4.4 Mutation in TRPM7's 14-3-30-binding sites affect the distribution of the channel in polarized epithelial cells**

Having found that 14-3-30 binds to the channel, we were motivated to understand its functional impact on TRPM7. 14-3-3 proteins have also been shown to regulate the cellular localization of ion channels and transporters (92-96). Because TRPM7 kinase-inactivation affected the channel's localization and the interaction of TRPM7 with 14-3-30 is autophosphorylation-dependent, we investigated whether mutations of 14-3-3-binding sites would affect the localization of the channel in OK cells (Figure 23).

Compared to TRPM7-WT, which was found localized at basal-lateral and apical membranes in  $69.29 \pm 2.4$  % of expressing cells, peripheral localization of TRPM-S1403A ( $45.09 \pm 2.7\%$ ) and TRPM7-S1567A ( $35.89 \pm 2.4\%$ ) in OK cells was significantly lower (Figure 23B). The reduced peripheral membrane localization of TRPM7-S1403A and TRPM7-S1567A correlated to some extent with the mutants' inability to interact with 14-3-30 (Figure 22A). To determine whether the defect in peripheral localization of TRPM7-S1403A and TRPM7-S1567A was due to the lack of phosphorylation-dependent 14-3-3 binding or the loss of phosphorylation at the residue, we created phosphomimetic substitutions of S1403 (TRPM7-S1403D and TRPM7-S1403E) and S1567 (TRPM7-S1567D and TRPM7-S1567E) and tested these mutants' localization in OK cells. The rationale is that if the defect in S1403A and S1567A localization was due to the mutants' inability to interact with 14-3-30, phosphomimetic substitutions of the residue would not rescue their intracellular localization, as phosphomimetic substitutions could not biochemically reconstitute the interaction of substrate proteins with 14-3-30. On the other hand, if the localization defects of TRPM7-S1403A and TRPM7-S1567A mutants were

due to a lack of phosphorylation at these sites, phosphomimetic substitutions would be predicted to rescue the phenotype. We found that when over expressed in OK cells, phosphomimetic substitution mutants TRPM7-S1403D ( $41.4 \pm 1.6\%$ ) and TRPM7-S1403E ( $50.26 \pm 2.95\%$ ) did not localize to the cell periphery more efficiently than TRPM7-S1403A ( $45.09 \pm 2.738\%$ ). Indeed, both TRPM7-S1403D and TRPM7-S1403E exhibited significantly reduced peripheral localization compared to the TRPM7-WT ( $63.82 \pm 1.9\%$ ) (Figure 24B). This inability of S1403 phosphomimetic substitutions to rescue the localization defect corresponds with the failure of the mutant to elicit an *in vitro* interaction with 14-3-3 $\theta$ , as previously described in Figure 22C. As for residue S1567, while the glutamate mutant TRPM7-S1567E had a significant increase in the level of peripheral localization ( $53.28 \pm 3.0\%$ ) compared to the TRPM7-S1567A ( $35.89 \pm 2.4\%$ ), the aspartate mutant TRPM7-S1567D exhibited a severe trafficking defect, with very few channels localizing to the cell periphery ( $1.5 \pm 0.6\%$ ) (Figure 24). Though the two S1567 phosphomimetic substitutions produced completely opposite effects, the observation that S1567E could partially rescue the protein's peripheral localization suggests that phosphorylation of S1567 could contribute to the regulation of TRPM7 trafficking through 14-3-3 binding-independent mechanisms. Similarly, we also observed that the TRPM7-S1502A/T1503A mutant, which does not strongly interact with 14-3-3 $\theta$ , had a significant reduction in peripheral membrane localization ( $51.23 \pm 3.8\%$ ) compared to the wildtype protein (Figure 23). Taken together, these results indicate a critical role for TRPM7 phosphorylation in regulating channel localization and suggest that the phosphorylation-dependent interaction of 14-3-3 $\theta$  with the channel may be involved in regulating post-translational trafficking of TRPM7.

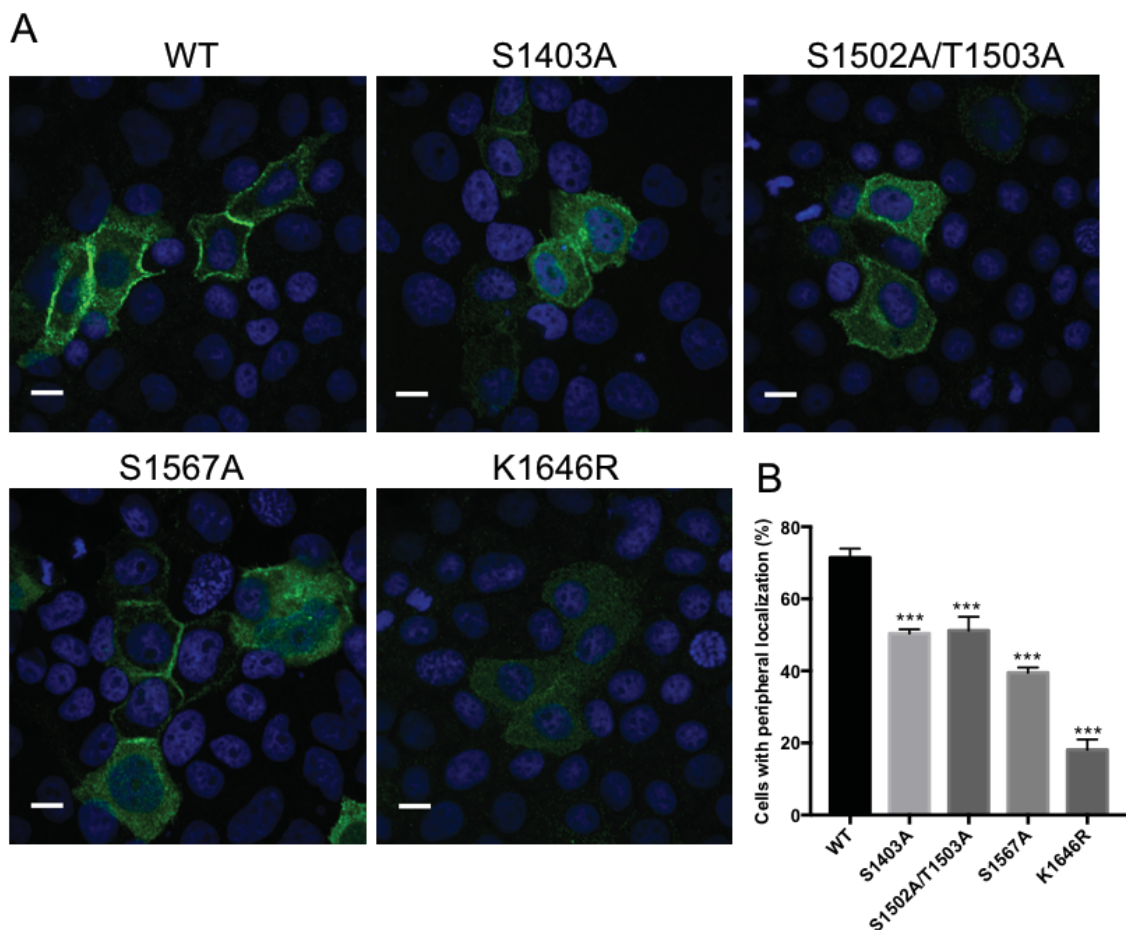


**Figure 23. Alanine substitution at TRPM7 phosphorylation sites alters TRPM7 localization in polarized epithelial cells.**

**(A)** Representative confocal images show cellular localization of HA-TRPM7-WT, S1403A, S1502A/T1503A, S1567A, and K1646R (green) in OK cells after 48h of expression (*Scale bar* 10 micron). **(B)** Quantification of the percentage of TRPM7-expressing OK cells with TRPM7 localized to basal-lateral or apical membranes. 400-600 cells from three independent experiments were examined (Mean  $\pm$  S.E.M, Student t-test, \*\*\*  $P < 0.0005$ ).

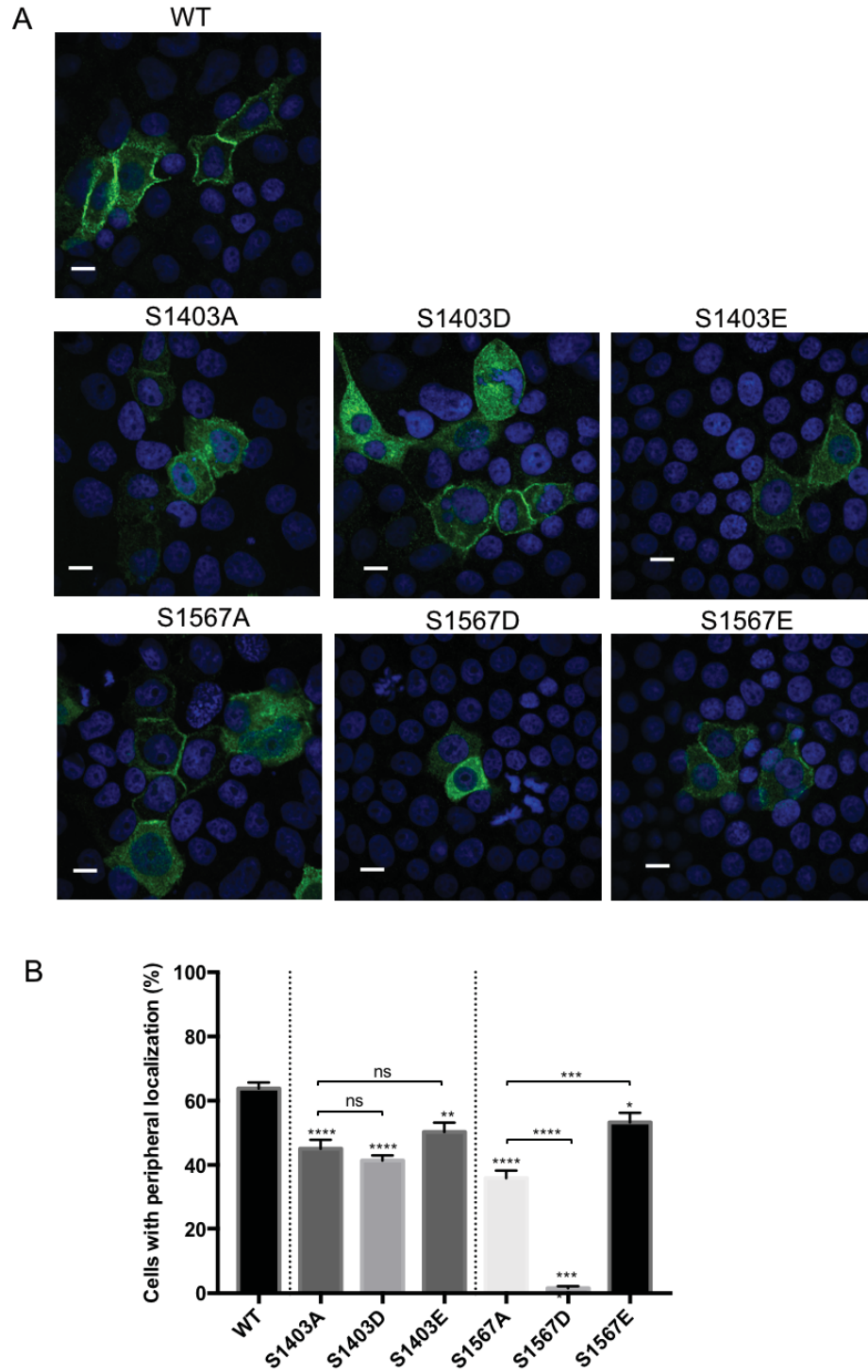


**Figure 24. Phosphomimetic substitutions at S1403 and S1567 differentially affects TRPM7's localization in polarized epithelial cells.**

(A) Representative confocal images show cellular localization of HA-TRPM7-WT, S1403A, S1403D, S1403E, S1567A, S1567D, and S1567E (green) in OK cells after 48 h of expression (*Scale bar* 10 micron). (B) Quantification of the percentage of TRPM7-expressing OK cells with TRPM7 localized to basal-lateral or apical membranes. 400-600 cells from three independent experiments examined (Mean  $\pm$  S.E.M, Student t-test, \*  $P < 0.05$ , \*\*\*  $P < 0.0005$ ).

#### **4.5 The interaction with 14-3-30 does not affect TRPM7 kinase's catalytic activity or the overall protein levels**

14-3-3 proteins have been shown to regulate the catalytic activity of many kinases (95,97,98). However, our data suggest that 14-3-30 binding with TRPM7 does not directly stimulate TRPM7's kinase activity (Figure 25). We immunopurified HA-TRPM7 and GFP-TRPM7-Cterm from HEK-293T cells and performed *in vitro* kinase assays using MBP as substrate in the presence of 5 µg of bacterially purified GST, GST-14-3-30-K49E, or GST-14-3-30 proteins. The addition of GST-14-3-30 proteins did not produce any significant change in the kinase activities of TRPM7 (Figure 25A). We also tested the intrinsic kinase activity of TRPM7 mutants harboring mutations in the 14-3-30-binding sites. HA-TRPM7-WT, HA-TRPM7-S1403A, HA-TRPM7-S1502A/T1503A, and HA-TRPM7-S1567A were expressed in HEK-293T cells and immunoprecipitated by anti-HA agarose. *In vitro* kinase assays showed that the 14-3-3-binding deficient TRPM7 mutants have normal kinase activity compared to the WT protein (Figure 25B).

We also investigated whether heterologous overexpression of 14-3-30 in HEK-293 cells would affect TRPM7 protein levels (Figure 25C). HA-TRPM7 was co-transfected with an empty FLAG vector, FLAG-14-3-30-WT, or FLAG-14-3-30-K49E in HEK-293T cells. As we expected, 14-3-3 proteins are already abundantly expressed in HEK-293T cells and overexpression of FLAG-14-3-30 did not affect the TRPM7 protein levels.

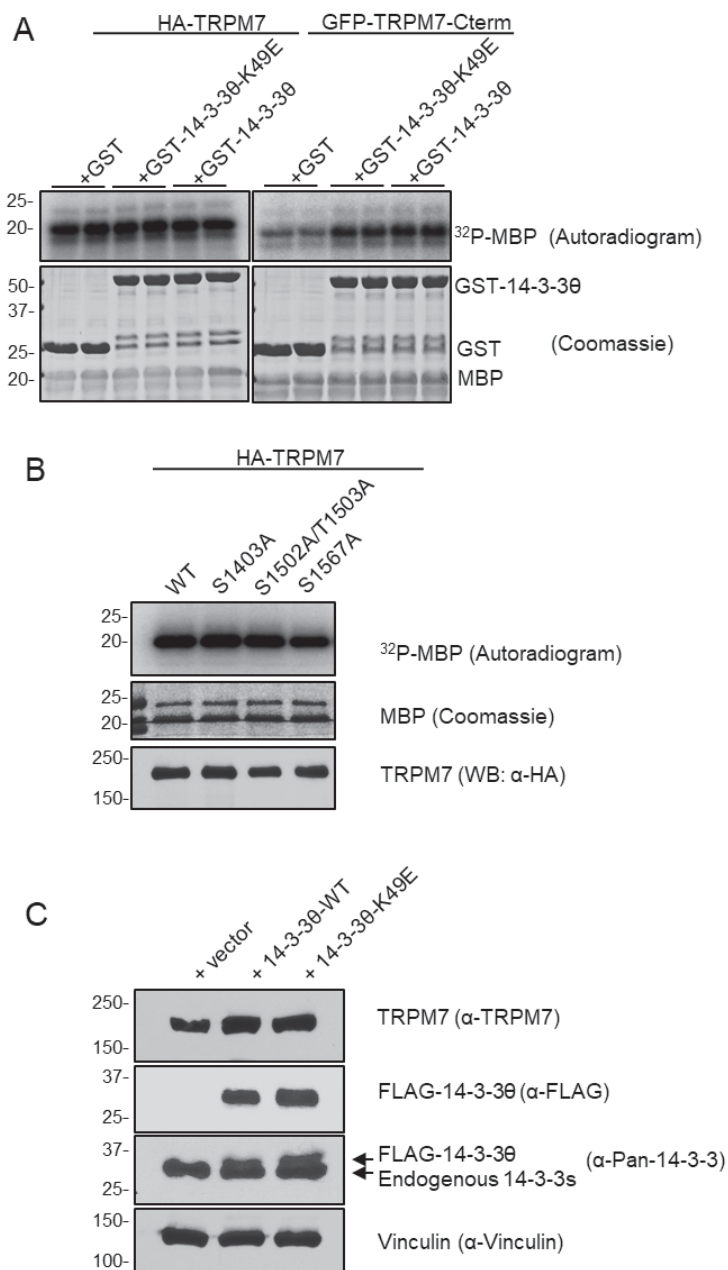


**Figure 25. Interaction with 14-3-3 $\theta$  does not affect TRPM7 kinase activity or protein levels.**

(A) Binding with 14-3-3 $\theta$  does not change TRPM7 kinase activity. HA-TRPM7 and GFP-TRPM7-Cterm proteins immunopurified from HEK-293T cells were subject to *in vitro* kinase reactions in the presence of 5  $\mu$ g of GST, GST-14-3-3 $\theta$ -K49E, or GST-14-3-3 $\theta$  proteins that are purified from bacteria. Proteins from the kinase assays were resolved by

SDS-PAGE and Coomassie staining. The incorporation of [ $\gamma$ - $^{32}$ P]ATP into the substrate MBP was assessed by autoradiography. (B) TRPM7 binding-deficient mutants have normal kinase activity. HA-TRPM7-WT, S1403A, S1502A/T1503A, and S1567A were expressed in HEK-293T cells and immunoprecipitated by anti-HA agarose. Proteins from the kinase reactions were resolved by SDS-PAGE and Coomassie staining. The incorporation of [ $\gamma$ - $^{32}$ P]ATP into the substrate MBP was assessed by autoradiography. Western blotting with an anti-HA antibody confirmed the equal loading of each TRPM7 variant. (C) Overexpression of 14-3-3 $\theta$  does not affect total TRPM7 protein levels. HA-TRPM7 was co-transfected with an empty FLAG vector, FLAG-14-3-3 $\theta$ -WT, or FLAG-14-3-3-K49E in HEK-293T cells. The total amounts of HA-TRPM7 and FLAG-14-3-3 $\theta$  in the lysates were assessed by SDS-PAGE and Western blotting with an anti-TRPM7 antibody and an anti-FLAG antibody respectively. A pan-14-3-3 antibody that recognizes all different 14-3-3 isoforms was used to compare the protein levels of transfected FLAG-14-3-3 $\theta$  with endogenous 14-3-3 proteins. Blotting of vinculin was used to demonstrate equal loading of samples.

## DISCUSSION

The aim of my thesis project is to understand how the unique channel-kinase TRPM7 is regulated by autophosphorylation and how the kinase activity of TRPM7 is itself regulated. We deployed LC-MS/MS to survey phosphorylation sites present on the protein using various expression constructs, examining phosphorylation both *in vivo* and *in vitro*. Here in the discussion, we propose mechanisms of actions for several potential regulatory phosphorylation sites we identified on TRPM7 (Figure 26) and propose a model by which kinase activity of TRPM7 affects the protein stability and cellular localization of the channel (Figure 27).

First, we identified two regulatory autophosphorylation sites that directly affect the kinase activity of TRPM7: S1565 and S1777. Residue S1565 is located on the alpha-helical exchange domain NH<sub>2</sub>-terminal to the kinase's catalytic domain. Although the exchange segment is essential for TRPM7 kinase dimerization and activation, our evidence suggests that S1565 phosphorylation does not directly affect the dimerization of the kinase. Instead, phosphomimetic substitutions at S1565 led to inactivation of the kinase's catalytic activity whereas substitution with alanine had no effect. Molecular modeling indicates that S1565, located on the exchange domain helix of one TRPM7 kinase monomer, is orientated toward the negatively charged surface of the N/D loop of the other kinase monomer within the dimer. The N/D loops have been speculated to participate in substrate binding and to control access of the substrate to the active sites of other alpha-kinase members such as MHCKs and eEF2K (71,73,99). Phosphorylation of TRPM7 S1565 would be predicted to cause electrostatic repulsion of the N/D loop away from S1565, which could adversely

affect substrate binding to the active site of the kinase. This “trans-inactivation” of the TRPM7 kinase dimer, mediated by phosphorylation of one exchange domain and the N/D loop displacement of the other monomer, is unique to the regulation of TRPM7 kinase activity, as other members of the alpha-kinase family do not have this dimerization feature.

Located on the same exchange domain as S1565, there is another highly frequently phosphorylated residue: S1567. S1567 was one of the most prominent autophosphorylation sites on the overexpressed TRPM7 identified in our study and has also been frequently observed in previous studies (42,59,60). It is not clear yet as to whether the phosphorylation S1565 and S1567 affects one and another. Unlike that of the S1565, the side chain of S1567 is exposed toward the surface of the protein. The exchange domain itself is an alpha helix, a preferred feature for substrates of the alpha-kinases, and is in proximity to the catalytic core of TRPM7 kinase. These features could explain why S1567 is a highly phosphorylated site. Yet, our analysis did not find evidence of TRPM7 S1567 phosphorylation directly affecting the catalytic activity of TRPM7. It is worth noting that both S1565 and S1567 are conserved on TRPM6’s exchange domain (equivalent to TRPM6 S1722 and T1724) and that TRPM6 T1724 is also frequently phosphorylated. The functional significance of S1567 phosphorylation remains largely unknown but may affect the localization of the channel, as will be discussed below.

Our study also identified S1777, located at the kinase’s catalytic center, as a mediator of TRPM7 kinase activity. We found that alanine mutation of TRPM7 S1777 enhanced the catalytic activity of the kinase, potentially making TRPM7-S1777A a “gain-of-function” mutant that could potentially be used for identifying physiologically relevant substrates of TRPM7. However, phosphomimetic substitutions at S1777 caused TRPM7

kinase inactivation. Molecular modeling studies suggest that phosphorylation of S1777 could potentially cause an electrostatic perturbation at the kinase's catalytic center, leading to a stop signal for TRPM7 catalysis.

Given that the proposed mechanisms for the regulation of TRPM7's kinase activity by S1565 and S1777 are derived from *in vitro* studies, future studies will be directed at determining whether phosphorylation of S1565 and S1777 plays a functional role *in vivo*. It is interesting that the phosphorylation of both S1565 and S1777 generated negative signals that led to an inactivation of TRPM7 kinase activity. Given what we have observed about the effect of TRPM7 kinase-inactivation on its the protein stability and cellular localization, it would be important to understand how these regulatory signals are regulated *in vivo* and whether they directly affect the cellular activities of TRPM7 by controlling TRPM7's kinase activity.

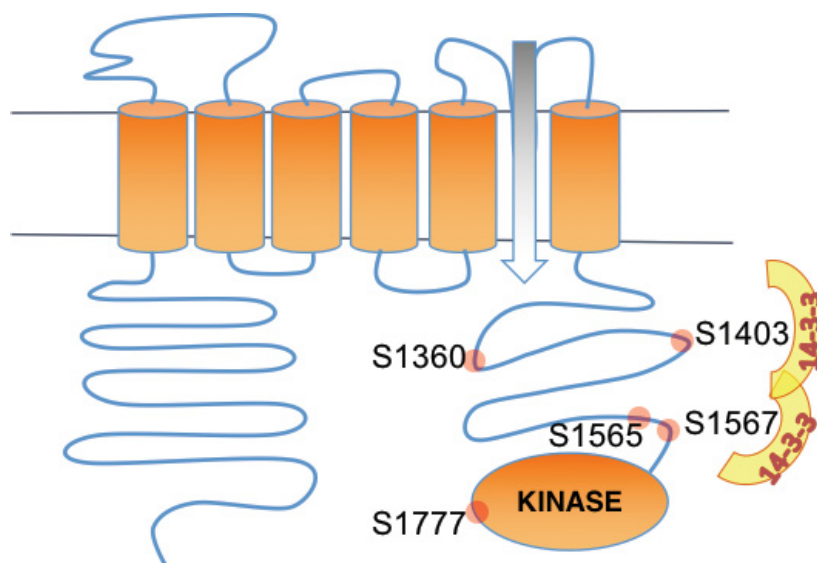


**Figure 26. Summary of identified regulatory TRPM7 phosphorylation sites.**

Residue S1565 and S1777 are regulatory sites for TRPM7's kinase activity. Phosphorylation of S1565 and S1777 leads to kinase inactivation, either by structurally affecting the access of substrate to the kinase or disrupting the electrostatics at the catalytic center of the kinase. Residue S1360 is a master regulator of post-translational processing of TRPM7, whose phosphorylation mediates TRPM7 protein stability and surface trafficking. Phosphorylated S1403 and S1567 constitute binding sites for signaling protein 14-3-30 and contribute to regulation of the cellular localization of the channel in polarized epithelial cells.

Having completed the *in vitro* analysis of mechanisms that modulate the kinase activity of TRPM7, we continued with the examination of the *in vivo* phosphorylation profiles of TRPM7 in order to have a better understanding of the function and regulation of TRPM7 in a physiologically relevant environment. We speculate that the *in vivo* phosphorylation sites of TRPM7 might vary depending on whether the protein is present on the cell surface, which is the case when TRPM7 is constitutively expressed in mammalian HEK-293 cells at a low basal level, or located in intracellular compartments such as the ER, which is where the channel is predominantly found when transiently expressed in the cells. Localization of TRPM7 to cell periphery reflect the channels in their final equilibrate states whereas TRPM7 in the intracellular compartments represent the proteins at various biosynthesis stages. Also, our previous studies found that overexpression of TRPM7 causes cell stress, which could also potentially influence the phosphorylation state of TRPM7 (100). To this end, we expressed TRPM7 under both overexpressed and constitutively expressed conditions in HEK-293 cells. Indeed, we found that the phosphorylation pattern detected for constitutively and lowly expressed TRPM7 differed from the one obtained for transiently overexpressed protein. On the lowly and constitutively expressed TRPM7, we found that residue S1360 was the most frequently phosphorylated residue *in vivo*, instead of residue S1567 found on the overexpressed protein. We acknowledge that this observation could be cell types specific to HEK-293 cells may vary under differential conditions.

With regard to TRPM7/TRPM6 *in vivo* heteromeric interactions, previous studies have reported that TRPM6 can cross-phosphorylate TRPM7 and that the TRPM6 kinase activity affects the intracellular localization of TRPM7. It was previously reported that co-

expression of TRPM6-WT, but not the TRPM6 kinase-dead mutant, caused the normally cellularly diffuse TRPM7 staining in HEK-293 cells to change to intracellular clusters (64). Our analysis of TRPM6/TRPM7 phosphorylation indeed identified sites on TRPM7 that are cross-phosphorylated by TRPM6, many of which overlap with TRPM7's autophosphorylation sites (such as S1224, S1255, S1299, S1403, S1565, S1567, and S1693). We speculate that these shared phosphorylation residues could potentially serve as regulatory signals governing the activity of TRPM7 in mammalian cells. We also found that TRPM6 is readily autophosphorylated *in vivo* and shares many conserved phosphorylation sites with TRPM7 (e.g., the aforementioned T1824 on TRPM6's exchange segment). TRPM6 has a more specific tissue distribution in kidney and colon, which is in contrast to the ubiquitously expressed pattern of TRPM7 (6,10,27). Therefore, our analysis of TRPM6 phosphorylation serves as an excellent starting point for investigating how the kinase activity of TRPM6 regulates this closely related yet functionally non-redundant homolog of TRPM7, and how these two channel-kinases may be regulated differently by their own kinase activities.

One important aim of our current investigations of TRPM7 kinase activity is to understand whether TRPM7 is functionally regulated by its intrinsic kinase activity. We focused our investigation on the role of TRPM7's kinase activity in controlling protein stability and intracellular localization of the channel (Figure 27).

Based on the previous observation that TRPM7 kinase mutants have lower protein expression levels compared to the WT, we continued our investigation into whether kinase-inactivation leads to a less stable protein with a shorter half-life. Indeed, using a

cycloheximide chase assay, we found that the kinase-inactive TRPM7 has a faster turnover rate than the WT TRPM7 when overexpressed in HEK-293 cells. We subsequently found that the TRPM7 kinase-inactive mutant has a higher level of ubiquitylation than the WT channel and that proteasome inhibition is effective in preventing degradation of the TRPM7 kinase mutant. All of these findings suggest that kinase inactivation of TRPM7 makes the channel more susceptible to proteasome-mediated degradation and that TRPM7's kinase activity is important in maintaining the stability of the protein.

We also inspected the effects of kinase-inactivation on the cellular localization of the channel. Our previous investigation of TRPM7 localization was hindered by the fact that heterologously expressed TRPM7 in HEK-293 cells tend to accumulate at perinuclear structures, whereas constitutively expressed TRPM7 levels were too low for immunocytochemical analysis. In this present study, we adopted the proximal tubule epithelial cell line OK cells as a cellular model to examine the cellular localization of TRPM7. OK cells are polarized epithelial cells frequently used to study the localization of ion channels and transporters that are natively expressed in the kidney proximal tubule (83). Our immunocytochemical analysis revealed that TRPM7 kinase inactivation led to intracellular retention of the channel in OK cells whereas TRPM7 WT protein readily localized to the cell periphery. A closer examination of the TRPM7 WT localization in OK cells found that when heterologously expressed, TRPM7 is more readily localized at the basal-lateral membrane in the OK cells and to a lesser extent at the apical membrane. In polarized kidney epithelial cells, the apical membrane should be where ion exchange occurs between the cells and the tubular fluid (83). We suspect that the limited localization of TRPM7 to the apical membrane is likely due to a shortage of scaffolding proteins to

properly traffic the overexpressed TRPM7 to the apical membrane, where we expect the channel to be normally localized. Nevertheless, OK cells provided us with a physiologically relevant platform to investigate the role of the TRPM7 kinase in regulating the cellular localization of the channel.

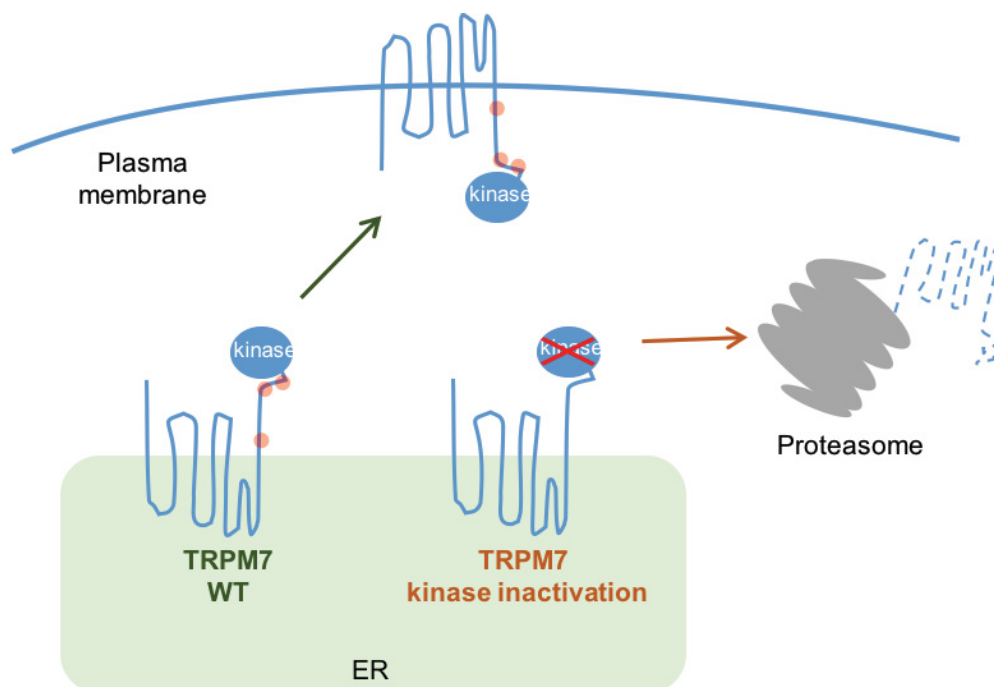


**Figure 27. Proposed model of TRPM7 kinase function in mediating TRPM7 protein stability and cellular localization.**

TRPM7 kinase activity is important for post-translational processing of the channel. Inactivation of TRPM7 kinase leads to a faster turnover of the protein through proteasome-mediated degradation and intracellular retention of the channel. We propose that a key regulatory residue, S1360 is phosphorylated first, either by TRPM7's intrinsic kinase activity or other extrinsic cellular kinases. The phosphorylation of S1360 provides a permissive signal for TRPM7 biosynthesis and cellular trafficking. Once a properly folded TRPM7 becomes fully activated and exits the ER, other autophosphorylation events may contribute to the regulation of the channel's protein stability, surface trafficking, and interaction with other cellular proteins. Red dots: TRPM7 phosphorylated sites.

Inspired by the exciting observation that TRPM7 kinase inactivation leads to faster protein turnover and defects in cellular localization, we continued our investigation into the role of phosphorylation of specific residues in mediating TRPM7 protein stability and localization. By screening a panel of TRPM7 mutants where alanine substitutions were introduced to frequently identified TRPM7 phosphorylation sites, we found that the alanine mutation at S1360, the most frequently *in vivo* phosphorylation sites identified on the constitutively expressed TRPM7, renders the protein sensitive to MG132-induced protein accumulation, a phenotype observed for the TRPM7 kinase-inactive mutants. More significantly, phosphomimetic substitutions at this site reversed the MG132 sensitivity of the S1360 alanine mutant, suggesting that S1360 phosphorylation protects TRPM7 from being targeted for proteasome degradation. Following our discovery of the role of S1360 phosphorylation on TRPM7 protein stability, we next examined the effect of S1360 mutations on the localization of the channel in OK cells. Remarkably, while the TRPM7-S1360A mutant exhibited phenotypes of intracellular retention, S1360 phosphomimetic substitutions effectively rescued the channel to peripheral localizations in OK cells. These results suggest that S1360 phosphorylation not only mediates proteasome-dependent turnover of TRPM7 but also play an important role in facilitating the surface trafficking of the channel in polarized epithelial cells.

Interestingly, our MS analysis found that S1360 was also phosphorylated on the overexpressed TRPM7 kinase-inactive mutant, either expressed alone or co-expressed with TRPM6. It is possible that S1360 is both an autophosphorylation site and a site targeted by other extrinsic kinases including TRPM6. We attempted to introduce phosphomimetic substitutions on S1360 for the kinase-inactive TRPM7 mutant but were unable to rescue

the kinase mutant from being targeted by the proteasome, which suggests that there are other regulatory autophosphorylation sites involved in orchestrating the posttranslational processing of the protein. We speculate that S1360 phosphorylation is a master regulatory signal for TRPM7 biosynthesis and trafficking, acting as a first step to ensuring that a fully translated and functionally assembled TRPM7 can exit the ER and be trafficked to designated cellular locations (Figure 27). Biochemically, TRPM7 S1360 phosphorylation may interfere with ubiquitylation of TRPM7, possibly by preventing the binding of proteasome-related proteins such as E3 ubiquitin-ligases with TRPM7. Given the significant revelations about this specific residue, further investigation is required to unravel the *in vivo* intracellular signals that mediate the phosphorylation of this key regulatory residue.

In addition to directly affecting TRPM7's biophysical activity, we speculate that the kinase function of TRPM7 could impose regulatory functions to the channel by mediating the interaction of TRPM7 with other intracellular proteins. We placed our attention onto the signaling protein 14-3-3 $\theta$ , which was identified as a TRPM7 binding partner in one of our earlier studies (76). 14-3-3 $\theta$  belongs to a family of phospho-binding proteins regulating the activities of a diverse range of cellular proteins. Through biochemical analysis, we discovered that TRPM7 interacts with 14-3-3 $\theta$  in a kinase-dependent manner on phosphorylated S1403 and S1567. Our study did not find a direct impact of 14-3-3 $\theta$  binding on TRPM7's protein levels or kinase activity, but did uncover a role for 14-3-3 $\theta$ 's interaction in mediating TRPM7 intracellular localization. In OK cells, we found that alanine mutation at the major 14-3-3 binding site on TRPM7 (TRPM7-

S1403A) significantly interfered with localization of the channel to basal-lateral and apical membranes. Phosphomimetic substitutions of S1403 (TRPM7-S1403D and S1403E) similarly exhibited defects in peripheral localization, agreeing with previous findings that phosphomimetic substitutions of the major 14-3-3 $\theta$  binding site are not effective in rescuing the interaction between TRPM7 and 14-3-3 $\theta$ . These results indicate that it is the disruption of phosphorylation-dependent 14-3-3 $\theta$  interaction, not a lack of phosphorylation at this residue, that contributes to the defect of localization of the mutant channels. Combining the biochemical analysis of TRPM7 and 14-3-3 $\theta$  interaction and the observations of TRPM7 mutants' cellular localization, we propose that autophosphorylation-induced 14-3-3 $\theta$  binding could be part of the mechanisms by which the kinase activity of TRPM7 regulates the trafficking and localization of the channel. This hypothesis is supported by a recent discovery that several 14-3-3 isoforms (14-3-3 $\theta$ , 14-3-3 $\epsilon$ , and 14-3-3 $\beta$ ) are enriched in TRPM7-containing intracellular vesicles, signifying a possibility of 14-3-3 proteins regulating TRPM7 localization by affecting vesicle trafficking (101).

Of course, we also speculate that there are 14-3-3 $\theta$ -independent mechanisms that may also affect TRPM7's localization. For example, TRPM7 exhibited peripheral localization defects when S1567, the weaker 14-3-3 $\theta$  binding site, was mutated to either alanine or aspartate but was partially rescued when the S1567 was replaced with a glutamate substitution. S1567 itself is a frequently phosphorylated residue of TRPM7, as discussed above, and therefore could mediate TRPM7 localization through both 14-3-3 $\theta$ -dependent and independent manners. We also found that mutation of TRPM7-S1502/T1503, which does not mediate 14-3-3 binding to the channel, also disrupted

TRPM7 localization in the OK cells. Thus, additional work is needed to determine how other TRPM7 phosphorylation sites affect the trafficking of the channel and whether other cellular proteins are involved in such regulation in different cell types and under different physiological conditions.

In summary, our comprehensive analysis of TRPM7 phosphorylation has given us significant insights into the function and regulation of this unique channel-kinase. Our discovery that phosphorylation of TRPM7-S1565 inactivates kinase activity without affecting kinase-dimerization provides a mechanism by which TRPM7 kinase catalytic activity can be controlled. Our analysis of TRPM7 kinase function revealed that TRPM7's intrinsic kinase activity could potentially regulate proteasome-mediated degradation of the channel and targeting of the channel to the proper cellular location in polarized epithelial cells. We identified that phosphorylation of residue S1360 is involved in both protein stability and cellular localization of the channel, highlighting a role for S1360 as a master regulator of TRPM7 posttranslational processing. Other phosphorylation events at residues such as S1403 and S1567 likely also contribute to the trafficking of the channel in epithelial cells. We believe that the kinase-induced interaction of TRPM7 with a signaling protein 14-3-3 could be a part of the machinery that mediates TRPM7 intracellular trafficking.

The findings that the kinase activity of TRPM7 functionally regulates the channel protein stability and cellular localization finally allows us to answer the question of why Nature endows an ion channel its own kinase function. TRPM7-mediated ion conductance is essential for early embryonic development and the proliferation and survival of differentiated cells. The intrinsic kinase activity of TRPM7 would allow a robust regulation

of the channel in response to different environmental stimulations at various developmental stages. Since TRPM7 is heavily phosphorylated *in vivo*, we speculate that each of the autophosphorylation sites could impose unique regulatory mechanisms to the ion channel in response to various cellular signals. We acknowledge that the effect of kinase-inactivation on TRPM7 protein stability and localization may be cell-type specific, and would require further exploration using different cell types.

Recently TRPM7 kinase-inactivation knockin mice have been generated in order to better understand the physiological significance of TRPM7 kinase activity. Many novel physiological phenotypes have been attributed to TRPM7 kinase inactivation in processes such as mast cell degranulation, T cell gut-homing and proliferation, ameloblast differentiation, and platelet cell survival (44-49). In light of our discovery on the role of TRPM7 kinase activity on channel protein stability and localization, extra care must be taken in teasing apart the mechanistic origins of the observed phenotypes: is it due to a loss of intrinsic TRPM7 kinase activity or a disruption of the regulation of the channel. Meanwhile, TRPM7's kinase activity has been associated with a wide range of cellular activities, including phosphorylation of histones, EF2K, and STIM, and regulation of gene transcription, protein translation, and store-dependent  $Ca^{2+}$  entry (49,51,57). Therefore, a further understanding of mechanisms and *in vivo* signaling pathways that regulate TRPM7 kinase activity are essential in deciphering the function and regulation of the channel in mammalian cells.

## REFERENCES

1. Nadler, M. J., Hermosura, M. C., Inabe, K., Perraud, A. L., Zhu, Q., Stokes, A. J., Kurosaki, T., Kinet, J. P., Penner, R., Scharenberg, A. M., and Fleig, A. (2001) LTRPC7 is a Mg-ATP-regulated divalent cation channel required for cell viability. *Nature* **411**, 590-595
2. Runnels, L. W., Yue, L., and Clapham, D. E. (2001) TRP-PLIK, a bifunctional protein with kinase and ion channel activities. *Science* **291**, 1043-1047
3. Ryazanova, L. V., Pavur, K. S., Petrov, A. N., Dorovkov, M. V., and Ryazanov, A. G. (2001) Novel type of signaling molecules: protein kinases covalently linked with ion channels. *Mol Biol* **35**, 271-283
4. Monteilh-Zoller, M. K., Hermosura, M. C., Nadler, M. J., Scharenberg, A. M., Penner, R., and Fleig, A. (2003) TRPM7 provides an ion channel mechanism for cellular entry of trace metal ions. *J Gen Physiol* **121**, 49-60
5. Ryazanov, A. G. (2002) Elongation factor-2 kinase and its newly discovered relatives. *FEBS let* **514**, 26-29
6. Schlingmann, K. P., Weber, S., Peters, M., Niemann Nejsum, L., Vitzthum, H., Klingel, K., Kratz, M., Haddad, E., Ristoff, E., Dinour, D., Syrrou, M., Nielsen, S., Sassen, M., Waldegger, S., Seyberth, H. W., and Konrad, M. (2002) Hypomagnesemia with secondary hypocalcemia is caused by mutations in TRPM6, a new member of the TRPM gene family. *Nat Genet* **31**, 166-170
7. Fleig, A., and Chubanov, V. (2014) *Mammalian Transient Receptor Potential (TRP) Cation Channels: Volume I*. 5th Ed., Springer Berlin Heidelberg, Heidelberg
8. Hofmann, T., Chubanov, V., Chen, X., Dietz, A. S., Gudermann, T., and Montell, C. (2010) *Drosophila* TRPM channel is essential for the control of extracellular magnesium levels. *PloS one* **5**, e10519
9. Lambie, E. J., Bruce, R. D., 3rd, Zielich, J., and Yuen, S. N. (2015) Novel alleles of *gon-2*, a *C. elegans* ortholog of mammalian TRPM6 and TRPM7, obtained by genetic reversion screens. *PloS one* **10**, e0143445
10. Fonfria, E., Murdock, P. R., Cusdin, F. S., Benham, C. D., Kelsell, R. E., and McNulty, S. (2006) Tissue distribution profiles of the human TRPM cation channel family. *J Recept Signal Transduct* **26**, 159-178
11. Jin, J., Desai, B. N., Navarro, B., Donovan, A., Andrews, N. C., and Clapham, D. E. (2008) Deletion of *trpm7* disrupts embryonic development and thymopoiesis without altering Mg<sup>2+</sup> homeostasis. *Science* **322**, 756-760

12. Liu, W., Su, L. T., Khadka, D. K., Mezzacappa, C., Komiya, Y., Sato, A., Habas, R., and Runnels, L. W. (2011) TRPM7 regulates gastrulation during vertebrate embryogenesis. *Dev Biol* **350**, 348-357
13. Jin, J., Wu, L.J., Jun, J., Cheng, X., Xu, H., Andrews, N. C., and Clapham, D. E. (2012) The channel kinase, TRPM7, is required for early embryonic development. *Proc the Natl Acad Sci U S A* **109**, E225–E233
14. Elizondo, M. R., Arduini, B. L., Paulsen, J., MacDonald, E. L., Sabel, J. L., Henion, P. D., Cornell, R. A., and Parichy, D. M. (2005) Defective skeletogenesis with kidney stone formation in dwarf zebrafish mutant for *trpm7*. *Curr Biol* **15**, 667-671
15. McNeill, M. S., Paulsen, J., Bonde, G., Burnight, E., Hsu, M. Y., and Cornell, R. A. (2007) Cell death of melanophores in zebrafish *trpm7* mutant embryos depends on melanin synthesis. *J Invest Dermatol* **127**, 2020-2030
16. Yee, N. S., Zhou, W., and Liang, I. C. (2011) Transient receptor potential ion channel *Trpm7* regulates exocrine pancreatic epithelial proliferation by  $Mg^{2+}$ -sensitive *Socs3a* signaling in development and cancer. *Dis Models Mech* **4**, 240-254
17. Decker, A. R., McNeill, M. S., Lambert, A. M., Overton, J. D., Chen, Y. C., Lorca, R. A., Johnson, N. A., Brockerhoff, S. E., Mohapatra, D. P., MacArthur, H., Panula, P., Masino, M. A., Runnels, L. W., and Cornell, R. A. (2014) Abnormal differentiation of dopaminergic neurons in zebrafish *trpm7* mutant larvae impairs development of the motor pattern. *Dev Biol* **386**, 428-439
18. Schmitz, C., Perraud, A. L., Johnson, C. O., Inabe, K., Smith, M. K., Penner, R., Kurosaki, T., Fleig, A., and Scharenberg, A. M. (2003) Regulation of vertebrate cellular  $Mg^{2+}$  homeostasis by TRPM7. *Cell* **114**, 191-200
19. Clark, K., Langeslag, M., van Leeuwen, B., Ran, L., Ryazanov, A. G., Figdor, C. G., Moolenaar, W. H., Jalink, K., and van Leeuwen, F. N. (2006) TRPM7, a novel regulator of actomyosin contractility and cell adhesion. *EMBO J* **25**, 290-301
20. Su, L. T., Agapito, M. A., Li, M., Simonson, W. T., Huttenlocher, A., Habas, R., Yue, L., and Runnels, L. W. (2006) TRPM7 regulates cell adhesion by controlling the calcium-dependent protease calpain. *J Biol Chem* **281**, 11260-11270
21. Du, J., Xie, J., Zhang, Z., Tsujikawa, H., Fusco, D., Silverman, D., Liang, B., and Yue, L. (2010) TRPM7-mediated  $Ca^{2+}$  signals confer fibrogenesis in human atrial fibrillation. *Circ Res* **106**, 992-1003
22. Oh, H. G., and Chung, S. (2017) Activation of transient receptor potential melastatin 7 (TRPM7) channel increases basal autophagy and reduces amyloid beta-peptide. *Biochem Biophys Res Commun* **493**, 494-499

23. Schappe, M. S., Szteyn, K., Stremaska, M. E., Mendu, S. K., Downs, T. K., Seegren, P. V., Mahoney, M. A., Dixit, S., Krupa, J. K., Stipes, E. J., Rogers, J. S., Adamson, S. E., Leitinger, N., and Desai, B. N. (2018) Chanzyme TRPM7 mediates the  $\text{Ca}^{2+}$  influx essential for lipopolysaccharide-induced toll-like receptor 4 endocytosis and macrophage activation. *Immunity* **48**, 59-74
24. Tani, D., Monteilh-Zoller, M. K., Fleig, A., and Penner, R. (2007) Cell cycle-dependent regulation of store-operated I(CRAC) and  $\text{Mg}^{2+}$ -nucleotide-regulated MagNuM (TRPM7) currents. *Cell Calcium* **41**, 249-260
25. Faouzi, M., Kilch, T., Horgen, F. D., Fleig, A., and Penner, R. (2017) The TRPM7 channel kinase regulates store-operated calcium entry. *J Physiol* **595**, 3165-3180
26. Chubanov, V., Waldegger, S., Mederos y Schnitzler, M., Vitzthum, H., Sassen, M. C., Seyberth, H. W., Konrad, M., and Gudermann, T. (2004) Disruption of TRPM6/TRPM7 complex formation by a mutation in the *TRPM6* gene causes hypomagnesemia with secondary hypocalcemia. *Proc the Natl Acad Sci U S A* **101**, E2894-E2899
27. Walder, R. Y., Landau, D., Meyer, P., Shalev, H., Tsolia, M., Borochoowitz, Z., Boettger, M. B., Beck, G. E., Englehardt, R. K., Carmi, R., and Sheffield, V. C. (2002) Mutation of *TRPM6* causes familial hypomagnesemia with secondary hypocalcemia. *Nat Genet* **31**, 171-174
28. Coulter, M., Colvin, C., Korf, B., Messiaen, L., Tuanama, B., Crowley, M., Crossman, D. K., and McCormick, K. (2015) Hypomagnesemia due to two novel *TRPM6* mutations. *J Pediatr Endocrinol Metab* **28**, 1373-1378
29. Astor, M. C., Lovas, K., Wolff, A. S., Nedrebo, B., Bratland, E., Steen-Johnsen, J., and Husebye, E. S. (2015) Hypomagnesemia and functional hypoparathyroidism due to novel mutations in the Mg-channel TRPM6. *Endocr Connect* **4**, 215-222
30. Ryazanova, L. V., Rondon, L. J., Zierler, S., Hu, Z., Galli, J., Yamaguchi, T. P., Mazur, A., Fleig, A., and Ryazanov, A. G. (2010) TRPM7 is essential for  $\text{Mg}^{2+}$  homeostasis in mammals. *Nat Commun* **1**, 109
31. Aarts, M., Iihara, K., Wei, W. L., Xiong, Z. G., Arundine, M., Cerwinski, W., MacDonald, J. F., and Tymianski, M. (2003) A key role for TRPM7 channels in anoxic neuronal death. *Cell* **115**, 863-877
32. Zhang, J., Zhao, F., Zhao, Y., Wang, J., Pei, L., Sun, N., and Shi, J. (2011) Hypoxia induces an increase in intracellular magnesium via transient receptor potential melastatin 7 (TRPM7) channels in rat hippocampal neurons *in vitro*. *J Biol Chem* **286**, 20194-20207

33. Guilbert, A., Gautier, M., Dhennin-Duthille, I., Haren, N., Sevestre, H., and Ouadid-Ahidouch, H. (2009) Evidence that TRPM7 is required for breast cancer cell proliferation. *Am J Physiol Cell Physiol* **297**, C493-502
34. Middelbeek, J., Kuipers, A. J., Henneman, L., Visser, D., Eidhof, I., van Horsen, R., Wieringa, B., Canisius, S. V., Zwart, W., Wessels, L. F., Sweep, F. C., Bult, P., Span, P. N., van Leeuwen, F. N., and Jalink, K. (2012) TRPM7 is required for breast tumor cell metastasis. *Cancer Res* **72**, 4250-4261
35. Sun, Y., Selvaraj, S., Varma, A., Derry, S., Sahmoun, A. E., and Singh, B. B. (2013) Increase in serum  $\text{Ca}^{2+}/\text{Mg}^{2+}$  ratio promotes proliferation of prostate cancer cells by activating TRPM7 channels. *J Biol Chem* **288**, 255-263
36. Wang, J., Liao, Q. J., Zhang, Y., Zhou, H., Luo, C. H., Tang, J., Wang, Y., Tang, Y., Zhao, M., Zhao, X. H., Zhang, Q. Y., and Xiao, L. (2014) TRPM7 is required for ovarian cancer cell growth, migration and invasion. *Biochem Biophys Res Commun* **454**, 547-553
37. Yee, N. S., Kazi, A. A., Li, Q., Yang, Z., Berg, A., and Yee, R. K. (2015) Aberrant over-expression of TRPM7 ion channels in pancreatic cancer: required for cancer cell invasion and implicated in tumor growth and metastasis. *Biol Open* **4**, 507-514
38. Gao, S. L., Kong, C. Z., Zhang, Z., Li, Z. L., Bi, J. B., and Liu, X. K. (2017) TRPM7 is overexpressed in bladder cancer and promotes proliferation, migration, invasion and tumor growth. *Oncol Rep* **38**, 1967-1976
39. Chen, L., Cao, R., Wang, G., Yuan, L., Qian, G., Guo, Z., Wu, C. L., Wang, X., and Xiao, Y. (2017) Downregulation of TRPM7 suppressed migration and invasion by regulating epithelial-mesenchymal transition in prostate cancer cells. *Med Oncol* **34**, 127
40. Hermosura, M. C., Monteilh-Zoller, M. K., Scharenberg, A. M., Penner, R., and Fleig, A. (2002) Dissociation of the store-operated calcium current ICRAC and the Mg-nucleotide-regulated metal ion current MagNuM. *J Physiol* **539**, 445-458
41. Demeuse, P., Penner, R., and Fleig, A. (2006) TRPM7 channel is regulated by magnesium nucleotides via its kinase domain. *J Gen Physiol* **127**, 421-434
42. Matsushita, M., Kozak, J. A., Shimizu, Y., McLachlin, D. T., Yamaguchi, H., Wei, F. Y., Tomizawa, K., Matsui, H., Chait, B. T., Cahalan, M. D., and Nairn, A. C. (2005) Channel function is dissociated from the intrinsic kinase activity and autophosphorylation of TRPM7/ChaK1. *J Biol Chem* **280**, 20793-20803
43. Kaitsuka, T., Katagiri, C., Beesetty, P., Nakamura, K., Hourani, S., Tomizawa, K., Kozak, J. A., and Matsushita, M. (2014) Inactivation of TRPM7 kinase activity does not impair its channel function in mice. *Sci Rep* **4**, 5718

44. Ryazanova, L. V., Hu, Z., Suzuki, S., Chubanov, V., Fleig, A., and Ryazanov, A. G. (2014) Elucidating the role of the TRPM7 alpha-kinase: TRPM7 kinase inactivation leads to magnesium deprivation resistance phenotype in mice. *Sci Rep* **4**, 7599
45. Zierler, S., Sumoza-Toledo, A., Suzuki, S., Duill, F. O., Ryazanova, L. V., Penner, R., Ryazanov, A. G., and Fleig, A. (2016) TRPM7 kinase activity regulates murine mast cell degranulation. *J Physiol* **594**, 2957-2970
46. Romagnani, A., Vettore, V., Rezzonico-Jost, T., Hampe, S., Rottoli, E., Nadolni, W., Perotti, M., Meier, M. A., Hermanns, C., Geiger, S., Wennemuth, G., Recordati, C., Matsushita, M., Muehlich, S., Proietti, M., Chubanov, V., Gudermann, T., Grassi, F., and Zierler, S. (2017) TRPM7 kinase activity is essential for T cell colonization and alloreactivity in the gut. *Nat Commun* **8**, 1917
47. Beesetty, P., Wiczerzak, K. B., Gibson, J. N., Kaitsuka, T., Luu, C. T., Matsushita, M., and Kozak, J. A. (2018) Inactivation of TRPM7 kinase in mice results in enlarged spleens, reduced T-cell proliferation and diminished store-operated calcium entry. *Sci Rep* **8**, 3023
48. Ogata, K., Tsumuraya, T., Oka, K., Shin, M., Okamoto, F., Kajiyama, H., Katagiri, C., Ozaki, M., Matsushita, M., and Okabe, K. (2017) The crucial role of the TRPM7 kinase domain in the early stage of amelogenesis. *Sci Rep* **7**, 18099
49. Gotru, S. K., Chen, W., Kraft, P., Becker, I. C., Wolf, K., Stritt, S., Zierler, S., Hermanns, H. M., Rao, D., Perraud, A. L., Schmitz, C., Zahedi, R. P., Noy, P. J., Tomlinson, M. G., Dandekar, T., Matsushita, M., Chubanov, V., Gudermann, T., Stoll, G., Nieswandt, B., and Braun, A. (2017) TRPM7 (transient receptor potential melastatin-like 7 channel) kinase controls calcium responses in arterial thrombosis and stroke in mice. *Arterioscler Thromb Vasc Biol* **38**, 344-352
50. Desai, B. N., Krapivinsky, G., Navarro, B., Krapivinsky, L., Carter, B. C., Febvay, S., Dellinger, M., Penumaka, A., Ramsey, I. S., Manasian, Y., and Clapham, D. E. (2012) Cleavage of TRPM7 releases the kinase domain from the ion channel and regulates its participation in Fas-induced apoptosis. *Dev Cell* **22**, 1149-1162
51. Krapivinsky, G., Krapivinsky, L., Manasian, Y., and Clapham, D. E. (2014) The TRPM7 chanzyme is cleaved to release a chromatin-modifying kinase. *Cell* **157**, 1061-1072
52. Krapivinsky, G., Krapivinsky, L., Renthal, N. E., Santa-Cruz, A., Manasian, Y., and Clapham, D. E. (2017) Histone phosphorylation by TRPM6's cleaved kinase attenuates adjacent arginine methylation to regulate gene expression. *Proc the Natl Acad Sci U S A* **114**, E7092-E7100

53. Clark, K., Middelbeek, J., Lasonder, E., Dulyaninova, N. G., Morrice, N. A., Ryazanov, A. G., Bresnick, A. R., Figdor, C. G., and van Leeuwen, F. N. (2008) TRPM7 regulates myosin IIA filament stability and protein localization by heavy chain phosphorylation. *J Mol Biol* **378**, 790-803
54. Clark, K., Middelbeek, J., Dorovkov, M. V., Figdor, C. G., Ryazanov, A. G., Lasonder, E., and van Leeuwen, F. N. (2008) The alpha-kinases TRPM6 and TRPM7, but not eEF-2 kinase, phosphorylate the assembly domain of myosin IIA, IIB and IIC. *FEBS let* **582**, 2993-2997
55. Dorovkov, M. V., and Ryazanov, A. G. (2004) Phosphorylation of annexin I by TRPM7 channel-kinase. *J Biol Chem* **279**, 50643-50646
56. Deason-Towne, F., Perraud, A. L., and Schmitz, C. (2012) Identification of Ser/Thr phosphorylation sites in the C2-domain of phospholipase C gamma2 (PLC $\gamma$ 2) using TRPM7-kinase. *Cell Signal* **24**, 2070-2075
57. Perraud, A. L., Zhao, X., Ryazanov, A. G., and Schmitz, C. (2011) The channel-kinase TRPM7 regulates phosphorylation of the translational factor eEF2 via eEF2-k. *Cell Signal* **23**, 586-593
58. Dorovkov, M. V., Beznosov, S. N., Shah, S., Kotlianskaia, L., and Kostiukova, A. S. (2008) Effect of mutations imitating the phosphorylation by TRPM7 kinase on the function of the N-terminal domain of tropomodulin. *Biofizika* **53**, 943-949
59. Clark, K., Middelbeek, J., Morrice, N. A., Figdor, C. G., Lasonder, E., and van Leeuwen, F. N. (2008) Massive autophosphorylation of the Ser/Thr-rich domain controls protein kinase activity of TRPM6 and TRPM7. *PLoS one* **3**, e1876
60. Kim, T. Y., Shin, S. K., Song, M. Y., Lee, J. E., and Park, K. S. (2012) Identification of the phosphorylation sites on intact TRPM7 channels from mammalian cells. *Biochem Biophys Res Commun* **417**, 1030-1034
61. Zhang, X., Huang, J., and McNaughton, P. A. (2005) NGF rapidly increases membrane expression of TRPV1 heat-gated ion channels. *EMBO J* **24**, 4211-4223
62. Shin, S. H., Lee, E. J., Hyun, S., Chun, J., Kim, Y., and Kang, S. S. (2012) Phosphorylation on the Ser824 residue of TRPV4 prefers to bind with F-actin than with microtubules to expand the cell surface area. *Cell Signal* **24**, 641-651
63. Schmitz, C., Dorovkov, M. V., Zhao, X., Davenport, B. J., Ryazanov, A. G., and Perraud, A.-L. (2005) The channel kinases TRPM6 and TRPM7 are functionally nonredundant. *J Biol Chem* **280**, 37763-37771

64. Brandao, K., Deason-Towne, F., Zhao, X., Perraud, A. L., and Schmitz, C. (2014) TRPM6 kinase activity regulates TRPM7 trafficking and inhibits cellular growth under hypomagnesic conditions. *Cell Mol Life Sci* **71**, 4853-4867
65. Ryazanov, A. G., Pavur, K. S., and Dorovkov, M. V. (1999) Alpha-kinases: a new class of protein kinases with a novel catalytic domain. *Curr Biol* **9**, R43-45
66. Yamaguchi, H., Matsushita, M., Nairn, A. C., and Kuriyan, J. (2001) Crystal structure of the atypical protein kinase domain of a TRP channel with phosphotransferase activity. *Mol Cell* **7**, 1047-1057
67. Drennan, D., and Ryazanov, A. G. (2004) Alpha-kinases: analysis of the family and comparison with conventional protein kinases. *Prog Biophys Mol Biol* **85**, 1-32
68. Crawley, S. W., and Cote, G. P. (2009) Identification of dimer interactions required for the catalytic activity of the TRPM7 alpha-kinase domain. *Biochem J* **420**, 115-122
69. van der Wijst, J., Blanchard, M. G., Woodroof, H. I., Macartney, T. J., Gourlay, R., Hoenderop, J. G., Bindels, R. J., and Alessi, D. R. (2014) Kinase and channel activity of TRPM6 are co-ordinated by a dimerization motif and pocket interaction. *Biochem J* **460**, 165-175
70. Steichen, J. M., Iyer, G. H., Li, S., Saldanha, S. A., Deal, M. S., Woods, V. L., and Taylor, S. S. (2010) Global consequences of activation loop phosphorylation on protein kinase A. *J Biol Chem* **285**, 3825-3832
71. Ye, Q., Crawley, S. W., Yang, Y., Cote, G. P., and Jia, Z. (2010) Crystal structure of the alpha-kinase domain of *Dictyostelium* myosin heavy chain kinase A. *Sci Signal* **3**, ra17
72. Crawley, S. W., Gharaei, M. S., Ye, Q., Yang, Y., Raveh, B., London, N., Schueler-Furman, O., Jia, Z., and Cote, G. P. (2011) Autophosphorylation activates *Dictyostelium* myosin II heavy chain kinase A by providing a ligand for an allosteric binding site in the alpha-kinase domain. *J Biol Chem* **286**, 2607-2616
73. Moore, C. E., Regufe da Mota, S., Mikolajek, H., and Proud, C. G. (2014) A conserved loop in the catalytic domain of eukaryotic elongation factor 2 kinase plays a key role in its substrate specificity. *Mol Cell Biol* **34**, 2294-2307
74. Tavares, C. D., Ferguson, S. B., Giles, D. H., Wang, Q., Wellmann, R. M., O'Brien, J. P., Warthaka, M., Brodbelt, J. S., Ren, P., and Dalby, K. N. (2014) The molecular mechanism of eukaryotic elongation factor 2 kinase activation. *J Biol Chem* **289**, 23901-23916

75. Ye, Q., Yang, Y., van Staalduinen, L., Crawley, S. W., Liu, L., Brennan, S., Cote, G. P., and Jia, Z. (2016) Structure of the *Dictyostelium* myosin-II heavy chain kinase A (MHCK-A) alpha-kinase domain apoenzyme reveals a novel autoinhibited conformation. *Sci Rep* **6**, 26634
76. Overton, J. D., Komiya, Y., Mezzacappa, C., Nama, K., Cai, N., Lou, L., Fedeles, S. V., Habas, R., and Runnels, L. W. (2015) Hepatocystin is essential for TRPM7 function during early embryogenesis. *Sci Rep* **5**, 18395
77. Kamitani, T., Kito, K., Nguyen, H. P., and Yeh, E. T. (1997) Characterization of NEDD8, a developmentally down-regulated ubiquitin-like protein. *J Biol Chem* **272**, 28557-28562
78. Morales, F. C., Takahashi, Y., Momin, S., Adams, H., Chen, X., and Georgescu, M. M. (2007) NHERF1/EBP50 head-to-tail intramolecular interaction masks association with PDZ domain ligands. *Mol Cell Biol* **27**, 2527-2537
79. Luo, Z. J., Zhang, X. F., Rapp, U., and Avruch, J. (1995) Identification of the 14.3.3 zeta domains important for self-association and Raf binding. *J Biol Chem* **270**, 23681-23687
80. Yaffe, M. B., Rittinger, K., Volinia, S., Caron, P. R., Aitken, A., Leffers, H., Gamblin, S. J., Smerdon, S. J., and Cantley, L. C. (1997) The structural basis for 14-3-3:phosphopeptide binding specificity. *Cell* **91**, 961-971
81. Fetrow, J. S. (1995) Omega loops: nonregular secondary structures significant in protein function and stability. *FASEB J* **9**, 708-717
82. Amanchy, R., Periaswamy, B., Mathivanan, S., Reddy, R., Tattikota, S. G., and Pandey, A. (2007) A curated compendium of phosphorylation motifs. *Nat Biotech* **25**, 285-286
83. Courjault, F., Gerin, B., Leroy, D., Chevalier, J., and Toutain, H. (1991) Morphological and biochemical characterization of the opossum kidney cell line and primary cultures of rabbit proximal tubule cells in serum-free defined medium. *Cell Biol Int* **15**, 1225-1234
84. Ichimura, T., Isobe, T., Okuyama, T., Takahashi, N., Araki, K., Kuwano, R., and Takahashi, Y. (1988) Molecular cloning of cDNA coding for brain-specific 14-3-3 protein, a protein kinase-dependent activator of tyrosine and tryptophan hydroxylases. *Proc the Natl Acad Sci U S A* **85**, E7084-E7088
85. Ichimura, T., Ito, M., Itagaki, C., Takahashi, M., Horigome, T., Omata, S., Ohno, S., and Isobe, T. (1997) The 14-3-3 protein binds its target proteins with a common site located towards the C-terminus. *FEBS let* **413**, 273-276

86. Watanabe, M., Isobe, T., Ichimura, T., Kuwano, R., Takahashi, Y., Kondo, H., and Inoue, Y. (1994) Molecular cloning of rat cDNAs for the zeta and theta subtypes of 14-3-3 protein and differential distributions of their mRNAs in the brain. *Brain Res Mol Brain Res* **25**, 113-121
87. Muslin, A. J., Tanner, J. W., Allen, P. M., and Shaw, A. S. (1996) Interaction of 14-3-3 with signaling proteins is mediated by the recognition of phosphoserine. *Cell* **84**, 889-897
88. Dougherty, M. K., and Morrison, D. K. (2004) Unlocking the code of 14-3-3. *J Cell Sci* **117**, 1875-1884
89. Dubois, T., Howell, S., Amess, B., Kerai, P., Learmonth, M., Madrazo, J., Chaudhri, M., Rittinger, K., Scarabel, M., Soneji, Y., and Aitken, A. (1997) Structure and sites of phosphorylation of 14-3-3 protein: role in coordinating signal transduction pathways. *J Protein Chem* **16**, 513-522
90. Johnson, C., Crowther, S., Stafford, M. J., Campbell, D. G., Toth, R., and MacKintosh, C. (2010) Bioinformatic and experimental survey of 14-3-3-binding sites. *Biochem J* **427**, 69-78
91. Ku, N. O., Liao, J., and Omary, M. B. (1998) Phosphorylation of human keratin 18 serine 33 regulates binding to 14-3-3 proteins. *EMBO J* **17**, 1892-1906
92. Gabriel, L., Lvov, A., Orthodoxou, D., Rittenhouse, A. R., Kobertz, W. R., and Melikian, H. E. (2012) The acid-sensitive, anesthetic-activated potassium leak channel, KCNK3, is regulated by 14-3-3 $\beta$ -dependent, protein kinase C (PKC)-mediated endocytic trafficking. *J Biol Chem* **287**, 32354-32366
93. Cho, C. H., Kim, E., Lee, Y. S., Yarishkin, O., Yoo, J. C., Park, J. Y., Hong, S. G., and Hwang, E. M. (2014) Depletion of 14-3-3 $\gamma$  reduces the surface expression of Transient Receptor Potential Melastatin 4b (TRPM4b) channels and attenuates TRPM4b-mediated glutamate-induced neuronal cell death. *Mol Brain Res* **7**, 52
94. Moeller, H. B., Slengerik-Hansen, J., Aroankins, T., Assentoft, M., MacAulay, N., Moestrup, S. K., Bhalla, V., and Fenton, R. A. (2016) Regulation of the water channel aquaporin-2 via 14-3-3 $\theta$  and - $\zeta$ . *J Biol Chem* **291**, 2469-2484
95. Kilisch, M., Lytovchenko, O., Arakel, E. C., Bertinetti, D., and Schwappach, B. (2016) A dual phosphorylation switch controls 14-3-3-dependent cell surface expression of TASK-1. *J Cell Sci* **129**, 831-842
96. Fernandez-Orth, J., Ehling, P., Ruck, T., Pankratz, S., Hofmann, M. S., Landgraf, P., Dieterich, D. C., Smalla, K. H., Kahne, T., Seebohm, G., Budde, T., Wiendl, H., Bittner, S., and Meuth, S. G. (2017) 14-3-3 Proteins regulate K2P5.1 surface expression on T lymphocytes. *Traffic* **18**, 29-43

97. Thorson, J. A., Yu, L. W., Hsu, A. L., Shih, N. Y., Graves, P. R., Tanner, J. W., Allen, P. M., Piwnica-Worms, H., and Shaw, A. S. (1998) 14-3-3 proteins are required for maintenance of Raf-1 phosphorylation and kinase activity. *Mol Cell Biol* **18**, 5229-5238
98. Van Der Hoeven, P. C., Van Der Wal, J. C., Ruurs, P., Van Dijk, M. C., and Van Blitterswijk, J. (2000) 14-3-3 isotypes facilitate coupling of protein kinase C- $\zeta$  to Raf-1: negative regulation by 14-3-3 phosphorylation. *Biochem J* **345 Pt 2**, 297-306
99. Yang, Y., Ye, Q., Jia, Z., and Cote, G. P. (2015) Characterization of the catalytic and nucleotide binding properties of the alpha-kinase domain of *Dictyostelium* myosin-II heavy chaink A. *J Biol Chem* **290**, 23935-23946
100. Su, L. T., Chen, H. C., Gonzalez-Pagan, O., Overton, J. D., Xie, J., Yue, L., and Runnels, L. W. (2010) TRPM7 activates m-calpain by stress-dependent stimulation of p38 MAPK and c-Jun N-terminal kinase. *J Mol Biol* **396**, 858-869
101. Abiria, S. A., Krapivinsky, G., Sah, R., Santa-Cruz, A. G., Chaudhuri, D., Zhang, J., Adstamongkonkul, P., DeCaen, P. G., and Clapham, D. E. (2017) TRPM7 senses oxidative stress to release Zn<sup>2+</sup> from unique intracellular vesicles. *Proc the Natl Acad Sci U S A* **114**, E6079-E6088

**ABBREVIATIONS**

a.a., amino acid

ATCC, American Type Culture Collection

AMPPNP, adenylyl-imidodiphosphate

ATP, adenosine 5-triphosphate

Bis-Tris, Bis-(2-hydroxy-ethyl)-amino-tris(hydroxymethyl)-methane

BSA, bovine serum albumin

CBP, calmodulin binding protein

CC, coiled-coil

CHX, cycloheximide

DAPI, 4',6-diamidino-2-phenylindole

D-MEM, Dulbecco's Modified Eagle Medium

DMSO, dimethyl sulfoxide

eEF2K, eukaryotic elongation factor-2 kinase

ER, endoplasmic reticulum

FBS, fetal bovine serum

GFP, green fluorescent protein

GSK, glycogen synthase kinase

GST, glutathione S-transferase

HA, hemagglutinin

HEK, human embryonic kidney

IP, immunoprecipitation

IPTG, isopropyl- $\beta$ -D-1-thiogalactopyranoside

LC-MS/MS, liquid chromatography tandem mass spectrometry

MagNuM, magnesium nucleotide-regulated metal ion

MBP, myelin basic protein

MHCK, myosin heavy chain kinase

MIC, magnesium-inhibited cation

MOPS, (3-(*N*-morpholino)propanesulfonic acid)

MS, mass spectrometry

NHERF, sodium-hydrogen antiporter 3 regulator

NEM, *N*-ethylmaleimide

N/D loop, asparagine/aspartate-containing loop

NIMA, never in mitosis gene a

OK, opossum kidney

PBS, phosphate buffered saline

PBST, phosphate buffered saline-1% Triton-X100

PCR, polymerase chain reaction

PDB, protein data bank

PKA, protein kinase A

PKC, protein kinase C

PLC, phospholipase C

PMSF, phenylmethane sulfonyl fluoride or phenylmethylsulfonyl fluoride

PVDF, polyvinylidene difluoride

SBP, streptavidin binding protein

SDS, sodium dodecyl sulfate

SDS-PAGE, sodium dodecyl sulfate-polyacrylamide gel electrophoresis

S/T, serine/threonine-rich

TET, tetracycline

TRP, transient receptor potential

TRPA, transient receptor potential ankyrin

TRPV, transient receptor potential vanilloid

TRPM, transient receptor potential melastatin

Tween 20, polyoxyethylenesorbitan monolaurate

Ub, ubiquitin

WT, wild-type

## APPENDICES

## Appendix 1. Site-directed Mutagenesis QuickChange Primers

	Top Primer	Bottom Primer
<b>mTRPM 7</b>		
S1255A	GCCCAGAAAGCTGCAGAAGCT AGTAAAGTGC	GCACTTTACTAGCTTCTGCAG CTTTCTGGGC
S1360A	CCCAAGTGCTGTTGCTCCCC AGAATTACG	CGTAATTCTGGGGGAGCAACA GCACTTGGG
S1360D	CCCAAGTGCTGTTGATCCCC AGAATTACG	CGTAATTCTGGGGGATCAACA GCACTTGGG
S1360E	CCCAAGTGCTGTTGAGCCCC AGAATTACG	CGTAATTCTGGGGGCTCAACA GCACTTGGG
S1403A	CCAACCAAATTTTCTGTGGCTA CCCCATCCCAGCC	GGCTGGGATGGGGTAGCCAC AGAAAATTTGGTTGG
S1403D	CCAACCAAATTTTCTGTGGAC ACCCCATCCCAGCC	GGCTGGGATGGGGTGTCCACA GAAAATTTGGTTGG
S1403E	CCAACCAAATTTTCTGTGGAG ACCCCATCCCAGCC	GGCTGGGATGGGGTCTCCACA GAAAATTTGGTTGG
S1502A/ T1503A	GCTGTAGTAGAAGAGCGGCGG CGGAAGACTCTCCAG	CTGGAGAGTCTTCCGCCGCGG CTCTTCTACTACAGC
S1502D/ S1503D	GCTGTAGTAGAAGAGCGGACG ACGAAGACTCTCCAG	CTGGAGAGTCTTCGTCTGTCG CTCTTCTACTACAGC
S1506A	GCGTCGACGGAAGACGCTCCA GAAGTCG	CGACTTCTGGAGCGTCTTCCG TCGACGC
S1554A	GCCCGTTTTGGATACAAATTA CTATTATGCAGCTGTGGAAAG	CTTTCCACAGCTGCATAATAG TAATTTGTATCCAAAACGGGC
S1554D	GCCCGTTTTGGATACAAATTA CTATTATGACGCTGTGGAAAG	CTTTCCACAGCGTCATAATAG TAATTTGTATCCAAAACGGGC
L1564P	CCTGATGAGGCCGTCACAGAG TATCCCTTCGTTCC	GGAACGAAGGGAATACTCTG TGACGGCCTCATCAGG
S1565A	GAGGTTGGCCAGAGTATTCC CTTCGTTCCCTGTACC	GGTACAGGAACGAAGGGAAT ACTCTGGGCCAACCTC
S1565D	GAGGTTGGACCAGAGTATTCC CTTCGTTCCCTGTACC	GGTACAGGAACGAAGGGAAT ACTCTGGTCCAACCTC
S1565A/ S1567A	GATGAGGTTGGCACAGGCTAT TCCCTTCGTTCCCTGTACCTCC	GGAGGTACAGGAACGAAGGG AATAGCCTGTGCCAACCTCAT C
S1567A	GAGGTTGTCACAGGCTATTCC CTTCGTTCCCTGTACC	GGTACAGGAACGAAGGGAAT AGCCTGTGACAACCTC
S1567D	GAGGTTGTCACAGGATATTCC CTTCGTTCCCTGTACC	GGTACAGGAACGAAGGGAAT ATCCTGTGACAACCTC
S1567E	GAGGTTGTCACAGGAGATTCC CTTCGTTCCCTGTACC	GGTACAGGAACGAAGGGAAT CTCCTGTGACAACCTC

S1588A	CCGTCTGGAGGAGGCTTCTCC CAGTATACTG	CAGTATACTGGGAGAAGCCTC CTCCAGACGG
S1588D	CCGTCTGGAGGAGGATTCTCC CAGTATACTG	CAGTATACTGGGAGAATCCTC CTCCAGACGG
S1596A	CCCAGTATACTGAATAACGCC ATGTCTTCATGGTCTCAGC	GCTGAGACCATGAAGACATG GCGTTATTCAGTATACTGGG
S1596D	CCCAGTATACTGAATAACGAC ATGTCTTCATGGTCTCAGC	GCTGAGACCATGAAGACATGT CGTTATTCAGTATACTGGG
S1613A	GGCCTCTGTGCCAAAATTGAG TTTTTAGCTAAAGAGGAAATG GG	CCCATTTCTCTTTAGCTAAA AACTCAATTTTGGCACAGAGG CC
S1613D	GGCCTCTGTGCCAAAATTGAG TTTTTAGATAAAGAGGAAATG GG	CCCATTTCTCTTTATCTAAAA ACTCAATTTTGGCACAGAGGC C
K1646R	GTCAGGGCATCTCTATATCATT AGGTCATTTCTTCCTGAGGTG	CACCTCAGGAAGAAATGACCT AATGATATAGAGATGCCCTGA C
S1647D	GTCAGGGCATCTCTATATCATT AAGGATTTTCTTCCTGAGGTG	CACCTCAGGAAGAAAATCCTT AATGATATAGAGATGCCCTGA C
T1655D	GAGGTGATAAACGACTGGTCA AGCATTTATAAAGAAGATACG G	CCGTATCTTCTTTATAAATGCT TGACCAGTCGTTTATCACCTC
S1658A	GAGGTGATAAACACATGGTCA GCCATTTATAAAGAAGATACG G	CCGTATCTTCTTTATAAATGG CTGACCATGTGTTTATCACCT C
S1658D	GAGGTGATAAACACATGGTCA GACATTTATAAAGAAGATACG G	CCGTATCTTCTTTATAAATGTC TGACCATGTGTTTATCACCTC
T1664D	GAAGATGACGTTCTACATCTC TGTCTCAGAGAAATACAACAA C	GTTGTTGTATTTCTCTGAGAC AGAGATGTAGAACGTCATCTT C
T1683A	GCAGCACAAAAGCTCGCATTT GCCTTTAATCAGATG	CATCTGATTAAAGGCAAATGC GAGCTTTTGTGCTGC
T1683D	GCAGCACAAAAGCTCGACTTT GCCTTTAATCAGATG	CATCTGATTAAAGGCAAAGTC GAGCTTTTGTGCTGC
S1693A	CAGATGAAACCCAAAGCCATA CCATATTCTCCAAGG	CCTTGGAGAATATGGTATGGC TTTGGGTTTCATCTG
S1693D	CAGATGAAACCCAAAGACATA CCATATTCTCCAAGG	CCTTGGAGAATATGGTATGTC TTTGGGTTTCATCTG
S1697D	CAGATGAAACCCAAATCCATA CCATATGATCCAAGG	CCTTGGATCATATGGTATGGA TTTGGGTTTCATCTG
T1722D	GGTTTGCTGTAGAAGAGTGCA TGGATGGTGAATTTAG	CTAAATTCACCATCCATGCAC TCTTCTACAGCAAACC
T1741A	CATTCCTACAAATGCTCTAGA AGAGATCATGCTAGCC	GGCTAGCATGATCTCTCTAG AGCATTTGTAGGAATG

T1741D	CATTCCTACAAATGACCTAGA AGAGATCATGCTAGCC	GGCTAGCATGATCTCTTCTAG GTCATTTGTAGGAATG
S1750A	GAGATCATGCTAGCCTTTGCC CACTGGACCTATG	CATAGGTCCAGTGGGCAAAG GCTAGCATGATCTC
S1750D	GAGATCATGCTAGCCTTTGAC CACTGGACCTATG	CATAGGTCCAGTGGTCAAAGG CTAGCATGATCTC
S1750E	GAGATCATGCTAGCCTTTGAG CACTGGACCTATG	CATAGGTCCAGTGCTCAAAGG CTAGCATGATCTC
T1753D	GCCACTGGGACTATGAATATA CCAGAGGGGAG	CTCCCCTCTGGTATATTCATA GTCCCAGTGGC
T1757D	GGACCTATGAATATGACAGAG GGGAGTTACTGG	CCAGTAACTCCCCTCTGTCAT ATTCATAGGTCC
T1774A	GGAGTGGGAGAAAACCTTGGCT GACCCATCTG	CAGATGGGTCAGCCAAGTTTT CTCCCCTCC
T1774D	GGAGTGGGAGAAAACCTTGGAT GACCCATCTG	CAGATGGGTCATCCAAGTTTT CTCCCCTCC
T1774E	GGAGTGGGAGAAAACCTTGGAG GACCCATCTG	CAGATGGGTCCTCCAAGTTTT CTCCCCTCC
S1777A	GGGAGAAAACCTTACTGACCC AGCTGTAATAAAAAGC	GCTTTTATTACAGCTGGGTCA GTCAAGTTTTCTCCC
S1777D	GGGAGAAAACCTTACTGACCC AGATGTAATAAAAAGC	GCTTTTATTACATCTGGGTCA GTCAAGTTTTCTCCC
S1777E	GGGAGAAAACCTTACTGACCC AGAGGTAATAAAAAGC	GCTTTTATTACCTCTGGGTCA GTCAAGTTTTCTCCC
S1777G	GGGAGAAAACCTTACTGACCC AGGGGTAATAAAAAGC	GCTTTTATTACCCCTGGGTCA GTCAAGTTTTCTCCC
S1777N	GGGAGAAAACCTTACTGACCC AAACGTAATAAAAAGC	GCTTTTATTACGTTTGGGTCA GTCAAGTTTTCTCCC
S1777Q	GGGAGAAAACCTTACTGACCC ACAGGTAATAAAAAGC	GCTTTTATTACCTGTGGGTCA GTCAAGTTTTCTCCC
S1786A	GCTGAAGAAAAAAGAGCCTGT GACATGGTTTTTGG	CCAAAACCATGTACAGGCT CTTTTTCTTCAGC
S1786D	GCTGAAGAAAAAAGAGACTGT GACATGGTTTTTGG	CCAAAACCATGTACAGTCT CTTTTTCTTCAGC
T1882A	CCAGATTTGAAGAGGAATGAC TACGCGCCTG	CAGGCGCGTAGTCATTCCTCT TCAAATCTGG
T1882D	GAAGAGGAATGACTACGACCC TGATAAAATTATATTCCTCAG G	CCTGAGGAAATATAATTTTAT CAGGGTCGTAGTCATTCCTCT TC
<b>hTRPM 6- K1804R</b>	CCGGGACAAGTTTTTCATTGTC AGGTCCTTTCTTCC	GGAAGAAAGGACCTGACAAT GAAAACCTGTCCCGG
<b>m14-3- 30-K49E</b>	CTGTCGGTGGCCTACGAAAAC GTGGTAGGG	CCCTACCACGTTTTTCGTAGGC CACCGACAG

**Appendix 2. Sequencing Primers for QuickChange Mutagenesis**

	<b>Sequencing Primer</b>
<b>mTRPM7</b>	
S1255	CCGGGTCACCTTTTGAAAGAGTGGAGCAGATGAGC
S1403	GAATTACGACAGAGACGACATGGG
S1502	CTGAAACATGTGGGTGCTGCTG
S1588	GTCACAGAGTATTCCCTTCGTTCC
K1646	GCTAGGCCTCTGTGCCAAAATTG
S1693	GATATCCTGAAGTCAGGGCATCTC
<b>hTRPM6-K1804R</b>	GTCCCGAGAGGAGATGGATGGGGGC
<b>m14-3-30-K49E</b>	CTGATCCAGAAGGCCAAGCTG

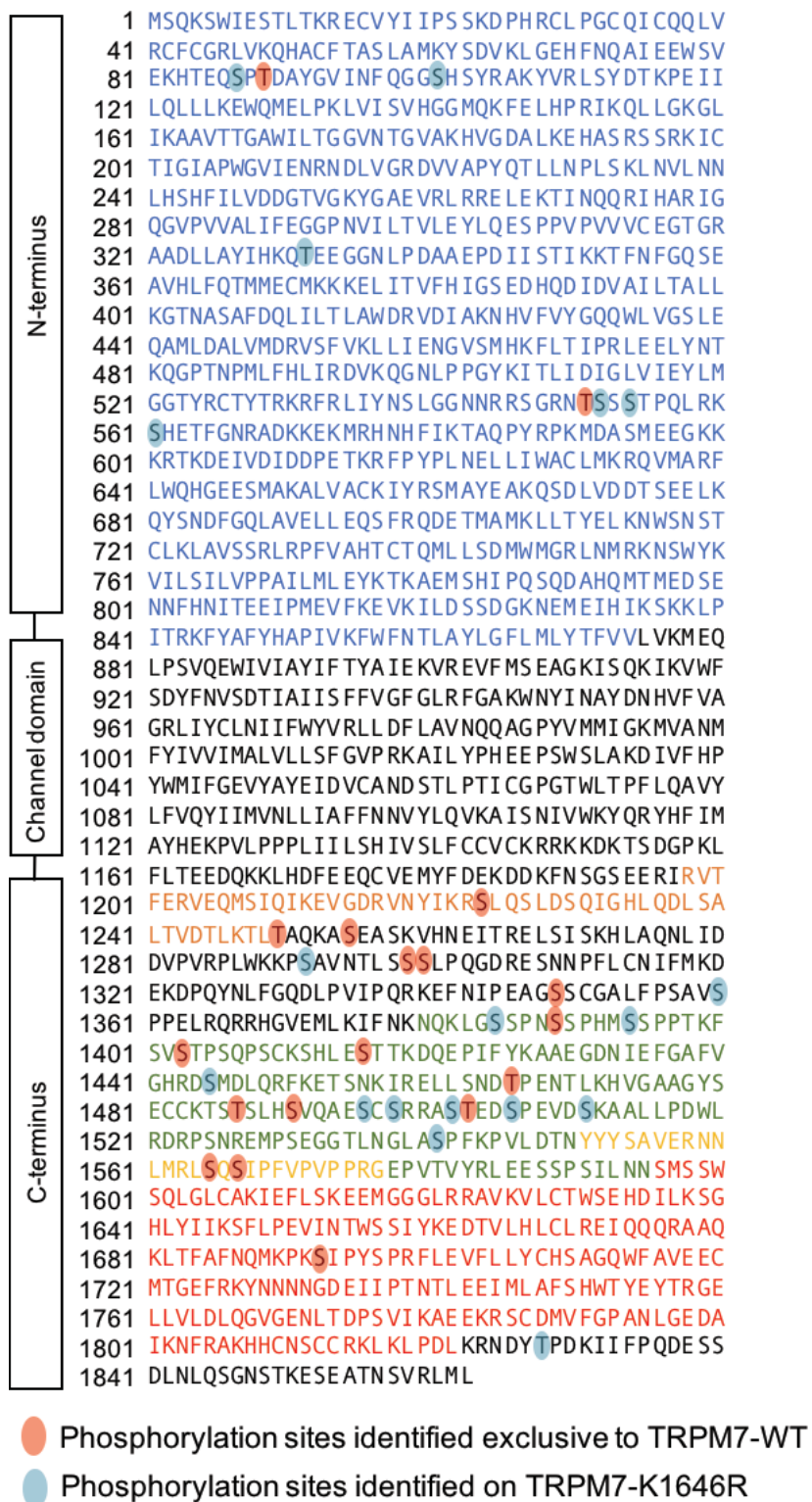
## Appendix 3. Summary of Phosphorylation Sites Identified on mTRPM7

N-terminus	1	MSQKSWIESTLTKRECVYI IPS SKD PHRCL PGC QI CQQLV
	41	RCFCGRLVKQHACF TAS LAMKY SDV KL GEH FNQAI EEW SV
	81	EKHTEQSPTDAYGV INF QGG <sup>S</sup> H SYRAKYVR LSYDTKPE II
	121	LQLLLKEWQME L PKLVI SVHGGMQK FE LHP RIKQL LGKGL
	161	IKA AVTTGAWIL TG VNTG VAKHVG DA LKE HAS RS SRK IC
	201	TIGIAPWGV I ENRNDLV GRD VV APY QT LLN PLS KL NVL NN
	241	LHSHF ILVDDGT VG KYGAE VRL RRE LE KTI NQQR I HAR IG
	281	QGV PVVAL IFEGGP NVI LTVLE YLQ ES PPV PVV VC EGT GR
	321	AADL LAYIHKQTEE GGN LP DAA EPD II STI KKT FNFGQ SE
	361	AVHL FQTMMECMKKEL ITVFH IGS EDHQD IDVAI LTALL
	401	KGTNASAFDQL I LT LAWDRVDI AKN HV FVY GQQWL VGS LE
	441	QAML DALVMDRV SF VKL LI ENG VSM HK FLT IPR LE ELY NT
	481	KQGPTNPML FHL IRDVK QGNLP PGY KI TLI DIG LV IEY LM
	521	GGTYRCTYTRKRFR LI YNS LGGNNR <sup>S</sup> GRNTSS STPQL RK
	561	SHETFGNRADKKEKMRH NH FIKTAQ PY RPKMDA SM EEGKK
	601	KRTKDEIVDIDDPE TKR FP YPL NEL LI WAC LMKRQVMARF
	641	LWQHGEESMAKALVACK IYRSMAYE AKQSD LVDDT SEE LK
	681	QYSNDFGQLAVELL EQS FRQDE TMA MKLLT YEL KNWSNST
	721	CLKLAVSSRL RPFVAHT CTQML LSDMWMGR LNM RKNSWYK
	761	VILS ILVPPAILML EYKTKAEM SHI PQ SQDAHQMT MED SE
	801	NNFHNI TEEI PMEV FKE VKILD <sup>S</sup> SDGKNEME IHIKSKKLP
	841	ITRKFYAFYHAP IVKFWFN TLA YLGF LMLY TFVVLVKMEQ
	881	LPSVQEWIVIAIYIF TYA IE KVR EVF MS EAGKIS QKIKVWF
	921	SDYFNVSDTIAIIS FFVGF GLRFGA KWN YI NAYDNHVFVA
961	GRLIYCLNII FWYV RLL DF LAVNQQAG PYVMMI GKMVANM	
1001	FYIVVIMALVLL SF GVP RKAIL YPHEE PSW SLAKD IVF HP	
1041	YWMI FGEVYAYE IDVCAND STL PTI CG PGTWLT PF LQAVY	
1081	LFVQYI IMVNL LIA FFNNVYLQVKA IS NIVWKY QR YHF IM	
1121	AYHEKPVLP PPLII LSH IV SLF CCVCKRRK KDK TS DGP KL	
1161	FLTEEDQKKLHDFE EQC VE MYF DEKDD KFN SGS EER I <sup>RVT</sup>	
1201	FERVEQMSIQI KEV GDRVNYIKR <sup>S</sup> LS <sup>S</sup> LD <sup>S</sup> QIGHL QDL SA	
1241	LTVDTLKTLT AQKA <sup>S</sup> EA <sup>S</sup> SKVHNEITRELSI <sup>S</sup> SKHLAQNL ID	
1281	DVPVRPLWKKPSAVNTL <sup>SS</sup> SLPQGDRE SNN PFL CN IFMKD	
1321	EKDPQYNLFGQDLP VIP QRKEF NIP EAGS <sup>S</sup> CGALF P <sup>S</sup> SAVS	
1361	PELRQR RHGVEML KIF NKNQK LGS <sup>S</sup> PN <sup>SS</sup> PHM <sup>SS</sup> PPTKF	
1401	SV <sup>S</sup> TPSQPSCKSHL E <sup>S</sup> TTKDQE PIF YKAAE GDN IE FGAFV	
1441	GHRD <sup>S</sup> MDLQRFKET SNK IRELL <sup>S</sup> NDTP ENT LKHVG AAG <sup>S</sup>	
1481	ECCKT <sup>S</sup> STLSVQAESC SRRAS <sup>S</sup> TED <sup>S</sup> SP EVD <sup>S</sup> SKAAL LPDWL	
1521	RDRP <sup>S</sup> NREMPSEGG <sup>T</sup> LNGLA <sup>S</sup> SP FKP VL DTN <sup>YYY</sup> SAVERNN	
1561	LMRL <sup>S</sup> Q <sup>S</sup> IPFVPVP PRG EPVTVYRL EE SSP SIL NN <sup>SMS</sup> SW	
1601	SQLGLCAKIEFL <sup>S</sup> KEEMGG LRRAVKV LCTWSEHD ILKSG	
1641	HLYI IKSFLPEVIN TWS <sup>S</sup> SI YKEDTVLH LCL REI QQQRAAQ	
1681	KL <sup>T</sup> FAFNQMKPK <sup>S</sup> SI PYS PR FLE VFL LYCHS AGQWF AVE EC	
1721	MTGEFRKYNNNGDEII PTNTL <sup>S</sup> EEI ML AFS HWT YE YTRGE	
1761	LLVLDLQGVGENLT DP <sup>S</sup> VI KAE EKR SC DMV FGP AN LGE DA	
1801	IKNFRAKHHCNSCC RKL KL PDL KRNDY <sup>T</sup> TPDKII FPQDE <sup>SS</sup>	
1841	DLNLQ <sup>S</sup> GN <sup>S</sup> STKESEATN <sup>S</sup> SVRLML	
Channel domain		
C-terminus		

 Phosphorylation sites identified exclusive to TRPM7-WT

 Phosphorylation sites identified on TRPM7-K1646R

## Appendix 4. Summary of Transphosphorylation Sites on mTRPM7 Introduced by Heterologously Expressed hTRPM6



## Appendix 5. Summary of Phosphorylation Sites Identified on hTRPM6

N-terminus	1	MKEQPVLERLQ	S	Q	K	S	W	I	K	G	V	F	D	K	R	E	C	S	T	I	P	S	S	K	N	P	H	R	C	T											
	41	PVCQVCQNL	I	R	C	Y	C	G	R	L	I	G	D	H	A	G	I	D	Y	S	W	T	I	S	A	A	K	G	K	E	S	E	Q								
	81	WSVEKHTTK	S	P	T	D	T	F	G	T	I	N	F	Q	D	G	E	H	T	H	A	K	Y	I	R	T	S	Y	D	T	K	L									
	121	DHLLHLMLKEWKME	L	P	K	L	V	I	S	V	H	G	I	Q	N	F	T	M	P	S	K	F	K	E	I	F	S														
	161	QGLVKA	A	E	T	T	G	A	W	I	I	T	E	G	I	N	T	G	V	S	K	H	V	G	D	A	L	K	S	H	S	L	R								
	201	KI	W	T	V	G	I	P	P	W	G	V	I	E	N	Q	R	D	L	I	G	K	D	V	V	C	L	Y	Q	T	L	D	N	P	L	S	K	L	T	T	
	241	L	N	S	M	H	S	H	F	I	L	S	D	D	G	T	V	G	K	Y	G	N	E	M	K	L	R	R	N	L	E	K	Y	L	S	L	Q	K	I	H	
	281	R	S	R	Q	G	V	P	V	V	G	L	V	V	E	G	P	N	V	I	L	S	V	W	E	T	V	K	D	K	D	P	V	V	C	E	G	T			
	321	R	A	A	D	L	L	A	F	T	H	K	H	L	A	D	E	G	M	L	R	P	Q	V	K	E	E	I	I	C	M	I	Q	N	T	F	N	F	S	L	K
	361	Q	S	K	H	L	F	Q	I	L	M	E	C	M	V	H	R	D	C	I	T	I	F	D	A	D	S	E	E	Q	D	L	D	L	A	I	L	T	A	L	
	401	L	K	G	T	N	L	S	A	S	E	Q	L	N	L	A	M	A	W	D	R	V	I	A	K	K	H	I	L	I	Y	E	Q	H	W	K	P	D	A	L	
	441	E	Q	A	M	S	D	A	L	V	M	D	R	V	D	F	V	K	L	L	I	E	Y	G	V	N	L	H	R	F	L	T	I	P	R	L	E	E	L	Y	N
481	T	K	Q	G	P	T	N	T	L	L	H	H	L	V	Q	D	V	K	Q	H	T	L	L	S	G	Y	R	I	T	L	I	D	I	G	L	V	V	E	Y	L	
521	I	G	R	A	R	S	N	Y	T	R	K	H	F	R	A	L	Y	N	N	L	Y	R	K	Y	K	H	Q	R	H	S	S	G	N	R	N	E	S	A	E		
561	S	T	L	H	S	Q	F	I	R	T	A	Q	P	Y	K	F	K	E	K	S	I	V	L	H	K	S	R	K	K	S	K	E	Q	N	V	S	D	D	P	E	
601	S	T	G	F	L	Y	P	Y	N	D	L	L	V	W	A	V	L	M	K	R	Q	K	M	A	M	F	F	W	Q	H	G	E	E	A	T	V	K	A	V	I	
641	A	C	I	L	Y	R	A	M	A	E	A	K	E	S	H	M	V	D	D	A	S	E	E	L	K	N	Y	S	K	Q	F	G	Q	L	A	L	D	L	F		
681	E	K	A	F	K	Q	N	E	R	M	A	M	T	L	L	T	Y	E	L	R	N	W	S	N	S	T	C	L	K	L	A	V	S	G	G	L	R	P	F	V	
721	S	H	T	C	T	Q	M	L	L	T	D	M	W	M	G	R	L	K	M	R	K	N	S	W	L	K	I	I	S	I	I	L	P	T	I	L	T	L			
761	E	F	K	S	K	A	E	M	S	H	V	P	Q	S	Q	D	F	Q	F	M	W	Y	S	D	Q	N	A	S	S	K	E	S	A	S	V	K	E	Y			
801	D	L	E	R	G	H	D	E	K	L	D	E	N	Q	H	F	G	L	E	S	G	H	Q	L	P	W	T	R	K	V	Y	E	F	Y	S	A	P	I	V		
841	K	F	W	F	Y	T	M	A	L	A	F	L	M	L	F	T	Y	T	V	L	V	E	M	Q	P	Q	P	S	V	Q	E	W	L	V	S	I	Y	I	F		
881	T	N	A	I	E	V	V	R	E	I	C	I	S	E	P	G	K	F	T	Q	K	V	K	W	I	S	E	Y	W	N	L	T	E	T	V	A	I	G	L		
921	F	S	A	G	F	V	L	R	W	G	D	P	P	F	H	T	A	G	R	L	I	Y	C	I	D	I	I	F	W	F	S	R	L	D	F	F	A	V	N		
961	Q	H	A	G	P	Y	V	T	M	I	A	K	M	T	A	N	M	F	Y	I	V	I	I	M	A	I	V	L	L	S	F	G	V	A	R	K	A	I	L	S	
1001	P	K	E	P	P	S	W	S	L	A	R	D	I	V	F	E	P	Y	W	M	I	Y	G	E	V	A	G	E	I	D	V	C	S	S	Q	P	S	C	P		
1041	P	G	S	F	L	T	P	F	L	Q	A	V	Y	L	F	V	Q	Y	I	M	V	N	L	I	A	F	F	N	N	V	Y	L	D	M	E	S	I	S			
1081	N	N	L	W	K	Y	N	R	Y	R	I	M	T	Y	H	E	K	P	W	L	P	P	L	I	L	S	H	V	G	L	L	R	R	L	C	C					
1121	H	R	A	P	H	D	Q	E	E	G	D	V	G	L	K	L	Y	L	S	K	E	D	L	K	L	H	D	F	E	Q	C	V	E	K	Y	F	H				
1161	K	M	E	D	V	N	C	S	C	E	E	R	I	R	V	T	S	E	R	V	T	E	M	Y	F	Q	L	K	E	M	N	E	K	V	S	F	I	K	D	S	
1201	L	L	S	L	D	S	Q	V	G	H	L	Q	D	L	S	A	L	T	V	D	T	L	K	V	L	S	A	V	D	T	L	Q	E	D	E	A	L	L	A	K	
1241	R	K	H	S	T	C	K	K	L	P	H	S	W	N	V	I	C	A	E	V	L	G	S	M	E	I	A	G	E	K	Y	Q	Y	S	M	P	S				
1281	S	L	L	R	S	L	A	G	G	R	H	P	P	R	V	Q	R	G	A	L	L	E	I	T	N	S	K	R	E	A	T	N	V	R	N	D	Q	E	R	Q	
1321	E	T	S	S	I	V	S	G	V	S	P	N	R	Q	A	H	S	K	Y	G	Q	F	L	V	P	S	N	L	K	R	V	P	F	S	A	E	T				
1361	V	L	P	L	S	R	P	S	V	P	D	V	L	A	T	E	Q	D	I	Q	T	E	V	L	V	H	L	T	G	Q	T	P	V	S	D	W	A	S			
1401	D	E	P	K	E	K	H	E	P	I	A	H	L	L	D	G	Q	D	K	A	E	Q	V	L	P	T	L	S	C	T	P	E	P	M	T	M	S	S	P		
1441	S	Q	A	K	I	M	Q	T	G	G	Y	V	N	W	A	F	S	E	G	D	E	T	G	V	F	S	I	K	K	W	Q	T	C	L	P	S	T				
1481	D	S	D	S	R	S	E	Q	H	Q	K	A	Q	D	S	S	L	S	D	N	S	T	R	S	A	Q	S	S	E	C	S	E	V	G	P	W	L	Q			
1521	P	N	T	S	F	W	I	N	P	L	R	R	Y	R	P	F	A	R	S	H	S	F	R	F	H	K	E	K	L	M	K	I	C	K	I	K	N	L	S		
1561	G	S	S	E	I	G	Q	G	A	W	V	K	A	M	L	T	K	D	R	R	L	S	K	K	K	N	T	Q	G	L	Q	V	P	I	I	T	V	N			
1601	A	C	S	Q	S	D	Q	L	N	P	E	P	G	E	N	S	I	S	E	E	Y	S	K	N	W	F	T	V	S	K	F	S	H	T	G	V	E	P	Y		
1641	I	H	Q	K	M	K	T	K	E	I	G	Q	C	A	I	Q	I	S	D	Y	L	K	Q	S	Q	E	D	L	S	K	N	S	L	W	N	S	R	S	T		
1681	L	N	R	N	S	L	L	K	S	I	G	V	D	K	I	S	A	S	L	K	S	P	Q	E	P	H	H	Y	S	A	I	E	R	N	N	L	M	R			
1721	L	S	Q	T	I	P	F	T	P	V	Q	L	F	A	G	E	E	I	T	V	Y	R	L	E	E	S	P	L	N	L	D	K	S	M	S	S	W	Q			
1761	R	G	R	A	A	M	I	Q	V	L	S	R	E	E	M	D	G	L	R	K	A	M	R	V	S	T	W	S	E	D	D	I	L	K	P	G	Q	V			
1801	F	I	V	K	S	F	L	P	E	V	V	R	T	W	H	K	I	F	Q	E	S	T	V	L	H	L	C	L	R	E	I	Q	Q	R	A	A	K	L			
1841	I	Y	T	F	N	Q	V	K	P	Q	T	I	P	Y	T	P	R	F	L	E	V	F	L	I	Y	C	H	S	A	N	Q	W	L	T	I	E	K	Y	M		
1881	G	E	F	R	K	Y	N	N	N	G	D	E	I	T	P	T	N	T	L	E	E	L	M	L	A	F	S	H	W	T	Y	E	Y	T	R	G	E	L			
1921	V	L	D	L	Q	G	V	G	E	N	L	T	D	P	S	V	I	K	P	E	V	K	Q	S	R	G	M	V	F	G	P	A	N	L	G	E	D	A	I		
1961	N	F	I	A	K	H	H	C	N	S	C	C</																													